CHARACTERIZING THE ROLE OF GENE REGULATORY FACTORS IN AGING DROSOPHILA PHOTORECEPTORS

by

Spencer Escobedo

A Dissertation

Submitted to the Faculty of Purdue University

In Partial Fulfillment of the Requirements for the degree of

Doctor of Philosophy

Department of Biochemistry

West Lafayette, Indiana

May 2022

THE PURDUE UNIVERSITY GRADUATE SCHOOL
STATEMENT OF COMMITTEE APPROVAL

Dr. Vikki M. Weake

Department of Biochemistry

Dr. James D Forney

Department of Biochemistry

Dr. Frederick S Gimble

Department of Biochemistry

Dr. Donald Ready

Department of Biological Sciences

Approved by:

Dr. Andrew D Mesecar

To my wife and parents, Jaime Rae Escobedo, Pamela Marie Gray and Raul Escobedo

TABLE OF CONTENTS

LIST OF TABLES

LIST OF FIGURES

ABSTRACT

Aging is associated with a decline in visual function and increased prevalence of ocular disease, correlating with changes in the transcriptome and epigenome of cells in the eye. The extended photoreceptor cell lifespan, in addition to its high metabolic needs due to phototransduction, makes it critical for these neurons to continually respond to the stresses associated with aging by mounting an appropriate gene expression response. My work, in collaboration with fellow lab members and colleagues, has focused on better understanding the regulatory mechanisms that result in age-dependent transcriptional changes in photoreceptors, and if these changes not only correlate with but cause the decrease in function with age. In order to better characterize photoreceptor specific changes my initial work first focused on expanding the gene expression toolkit for eye specific expression. In chapter 1 we describe a previously unnoticed sevenless mutation present in the majority of the TRiP RNAi collection. In chapter 2 we characterized the currently available eye- and photoreceptor-specific binary expression system drivers in *Drosophila*. Using a luciferase and fluorescent reporter, we characterized the relative expression and cell type-specificity of each driver in the 10-day old adult eye. Also, wecharacterized the expression pattern of these drivers in various developmental stages. We then compared several Gal4 drivers from the Bloomington Drosophila Stock Center (BDSC) including GMR-Gal4, longGMR-Gal4 and Rh1-Gal4 with newly developed Gal4 and QF2 drivers that are specific to different cell types in the adult eye. In addition, we generated drug-inducible Rh1-GSGal4 lines and compared their induced expression with an available GMR-GSGal4 line. Although both lines had significant induction of gene expression measured by luciferase activity, Rh1-GSGal4 was expressed at levels below the detection of the fluorescent reporter by confocal microscopy, while GMR-GSGal4 showed substantial reporter expression in the absence of drug by microscopy. This study systematically characterized and compared a large toolkit of eye- and photoreceptor-specific drivers, while also uncovering some of the limitations of currently available expression systems in the adult eye.

In chapter 3, we sought to untangle the more general neuronal age-dependent transcriptional signature of photoreceptors with that induced by light stress. To do this, we aged flies or exposed them to various durations of blue light, followed by photoreceptor nuclei-specific transcriptome profiling. Using this approach, we identified genes that are both common and

uniquely regulated by aging and light induced stress. Whereas both age and blue light induce expression of DNA repair genes and a neuronal-specific signature of death, both conditions result in downregulation of neurotransmitters important for synaptic transmission. Interestingly, blue light uniquely induced genes that directly counteract the overactivation of the phototransduction signaling cascade. Lastly, unique gene expression changes in aging photoreceptors included the downregulation of genes involved in membrane potential homeostasis and mitochondrial function, as well as the upregulation of immune response genes. We proposed that light stress contributes to the aging transcriptome of photoreceptors, but that there are also other environmental or intrinsic factors involved in age-associated photoreceptor gene expression signatures.

In chapter 4, we sought to test if age-associated changes in gene expression patterns in the eye directly contribute to the increased risk of retinal degeneration. To do this, we performed a targeted photoreceptor specific RNAi screen in *Drosophila* to identify gene regulatory factors that result in premature, age-dependent retinal degeneration. From an initial set of 155 RNAi lines each targeting a unique gene and spanning a diverse set of gene regulatory factors, we identified 18 high confidence target genes whose decreased expression in adult photoreceptors leads to premature and progressive retinal degeneration. The 18 target genes were enriched for factors involved in the regulation of transcription initiation, pausing, and elongation, suggesting that these processes are essential for maintaining the health of aging photoreceptors. To identify the genes regulated by these factors, we profiled the photoreceptor transcriptome in a subset of lines. Strikingly, two of the 18 target genes, *Spt5* and *domino*, show substantially similar changes in gene expression to those observed with advanced age.

Together, our data suggests that dysregulation of the mechanisms involved in transcription initiation and elongation plays a key role in shaping the transcriptome of aging photoreceptors. Further, our findings indicate that the age-dependent changes in gene expression not only correlate, but might also contribute to increased risk of retinal degeneration.

STATEMENT OF PUBLISHED WORK

Chapter 1 is a pre-copyedited manuscript published in *microPublication Biology*. The article was written by Spencer Escobedo with editorial contribution from Vikki Weake. Jonathan Zirin provided primers and PCR experiments. The version of record, Escobedo, SE; Zirin, J; Weake, VM (2019). TRiP stocks contain a previously uncharacterized loss-of-function sevenless allele. microPublication Biology. 10.17912/micropub.biology.000097 is available online at https://www.micropublication.org/journals/biology/micropub-biology-000097/. Chapter 2 is a pre-copyedited manuscript of an article published in the journal *Fly*. The article was written by Spencer Escobedo with editorial contribution from Vikki Weake and experimental contributions by Aashka Shah, Alyssa Easton and supervisor Hana Hall. Chapter 3 is a pre-copyedited manuscript which has been submitted for publication. The article was written by Spencer Escobedo with editorial contribution from Vikki Weake and experimental contributions from Sarah Stanhope and Ziyu Dong.

CHAPTER 1. TRIP STOCKS CONTAIN A PREVIOUSLY UNCHARACTERIZED LOSS-OF-FUNCTION SEVENLESS ALLELE

Declaration of collaborative work
The work described in this chapter was the collaborative effort of Spencer Escobedo, Jonathan Zirin, and Dr. Vikki Weake. Jonathan Zirin provided primer sequences and a portion of PCR experiments. All other experiments were performed by Spencer Escobedo. Spencer Escobedo and Dr. Vikki Weake wrote the manuscript with editorial feedback from the other author.

1.1 Description

The Transgenic RNAi Project (TRiP) has generated more than 12,000 transgenic RNAi fly stocks that have been distributed to the community via the Bloomington Drosophila Stock Center (Ni et al. 2007; Ni et al. 2011; Perkins et al. 2015). These stocks express long double-stranded RNA hairpins (dsRNAs) or short RNA hairpins (shRNAs) under GAL4/UAS control (Brand and Perrimon 1993), and provide powerful tools for targeted genetic screens. Unexpectedly, as part of a genetic screen examining retinal degeneration in flies, we identified a defect in eye development associated with many of the TRiP stocks. Drosophila have a compound eye composed of repeating units, termed ommatidia, that each contain eight photoreceptor cells (R cells 1 – 8) (Ready, Hansen and Benzer 1976). The light-sensing organelle, the rhabdomere, in seven of these photoreceptors can be directly visualized in wild-type flies using light microscopy either by optical neutralization or by examining the deep pseudopupil; R7/R8 are stacked on top of each other so only one is visible in a given vertical plane (Franceschini and Kirschfeld 1971).Whereas seven rhabdomeres could be counted per ommatidium in wild-type flies (Fig. 1A), a subset of the TRiP lines tested show characteristic loss of a single rhabdomere (Fig. 1A, Fig. 1B). This single photoreceptor loss phenotype is reminiscent of sevenless (sev) mutants; sev (FBgn0003366) encodes a receptor tyrosine kinase essential for development of R7; thus, loss of function sev mutations result in ommatidia that lack R7 (Harris et al. 1976; Simon, Bowtell and Rubin 1989). Preliminary observations suggested that the sev phenotype was X-linked and observed only in TRiP stocks containing a scute (sc) allele of unknown origin denoted sc*. Whole genome sequencing data for one of the TRiP stocks with the X chromosome containing this sc allele (y1 sc* v1) revealed the presence of an A>T mutation at position X:1107648 in sev, which would result in a premature stop codon at K665X. We tested several of the TRiP stocks that showed the sev phenotype using PCR

sequencing, and found that all contained the same mutation (Fig. 1C). We have named this new allele sev21. We note that we observed both sev21 and wild-type flies in BL32421, suggesting that this stock is mixed. Since this premature stop codon would result in a severely truncated protein, it is likely that the sev21 allele would represent a loss-of-function mutation. Supporting this, our newly identified sev21 allele did not complement the known sev14 loss-of-function allele (BL67947, BL32421, BL50662). Since stocks generated by the TRiP at Harvard Medical School and their collaborators at Tsinghua University show the sev phenotype, but stocks generated by TRiP collaborators at the National Institute of Genetics in Japan do not, we suspected that the mutation was likely present in the stocks used to balance the TRiP lines (BL35781 and BL32261). PCR sequencing revealed that both of these stocks carry the sev21 allele. Together, these data show that many of the TRiP RNAi stocks balanced with BL35781 or BL32261 contain a newly identified loss-of-function sev allele, sev21. TRiP stocks containing this sev21 allele, including both RNAi and sgRNA lines (TRiP-CRISPR Overexpression and KnockOut) (Port et al. 2014; Jia et al. 2018), will be annotated on Flybase and at BDSC. The presence of the sev21 mutation will not generally affect the use of these stocks, as the X chromosome is typically segregated out or heterozygous during experiments.

1.2 Reagents

Table 1.1. Stocks used in this study.

Stock ID	Reagents
BL25709	y^1 v^1 P{$y^{+t7.7}$=nos-phiC31\int.NLS}X; P{$y^{+t7.7}$=CaryP}attP40
BL25710	y^1 sc* v^1 P{$y^{+t7.7}$=nos-phiC31\int.NLS}X ; P{$y^{+t7.7}$=CaryP}attP2
BL35781	y^1 sc* v^1; In(2LR)Gla, wg^{Gla-1} $PPO1^{Bc}$/CyO
BL32261	y^1 sc* v^1; Dr^1 e^1/TM3, Sb^1
BL67947	y^1 sc* v^1; P{$y^{+t7.7}$ $v^{+t1.8}$=TRiP.HMS05772}attP40
BL32421	y^1 sc* v^1; P{ $y^{+t7.7}$ $v^{+t1.8}$=TRiP.HMS00416}attP2
BL50662	y^1 sc* v^1; P{ $y^{+t7.7}$ $v^{+t1.8}$=TRiP.HMC03063}attP2
BL42511	y^1 v^1; P{ $y^{+t7.7}$ $v^{+t1.8}$=TRiP.HMJ02076}attP40
BL5690	sev^{14}; $Ras85^{De2F}$/TM3, Sb^1
BL5691	sev^{14}; drk^{e0A}/CyO

Figure 1-1. Identification of a new sevenless (sev) allele in a subset of TRiP stocks. A) Representative images showing adult retinas imaged using optical neutralization for male flies from the TRiP collection that show wild type (BL42511) or sev (BL50662) phenotypes. White arrow indicates expected position of missing R7 rhabdomere. B) Summary table describing presence of the eye phenotype and sev mutation in tested TRiP stocks. Eye phenotypes were analyzed using optical neutralization on male flies. Note, BL35781 and BL32261 females were outcrossed to Oregon R males with y1 sc v1; +/CyO and y1 sc v1; +/TM3, Sb1 male progeny used to assess presence/absence of R7. C) Chromatogram showing sequence analysis of the sev gene in BL42511 and BL50662 stocks; the position of the 1107648A>T mutation corresponding to the new sev21 allele is shown.

Figure 1.1 continued

A

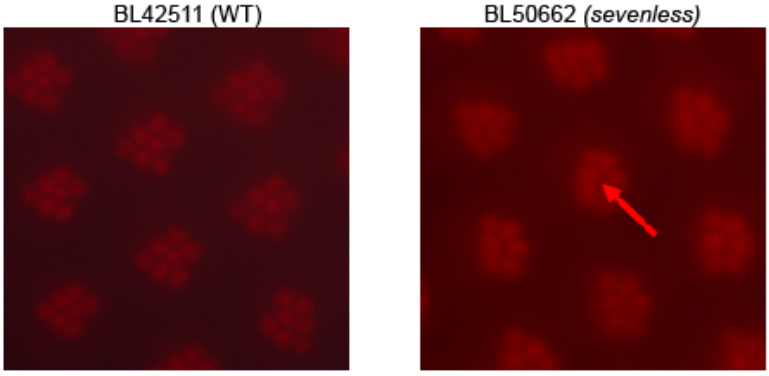

B

Bloomington Stock #	Genotype	Creator	Phenotype	1107648 A>T, K665X
BL25709	y^1 v^1 P{$y^{+t7.7}$=nos-phiC31\int.NLS}X; P{$y^{+t7.7}$=CaryP}attP40	TRiP	Wildtype	No
BL25710	y^1 sc* v^1 P{$y^{+t7.7}$=nos-phiC31\int.NLS}X; P{$y^{+t7.7}$=CaryP}attP2	TRiP	Sevenless	Yes
BL35781	y^1 sc* v^1; In(2LR)Gla, wg^{Gla-1} $PPO1^{Bc}$/CyO	TRiP	Sevenless*	Yes
BL32261	y^1 sc* v^1; Dr^1 e^1/TM3, Sb^1	TRiP	Sevenless*	Yes
BL67947	y^1 sc* v^1; P{$y^{+t7.7}$ $v^{+t1.8}$=TRiP.HMS05772}attP40	HMS	Sevenless	Yes
BL32421	y^1 sc* v^1; P{$y^{+t7.7}$ $v^{+t1.8}$=TRiP.HMS00416}attP2	HMS	Sevenless	Yes (heterozygous)
BL50662	y^1 sc* v^1; P{$y^{+t7.7}$ $v^{+t1.8}$=TRiP.HMC03063}attP2	HMC	Sevenless	Yes
BL42511	y^1 v^1; P{$y^{+t7.7}$ $v^{+t1.8}$=TRiP.HMJ02076}attP40	HMJ	Wildtype	No

C

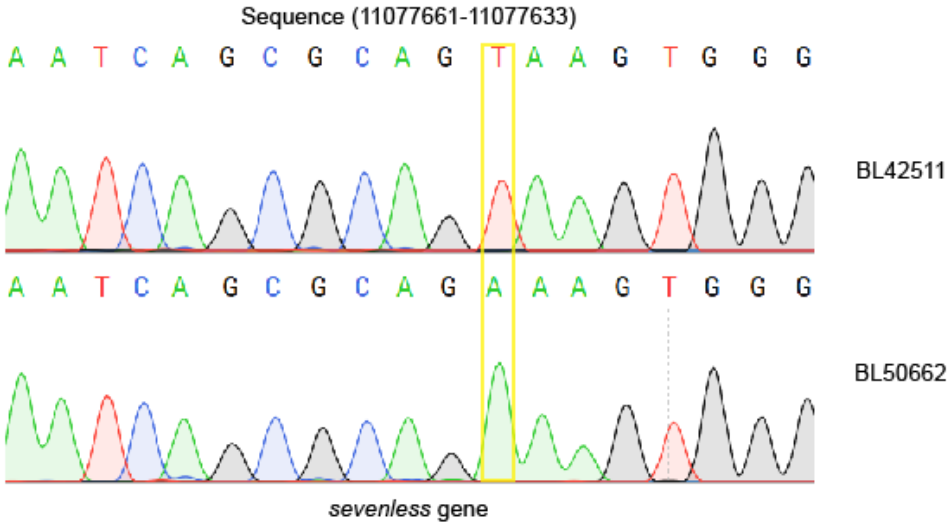

CHAPTER 2. CHARACTERIZING A GENE EXPRESSION TOOLKIT FOR EYE- AND PHOTORECEPTOR-SPECIFIC EXPRESSION IN DROSOPHILA

Declaration of collaborative work
The work described in this chapter was the collaborative effort of Spencer Escobedo, Aashka Shah, Alyssa Easton, Dr. Hana Hall and Dr. Vikki Weake. Aashka Shah helped in performing inducible Gal4 experiments, Alyssa Easton performed QF2 Driver inverse PCR experiments with supervision from Dr. Hana Hall. All other experiments were performed by Spencer Escobedo. Spencer Escobedo and Dr. Vikki Weake wrote the manuscript with editorial feedback from the other authors.

2.1 Introduction

The *Drosophila melanogaster* eye has been used as an important model system for studying cell-cell signaling during development, visual transduction, neurobiology, neurodegeneration, and aging[1–3]. The *Drosophila* eye is particularly amenable to genetic screens because flies with cell-lethal mutations expressed eye-specifically remain viable[4]. Thus, genetic tools to enable expression specifically in various cell types in the eye provide an important resource for the *Drosophila* community. In recent years, several different binary expression systems that enable tissue-specific gene expression have been developed for *Drosophila*[5]. The most established of these is the Gal4/UAS system adopted from yeast that utilizes the Gal4 transcription factor and its upstream activating sequence (UAS)[6,7]. In this system a temperature sensitive version of the Gal4 repressor, Gal80, allows for temporal regulation[8,9]. Recently, the QF/QUAS system derived from *Neurospora crassa* has emerged as another powerful binary expression system[10]. QF2/QUAS is analogous to the Gal4/UAS system, and uses the QF activator to drive expression of QUAS-transgenes. In addition, the QF/QUAS system offers a useful new means of temporal regulation in the form of a quinic acid inhibited QF repressor. This drug-inducible approach has advantages over the temperature sensitive Gal80 system because increased temperature can impact behavior, development and lifespan in *Drosophila* [11].

In this study, we focused on developing and characterizing several binary expression tools for use in the adult *Drosophila* eye. The *Drosophila* compound eye contains approximately 800 individual units called ommatidia, which are arranged in an orderly honeycomb like lattice[12]. This hexagonal lattice is composed of a total of twelve interommatidial cells (IOCs) surrounding each

ommatidium: six secondary pigment cells, three tertiary pigment cells and three sensory bristle cells[12]. Contained within each ommatidium lies an ordered array of eight photoreceptor (retinula, R) cells; the primary sensory neurons necessary for vision. The R1-R6 photoreceptors make up the outer trapezoidal arrangement with R7 stacked atop R8 near the center. Above these photoreceptor cells are two primary pigment cells and four cone cells, which are responsible for secreting the lens and pseudocone of each ommatidium. The adult *Drosophila* eye originates from the eye imaginal disc, a bi-layered invagination of the ectoderm that first forms in embryo[1]. This tissue continues to grow throughout larval development, and by early pupal development all cells of the adult eye are terminally differentiated[1].

There are several Gal4 drivers that have been widely used when studying eye development; however, many of these eye-specific Gal4 drivers have been less extensively characterized in tissues outside the developing eye and in specific cell types in the adult *Drosophila* eye. For instance, recent reports have noted that the commonly used *Sev-Gal4* and *GMR-Gal4* drivers have much broader expression profiles extending to neurons in the central nervous system (CNS) as well as in non-neuronal tissue such as the trachea and spiracles[13]. Additionally, the *GMR-Gal4* driver has been reported to cause disrupted ommatidia patterning and a visible rough eye phenotype in adults[14]. Here, we sought to systematically characterize the expression pattern of some of the existing eye-specific Gal4 drivers in the adult *Drosophila* eye. We also describe several new eye-specific binary expression drivers generated by our lab that can be used for different cell type-specific expression.

2.2 Materials and methods

2.2.1 Cloning and transgenic flies

Transgenic *Rh1-QF2* and *Rh1-GSGal4* flies were generated in the w^{1118} background using *P*-element transformation by BestGene (CA), and the chromosomal location of each insertion was determined using standard genetic techniques and inverse PCR[15]. To generate the *Rh1-QF2* flies, the QF2 (QF#7m1) coding sequence from pCasper-act(B)-QF2w-act_term (Addgene #46126)[16] was PCR amplified with 5' *XbaI* and 3' *EcoRI* restriction sites using the following primers: 5'-CCTCTAGAATGCCACCCAAGCGCAAAACGC-3' and 5'-TTGAATTCTCATTTCTTCTTTTTGTATGTATTAATG-3'. The QF2 PCR fragment was then

cloned into pCaSpeR-ninaE-forward containing the *ninaE* promoter and 3' region (kindly provided by J. O'Tousa) as an *XbaI/EcoRI* fragment to make pCaSpeR-ninaEp-QF2. To generate the *Rh1-GSGal4* flies, the Gene-switch Gal4 (Gal4-hPR-p65 fusion protein) coding sequence from pSwitch #1 (DGRC #1047)[17] was cloned into pCaSpeR-ninaE-reverse containing the *ninaE* promoter and 3' region (provided by J. O'Tousa) as a *NotI* fragment to make pCaSpeR-ninaEp-GeneswitchGal4. All plasmids generated in this study are listed in Table 1. To generate the *sRh1-Gal4* and *mRh1-Gal4*flies, the following regions of the *ninaE* promoter/enhancer region were PCR amplified with added 5' *NotI* and 3' *BglII* restriction sites: sRh1 209 bp fragment (-120/+67 bp) was amplified using 5'-CTTGCGGCCGCGTCGACACTTTCCTCTGCACATTG-3' and 5'-TTAAGATCTAGGGTTCCTGGATTCTGAATATTTC-3' from *Drosophila* genomic DNA; mRh1 532bp fragment (-450/+62bp) was amplified using 5'-CTTGCGGCCGCATAATCCAAGATTAGCAGAGCCCTC-3' and 5'-TTAAGATCTATTCTGAATATTTCACTGGGGCG-3' from pJRG40 (provided by J. Rister)[18]. The sRh1 or mRh1 promoter fragments were cloned into pBMPGal4LWL (Addgene #26270)[19] as *NotI/BglII* fragments to generate the pBMP-pRh1(-120/+67)-Gal4LWL and pBMP-pRh1(-450/+62)-Gal4LWL vectors and integrated in the *attP2* and *attP-9A* sites respectively using ΦC31-mediated transformation by BestGene (CA). All fly stocks used in this study are described in Table 2.

2.2.2 Fly stock maintenance, crosses and drug treatment

Flies were raised under a 12:12 hour light:dark cycle at 25°C on cornmeal agar fly food. Gal4 or QF2 driver flies were crossed with *UAS-Luc* (BDSC 61678) or *QUAS-Luc* (BDSC 64773) for luciferase assays, or with *20XUAS-6XmCherry* (BDSC 52268) or *10XQUAS-6XmCherry* (BDSC 52270) for confocal microscopy, and male progeny of the appropriate genotype were selected using visible markers. Mated male flies were collected ±1 day after eclosion and aged for 10 days with transfer to fresh food every 2-3 days for assays unless otherwise described. To induce *GSGal4* activity, 8-day-old flies were starved overnight and then placed in vials containing 3.2 mg/mL RU486 (Sigma) dissolved in 200 µL 1% (w/v) sucrose solution in ethanol or vehicle control (1% sucrose in ethanol) for 24 h prior to luciferase assays or microscopy.

2.2.3 Luciferase assays

Luciferase assays were performed as previously described20. Briefly, two heads from male flies of the appropriate age, genotype and/or drug treatment were homogenized in 100 □L of 1x Promega cell culture lysis reagent (#E153A, 25 mM Tris-phosphate pH 7.8, 2 mM DTT,10% glycerol, 1% Triton X-100) and 25 µL of homogenate was added to 50 µL of luciferase reagent (Promega, #E1500). Four biological replicates were conducted per genotype/drug treatment (2 biological replicates for GSGal4 drug duration experiments), and two technical replicates were conducted for each luciferase assay.

2.2.4 Confocal microscopy on live adult eyes

Confocal microscopy of mCherry fluorescent markers expressed in the eye was performed in live fly eyes as previously described21. Briefly, a small petri dish (60 x 15 mm) was filled halfway with 1.5% (w/v) agarose solution at 55°C. While the agarose was still unsolidified but slightly cooled, 5 - 10 anesthetized male flies were embedded into the surface of the agarose. Petri dishes were stored on ice to solidify the agarose and keep the flies anesthetized. To image flies, ice-cold water was added to the petri dish to cover the embedded flies. Using forceps under a dissecting microscope, the head of each fly was gently oriented to position the appearance of the pseudopupil into the middle of the eye. Although flies remain alive during imaging and can be recovered after this process, it is possible that this protocol results in some stress to the fly during the imaging process. Imaging was conducted with a Zeiss LSM780 confocal microscopy using a Zeiss Plan-Apochromat 40x/1.0 DIC M27 water dipping objective. Three biological replicates were conducted per genotype/drug treatment, and representative images are presented.

2.2.5 Embryo collection, fixation, and mounting

Embryos were collected by raising the appropriate mating cross in small cages on standard grape juice agar plates. Plates were changed every 18-24 h and stored at 4°C for up to 3 days. Embryos were fixed using standard formaldehyde fixation followed by 4′,6-diamidino-2-phenylindole (DAPI) staining[20], and mounted on a glass slide in VectaShield (Vector Laboratories, #H100010).

2.2.6 Larval and Pupal mounting

Wandering third instar larvae or late stage pupae of the appropriate genotype were collected from vials and transferred to Pyrex spot well plates. Larvae or pupae were then rinsed with PBS. For pupae, heads were dissected by cutting the most anterior section of the pupal case and then peeling back the case to reveal the heads. The heads were then cut and briefly washed in PBS. Either whole larvae or pupal heads were then mounted in VectaShield on a glass slide. A coverslip was secured over the larvae or pupal heads using dental wax as a bridge. Preparations were immediately imaged.

2.2.7 Fluorescence microscopy of embryos, larvae and pupal heads

All developmental tissues were imaged by fluorescence microscopy using a Leica DM6B-Z microscope equipped with a Leica DFC9000 camera using either a HC PL APO 10x/0.40 DRY (larvae, pupal heads) or HC PL APO 20x/0.70 DRY (embryos) objective.

2.3 Results:

2.3.1 Driver design for eye and photoreceptor-specific expression

We initially sought to develop a set of binary expression tools for the outer photoreceptors (R1 – R6) in the adult compound eye by taking advantage of regulatory elements in the *ninaE* gene, which encodes Rhodopsin 1, the light-sensing G-protein coupled receptor necessary for phototransduction[21]. Expression of the *ninaE* transcript is present at very low levels in pre-pupa, rises to high levels in 3-day old pupa, and persists at high levels throughout the life-span of adult flies[22]. In the larva, *ninaE* is expressed only in the light sensing Bolwig organ, while expression in adult eye is limited to R1 - R6, although expression has also been detected in the sensory neurons of the antennal Johnston's organ[23]. There are three Gal4 driver lines available from the Bloomington *Drosophila* Stock Center (BDSC) that include regulatory elements from *ninaE*: *GMR-Gal4*, *longGMR-Gal4*, and *Rh1-Gal4* (Table 2). The *GMR-Gal4* driver contains five copies of a 29 bp region of the *ninaE* promoter that includes a binding site for the Glass transcription factor (gl) flanked by the *Xho*I restriction site (35 bp total fragment size; Figure 1)[24]. In larva, *GMR-Gal4* has been reported to drive expression in all cells posterior to the morphogenic furrow

of the eye imaginal disc[25], and is also expressed in the midgut and salivary glands[26,27]. The expression in the midgut and salivary glands likely results from the presence of the *hsp70* minimal promoter in *GMR-Gal4*[28]. In adult flies, *GMR-Gal4* drives expression in R1 - R8 photoreceptor cells[25]. Although *GMR-Gal4* has been extensively used to drive expression in the developing eye[7,29], its high expression levels in the adult eye are associated with toxicity and retinal degeneration[14]. In contrast, the *longGMR-Gal4* driver contains five copies of a longer 38 bp fragment from the *ninaE* promoter containing the gl binding motif flanked by *Xho*I (43 bp total fragment size; Figure 1)[30]. *LongGMR-Gal4* is generally reported to be more photoreceptor specific than *GMR-Gal4*[30,31], however to our knowledge an extensive characterization of this driver has never been published. Whereas both the *GMR-Gal4* and *longGMR-Gal4* drivers are expressed during larval development in the eye imaginal disc[25,30], the longer 3 kb *ninaE* promoter fragment used in the *Rh1-Gal4* driver results in an expression pattern more similar to that of the endogenous *ninaE* gene, which is R1 - R6 specific[21,32,33]. *ninaE* is not expressed in the eye imaginal disc of larvae since its expression begins later into pupal development, after R cells are already differentiated, and persists through adulthood[33].

Table 2.1. Fly lines and chromosomal insertion sites. (*) indicates insertion sites determined by inverse PCR in this study.

Stock Name	**Source**	**Location (nearest gene)**	**Genotype**
UAS-Luc	BDSC 61678	3	*w^{1118};; 1P{UAS-LUC.D}3*
20XUAS-6XmCherry	BDSC 52268	*3L:11070538 (Mocs1)	*y^{1} w*; wg^{Sp-1}/CyO, P{Wee-P.ph0}$Bacc^{Wee-P20}$; P{$y^{+t7.7}$ w[+mC]=20XQUAS-6XmCherry-HA}attP2*
10XQUAS-6XmCherry	BDSC 52270	2L:2752799 (*attP2)*	*y^{1} w*; wg^{Sp-1}/CyO, P{Wee-P.ph0}$Bacc^{Wee-P20}$; P{$y^{+t7.7}$ w[+mC]=10XQUAS-6XmCherry-HA}attP2*
GMR-Gal4	BDSC 1104	*2R:10535014 (*lola*)	*w^{*}; P{w^{+mC}=GAL4-ninaE.GMR}12*
longGMR-Gal4	BDSC 8121	*3R: 15343048 (*CG6218*)	*cn bw; P{w^{+mC} =longGMR-Gal4}3/MKRS*
Rh1-Gal4 (3)	BDSC 8691	*3R: 6622632 (*sowi*)	*;;P{$ry^{+t7.2}$ =Rh1-Gal4}3, ry^{506}*
sRh1-Gal4	this study	3L:11070538 (*attP2)*	*w^{1118};;P{w^{+mC} =pRh1(-120/+67)-GAL4}attP2*
mRh1-Gal4	this study	*2R:7224205 (*pk*)	*w^{1118};P{w^{+mC} =pRh1(-450/+62)-GAL4}attP-91(43A1)*
GMR-GSGal4	BDSC 6758	*2R: 24786883 (*key*)	*w^{1118}; P{w^{+mC} =GMRinGS}11*
Rh1-GSGal4 (X)	this study	*X: 16278373 (*eas*)	*w^{1118}; P{w^{+mC} =Rh1inGS}X-9*
Rh1-GSGal4 (2)	this study	*2R: 24786883 (*key*)	*w^{1118}; P{w^{+mC} =Rh1inGS}2-3/CyO*
Q*UAS-Luc*	BDSC 64773	*3R:11808359 (*CIC-a*)	*y^{1} w*; M{$w^{[+mC}$=QUAS-Ppyr\LUC.G}ZH-86Fb*
Rh1-QF2 (2)	this study	*2L: 12507855 (*bun*)	*w^{1118}; P{w^{+mC}=ninaEp-QF2}/CyO*
Rh1-QF2 (3-1)	this study	*3L: 14205383 (*nuf*)	*w^{1118};; P{w^{+mC}=ninaEp-QF2}*
Rh1-QF2 (3-2)	this study	*3L: 20895359 (*Sfp77F*)	*w^{1118};; P{w^{+mC}=ninaEp-QF2}*
Rh1-QF2 (3-3)	This study	*3L: 14076958 (*bt1*)	*w^{1118};; P{w^{+mC}=ninaEp-QF2}/TM3, Sb*

Here, we focused on developing Gal4 drivers that were specific to outer photoreceptors but had varied expression levels compared to the existing *Rh1-Gal4* drivers. To do this, we used two fragments of the *ninaE* promoter that had previously been shown to control photoreceptor-specific expression but at much lower levels than that of the full-length region[34]. The smaller fragment (sRh1) consists of 189 bp of the *ninaE* promoter (3R:19888134-19888322, *ninaE* -120/+67) and the larger fragment (mRh1) consists of 512 bp (3R: 19888145-19888656), *ninaE* -450/+62) (Figure 1A). These two *ninaE* fragments, termed *small (s)* and *medium (m),* control Gal4 expression using the Integrase Swappable In vivo Targeting Element (INSITE) system[19]. INSITE allows for the Gal4 activator to be swapped out for other activators from an established library of activator donor plasmids using a system of Cre-Lox and phi31C recombination, all while maintaining the regulatory element. Thus, the *sRh1-Gal4* and *mRh1-Gal4* drivers described in this study can be readily crossed with other flies to generate Gal80, -QF or -LexA drivers, as necessary[35].

Next, we developed inducible Gal4 drivers for eye specific expression. An inducible *GMR-GSGal4* driver had previously been developed[36] and is available from the BDSC. Gene-switch Gal4 (GSGal4) contains the GMR regulatory elements, as described for *GMR-Gal4* above, that control expression of a fusion protein consisting of a mutant human progesterone receptor, the DNA binding domain of GAL4, and the activating domain of herpes simplex VP16 (GSGal4)[9]. Upon feeding flies with RU486 (mifepristone), GSGal4 is activated and results in the expression of target genes under control of the UAS regulatory element[17,37]. *GMR-GSGal4* expression is reported to be specific to the eye and ocelli in adult flies[25]. We created *Rh1-GSGal4* driver lines for outer photoreceptor specific inducible expression using the GSGal4 fusion protein under the control of a 3.8 kb fragment of the promoter (3R:19890993- 19888031) and 3' (3R: 19886438-19885743) regulatory elements of *ninaE* (Figure 1).

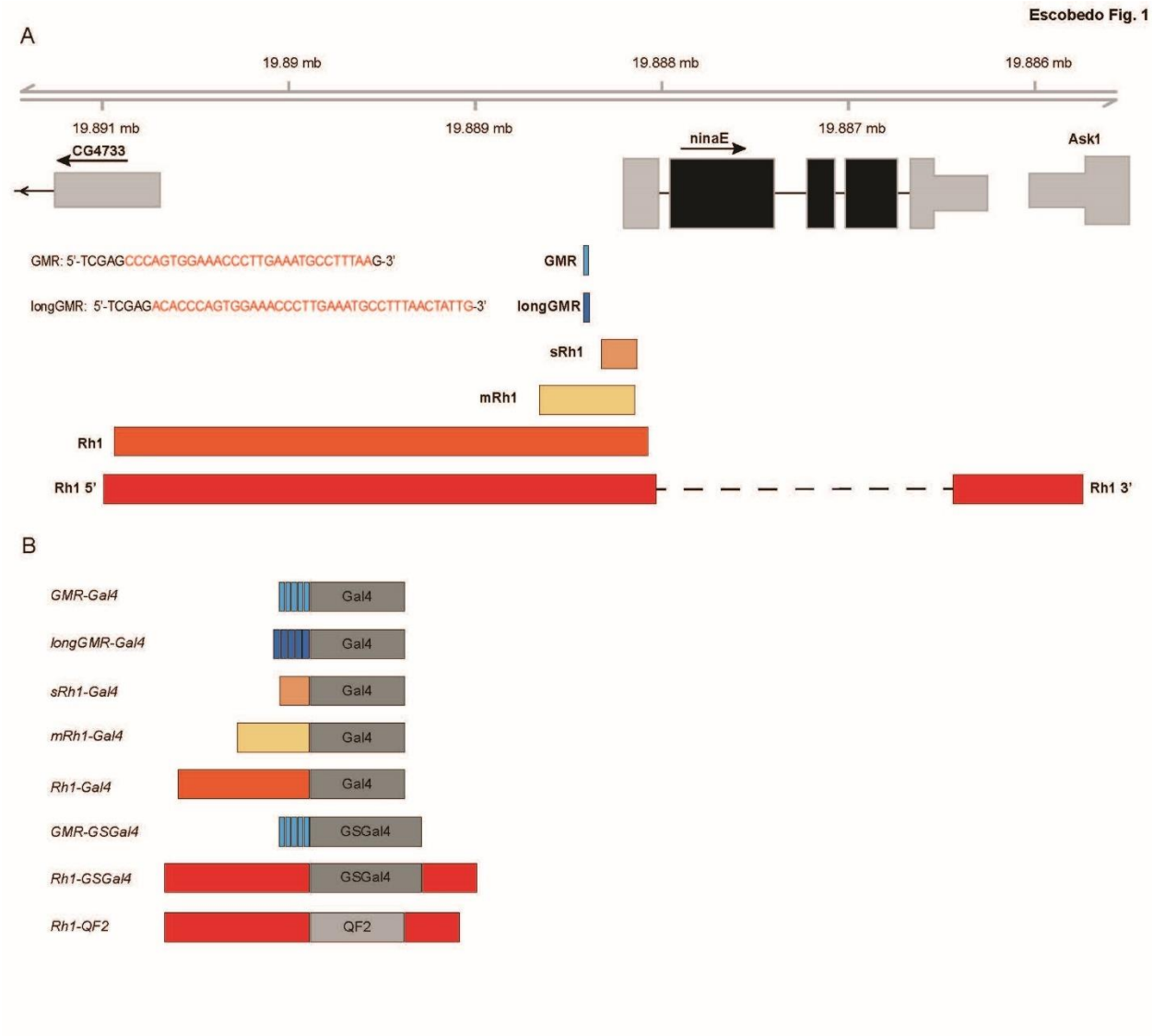

Figure 2-1. Overview of the *ninaE* regulatory regions used in the Gal4 and QF2 driver constructs. A) Schematic of the *ninaE* locus on chromosome 3 (3R:19,888,206) showing relative positions of the regulatory elements used in each of the driver constructs. Inset text shows the sequences of the Glass transcription factor binding site in the *ninaE* promoter that were pentamerized to generate the GMR or longGMR sequences. B) The different regulatory elements described in panel A drive expression of the Gal4, GSGal4 or QF2 drivers. The *sRh1-Gal4*, *mRh1-Gal4*, *Rh1-GSGal4* and *Rh1-QF2* drivers were generated in this study, and compared with the *Rh1-Gal4*, *GMR-Gal4* and *longGMR-Gal4* drivers available from the Bloomington Drosophila Stock Center.

Last, we generated QF2 drivers expressed in outer photoreceptors to provide an alternative binary expression system to Gal4. To generate *Rh1-QF2* driver lines, we placed the QF2 gene under the control of the same 3.8 kb fragment containing the 5' and 3' regulatory elements of *ninaE* used for *Rh1-GSGal4* (Figure 1). We used targeted ΦC31 integration for the *sRh1-Gal4* and *mRh1-Gal4* drivers to generate lines on chromosomes 3 and 2, respectively[38] (Table 2). We then used *P*-element integration to generate multiple lines for both the *Rh1-GSGal4* and *Rh1-QF2* drivers on different chromosomes. We selected at least one line on each of the chromosomes 2 and 3 for follow-up characterization of each driver, and determined the insertion position of each transgene using inverse PCR (Table 2). In addition, since the insertion position for the *GMR-Gal4*, *GMR-GSGal4*, *longGMR-Gal4* and *Rh1-Gal4* drivers had not previously been described and was not available on FlyBase, we also characterized the insertion position for each of these transgenes using inverse PCR (Table 2). As expected, all driver transgenes map to single insertion sites on the predicted chromosome. Importantly, no insertion sites mapped near genes that are involved in eye development or function.

Table 2.2. Plasmids generated in this study

Plasmid Name	Associated Fly stocks
pCaSpeR-ninaEp-QF2	*Rh1-QF2*
pCaSpeR-ninaEp-GeneswitchGal4	*Rh1-GSGal4*
pBMP-pRh1(-120/+67)-Gal4LWL	*sRh1-Gal4Rh1-Gal4*
pBMP-pRh1(-450/+62)-Gal4LWL	*mRh1-Gal4*

2.3.2 Characterization of driver expression pattern in the adult eye using a fluorescent reporter

Next, we examined the expression pattern of each of our newly generated drivers in the adult eye and compared this with the available *GMR-*, *longGMR-* and *Rh1-Gal4* drivers. To do this, we crossed each of the Gal4 and QF2 driver lines with *20XUAS-6XmCherry* (*UAS-mCherry*) or *10XQUAS-6XmCherry* (*QUAS-mCherry*) reporter lines, respectively, and examined the pattern

of red fluorescence in live 10-day old adult male eyes using confocal microscopy. Three independent flies were examined for each driver cross, and conclusions regarding cell-type expression were determined by evaluating the mCherry expression across the whole eye. Due to the curvature of the eye, the images presented show a progression from more distal outer ommatidial cells to the more proximal R cells along a center in radius. Likely due to the various levels of expression and therefore fluorescence intensity, differing laser strengths were used to image samples. Therefore, fluorescence intensity should only be compared between cells within the eye of a single fly, rather than between genotypes. To ensure that the higher laser strengths did not result in the misinterpretation of background signal, we have displayed our control lines (*UAS/QUAS-mCherry* alone) at the highest laser strength used. Using this approach, we observed *GMR-Gal4* driven mCherry expression in R1-R8 photoreceptors, as well as in the surrounding IOCs (Figure 2B). When we compared the mCherry expression pattern driven by *longGMR-Gal4* with *GMR-Gal4*, these were remarkably similar apart from the more obvious R cell patterning in *longGMR-Gal4*. In contrast to *GMR-Gal4* and *longGMR-Gal4*, the *Rh1-Gal4* driver resulted in mCherry expression specifically in R1 - R6 cells, as previously published, with no expression observed elsewhere in the eye (Figure 2B). Although the *ninaE* regulatory elements used to develop the *sRh1-Gal4* and *mRh1-Gal4* were originally described as photoreceptor-specific[34], these drivers show a broader expression profile in multiple cell types in the eye. The *sRh1-Gal4* driver resulted in distinct mCherry fluorescence in IOCs and relatively dim signal in photoreceptor cells. In contrast, the *mRh1-Gal4* driver had an mCherry expression profile closely resembling that of *Rh1-Gal4*, however, sparse mCherry fluorescence in IOCs was also present. Strikingly, the newly developed *Rh1-QF2* driver resulted in R1 - R6 photoreceptor specific mCherry expression, similar to that observed in the *Rh1-Gal4* driver (Figure 2C). Thus, the *Rh1-Gal4* and *Rh1-QF2* drivers are both specifically expressed in the outer photoreceptors R1 – R6, but not in other cells in the adult eye. Surprisingly, our newly developed *sRh1-Gal4* and *mRh1-Gal4*, although expressed in photoreceptors, are also expressed in other cells of the adult eye. Although the *longGMR-Gal4* driver was originally suggested to be more photoreceptor specific than *GMR-Gal4*, under our conditions, both *longGMR-Gal4* and *GMR-Gal4* show expression in multiple cell types in the adult eye including photoreceptors and the IOCs.

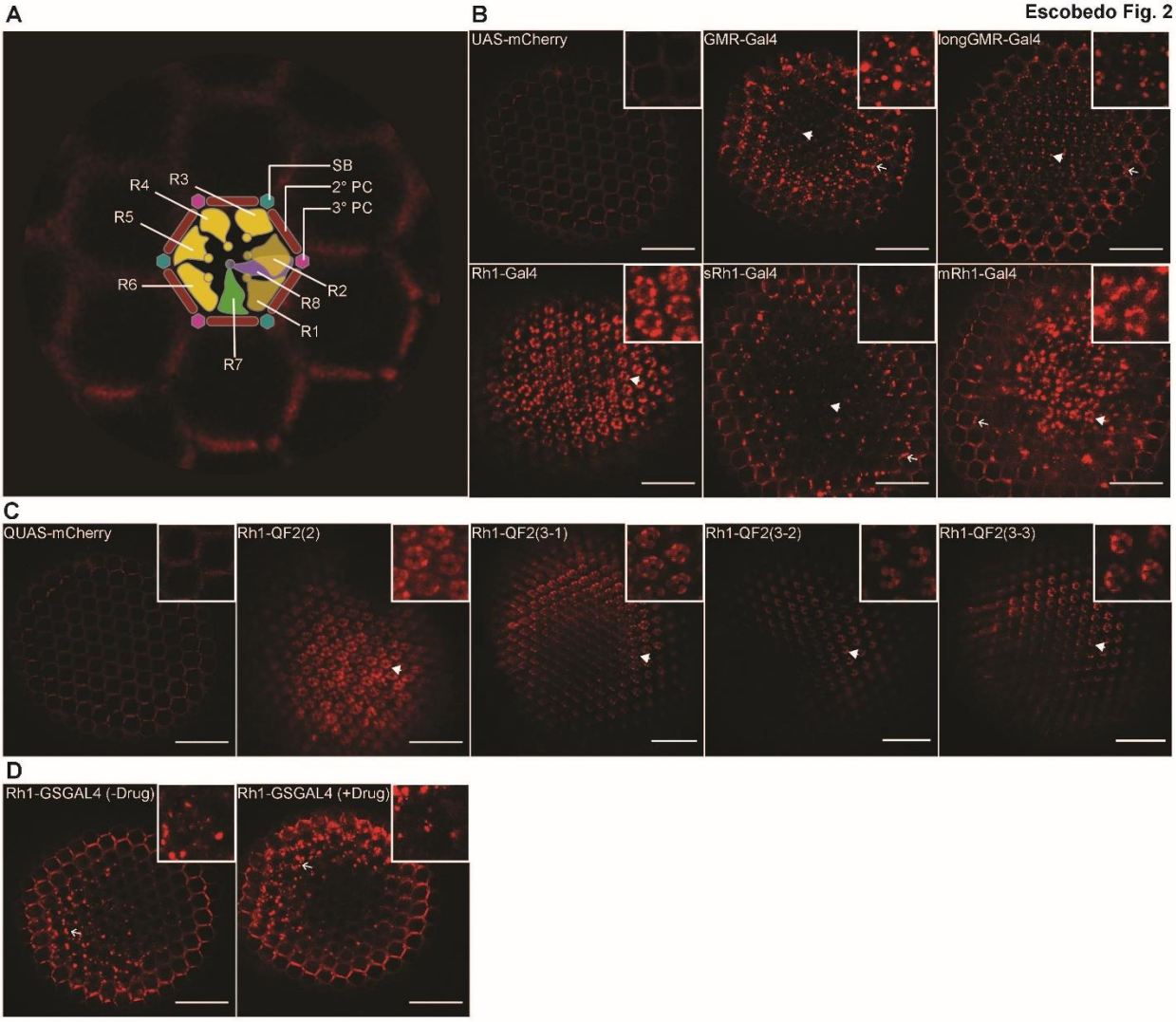

Figure 2-2. *Rh1* drivers are expressed specifically in adult photoreceptors, whereas *GMR*, *longGMR*, *sRh1* and *mRh1* drivers are expressed throughout the adult eye. The indicated Gal4 and QF2 driver lines were crossed to *UAS-mCherry* or *10XQUAS-QUAS-mCherry* flies, respectively, and confocal microscopy was conducted on 10-day old live adult male progeny. Representative images for each driver are shown (n = 3). Inset images show a magnified section of the eye. (A) Schematic depicting the location of cells in each ommatidium at a similar focal plane to that shown in each image. mCherry expression pattern for the (B) *GMR-Gal4*, *longGMR-Gal4*, *sRh1-Gal4*, *mRh1-Gal4*, and *Rh1-Gal4* drivers, relative to the *UAS-mCherry* control; (C) *Rh1-QF2* drivers and *QUAS-mCherry* control; (D) *GMR-GSGal4* + drug versus vehicle only control. Open and closed arrow heads point to interommatidial cells (IOCs) and R cells, respectively. Scale bar, 50 µm.

To test the cell specificity of the inducible GSGAL4 drivers, we used a similar approach by crossing GSGAL4 driver lines to *UAS-mCherry* and imaging 10-day old adult flies 24 hours after supplementing food with mifepristone. We observed *GMR-GSGal4* driven reporter fluorescence in all photoreceptor cells as well as in the pigment cells (Figure 2D). However, mCherry expression was also present in flies fed vehicle only, suggesting that GSGAL4 is also active independent of drug treatment in the eye (Figure 2D). Unfortunately, we were unable to detect reporter fluorescence in our *Rh1-GSGal4* lines, suggesting that the expression of, or induction by, this driver is below the limits of detection using the fluorescent reporter. Due to these results, we did not include the *GMR-GSGal4* or *Rh1-GSGal4* drivers in our developmental expression characterization (see next section).

2.3.3 Characterization of Gal4 and QF2 driver expression pattern during development

To further characterize these eye drivers, we sought to determine their expression patterns throughout different stages of fly development. Using the same genetic approach to evaluate the adult eye expression pattern, each driver line was crossed to the appropriate mCherry reporter. Late stage embryos (Figure 3), wandering third instar larvae (Figure 4), and late stage pupae (Figure 5) were then imaged using fluorescence microscopy to examine the expression pattern of each driver in various tissues at these three developmental stages. We imaged whole embryos and larvae to obtain a broad overview of the expression pattern of each driver in these developmental stages, and thus these images only provide general information about the expression pattern without the high spatial resolution like that obtained using the confocal imaging (Fig. 2). Similar to imaging conducted on the adult eye, differing laser strengths were used between drivers and developmental stages. As such, mCherry fluorescence intensity should only be evaluated for expression pattern, and not as a readout for expression level between driver lines. The relative expression level between drivers was evaluated in adult heads using a quantitative luciferase assay, which will be described in the next section (see Figure 6).

In embryos, we observed fluorescence for several of the eye drivers.*GMR-Gal4* had mCherry expression in the Bolwig's organ and Ring gland (Figure 3A), while *longGMR-Gal4* mCherry expression also appeared in the Bolwig's organ, as well as all major regions of the central nervous system, which include the central brain, optic lobes and ventral nerve cord (Figure 3A). Interesting, both the *sRh1-Gal4* and *mRh1-Gal4* drivers showed mCherry expression in the sensory

neurons of the peripheral nervous system (Figure 3A). In contrast, we did not detect mCherry expression in either the *Rh1-Gal4* or *Rh1-QF2* drivers (Figure 3A, B). Thus, four of the drivers designed for expression in the developing and/or adult eye also show expression in late stage embryos*: GMR-Gal4, longGMR-Gal4, sRh1-Gal4,* and *mRh1-Gal4*.

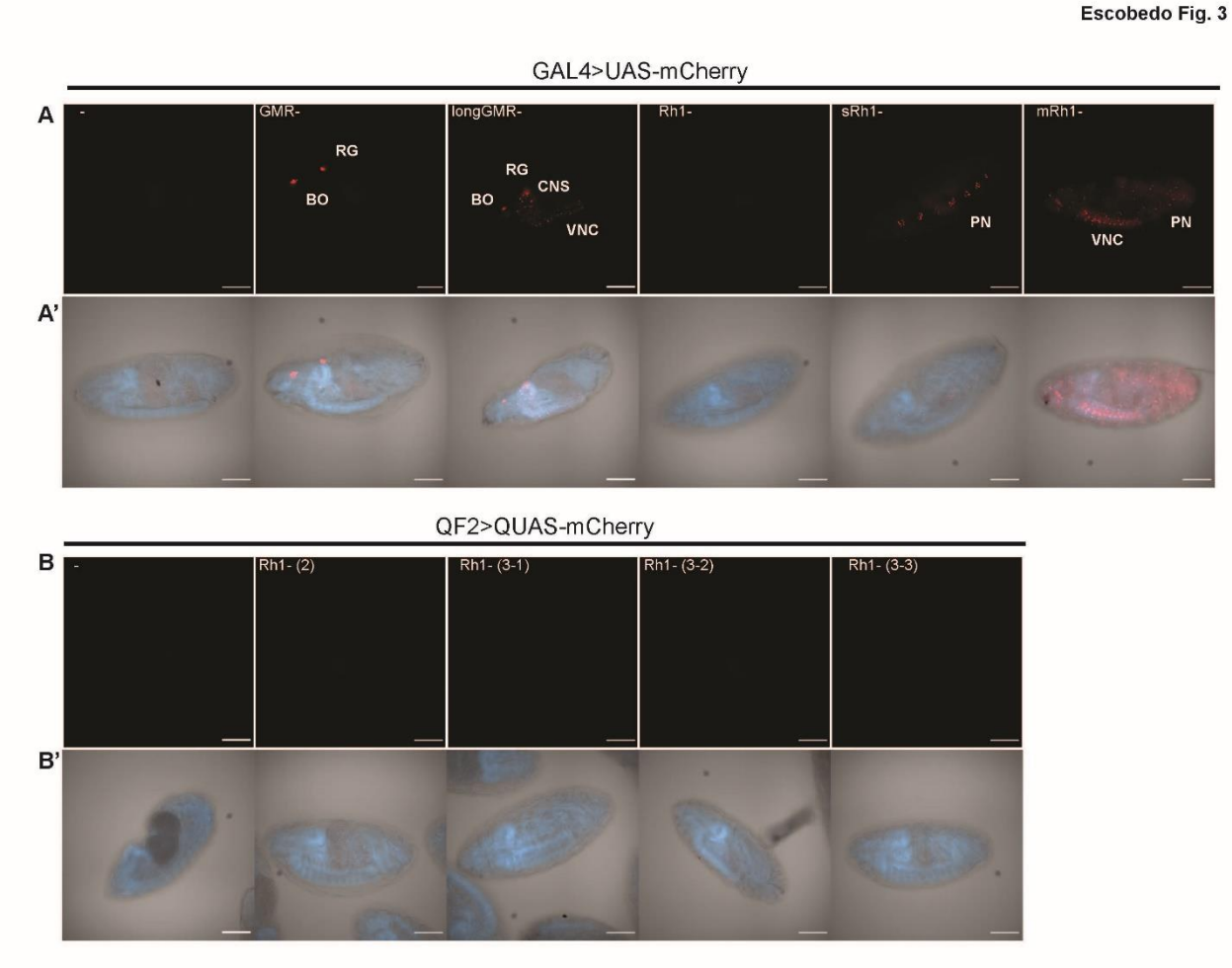

Figure 2-3. *GMR*, *longGMR*, *sRh1* and *mRh1* drivers are expressed in embryonic tissue, whereas *Rh1* drivers are not. The indicated GAL4 and QF2 driver lines were crossed to *UAS-mCherry* or *QUAS-mCherry* flies, respectively, and fluorescent microscopy was conducted on late stage embryos. (A, B) mCherry and (A', B') merged mCherry, DAPI and transmitted light (TL) images for (A, A') *GMR-Gal4, longGMR-Gal4, sRh1-Gal4, mRh1-Gal4, Rh1-Gal4, UAS-mCherry* control and (B, B') *Rh1-QF2* drivers and *QUAS-mCherry* control. Abbreviations for labeled tissues are as follows: (CNS) central nervous system; (VNC) ventral nerve cord; (PN) peripheral nervous system; (BO) Bolwig's organ; (RG) ring gland. Scale bar, 100 µm.

We next characterized the pattern of mCherry expression controlled by each driver in whole mounted wandering third instar larvae (Figure 4). *GMR-Gal4* resulted in mCherry expression in the eye antennal imaginal disc behind the propagating wave of the morphogenic furrow that begins to pattern the developing eye, in the optic stalk and optic lobe growth cones, as well as the trachea. *LongGMR-Gal4* resulted in mCherry expression in the salivary glands, tissue around the cephaloskeleton (mouth parts) and central nervous system (data for central nervous system not shown but available from PURR; see Data Availability). Interestingly, *sRh1-Gal4* also resulted in mCherry expression in salivary glands, which was so strong that salivary glands appeared violet in color under the dissecting scope (data not shown). *mRh1-Gal4* mCherry expression appeared in the ventral nerve cord and was also visible in the axonal projections and external sensory neurons of the peripheral nervous system. Similar to embryos, we did not observe any detectable mCherry expression driven by either the *Rh1-Gal4* driver or any of the *Rh1-QF2* drivers. Thus, as in embryos, *GMR-Gal4, longGMR-Gal4, sRh1-Gal4,* and *mRh1-Gal4* show expression patterns in additional larval tissues that are not related to eye development.

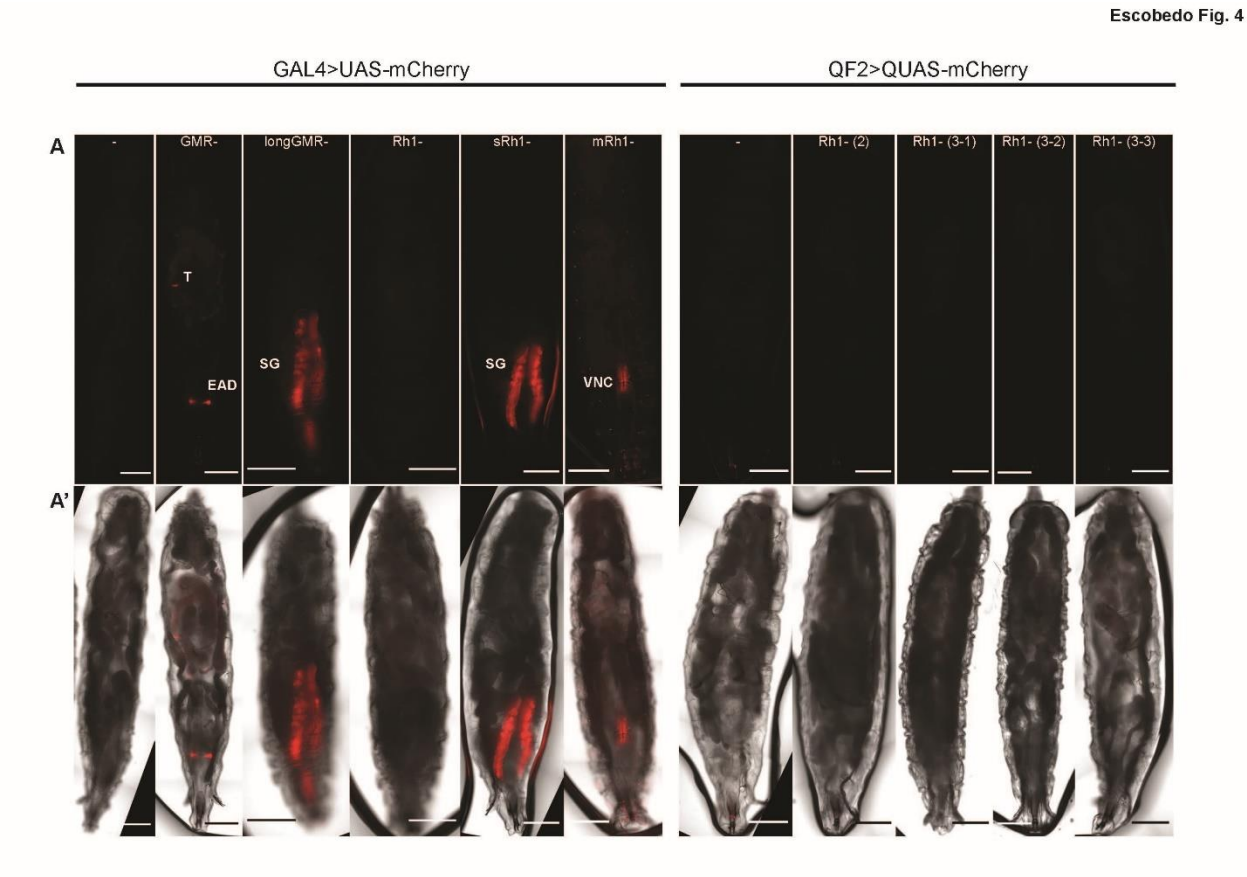

Figure 2-4. *GMR*, *longGMR*, *sRh1* and *mRh1* drivers are expressed in various larval tissues, whereas *Rh1* drivers have no detectable expression. The indicated GAL4 and QF2 driver lines were crossed to *UAS-mCherry* or *QUAS-mCherry* flies, respectively, and fluorescent microscopy was conducted on wandering third instar larvae. (A) mCherry and (A') merged mCherry, DAPI and transmitted light (TL) images for (A) *UAS-mCherry* control, *GMR-Gal4*, *longGMR-Gal4*, *sRh1-Gal4*, *mRh1-Gal4*, *Rh1-Gal4*, *QUAS-mCherry* control, and *Rh1-QF2* drivers. Abbreviations for labeled tissues are as follows: (VNC) ventral nerve cord; (PN) Peripheral nervous system; (EAD) eye antennal disc; (SG) salivary glands; (T) tracheal system; Scale bar, 500 µm.

Last, we investigated the expression pattern of these drivers in late stage pupal heads in which all cells of the eye have been terminally differentiated. These images provide data on the expression pattern in the eye, and within other tissues in the head including the brain. Using this approach, we observed strong mCherry expression in the eye and ocelli of *GMR-Gal4* and *longGMR-Gal4* drivers (additional data for ocelli is available in original z-stack images in PURR; see Data Availability) (Figure 5). *LongGMR-Gal4* also resulted in expression in small groups of cells in the mouth parts. We also observed expression of mCherry in the eyes of *sRh1-Gal4* flies, as well as in various regions of the antenna and mouth parts. *mRh1-Gal4* also resulted in mCherry expression in cells of the eye, as well as the lamina and central brain. As expected, *Rh1-QF2* drivers resulted in mCherry expression in eyes, without detectable expression in other regions of the head. Although some mCherry signal appears in the brain and punctae around the mouth parts in these images, comparison of all biological replicates with the QUAS control (-QF2) indicates that the weak signal is due to background from the QUAS transgene. Surprisingly, we could not detect fluorescence in the eye using the *Rh1-Gal4* driver, although confocal images in live flies confirmed that *Rh1-Gal4* drives expression in outer photoreceptors (Figure 2). The lack of detection of *Rh1-Gal4* may reflect its relatively low expression level (~5-fold lower than *sRh1-Gal4* in head extracts) when compared with the other drivers in this study (see below). Although we cannot exclude the possibility that *Rh1-Gal4* or the other drivers are expressed in other cells in the head, or indeed in other tissues during development, this expression level is below the detection of the fluorescent reporter used in our assays.

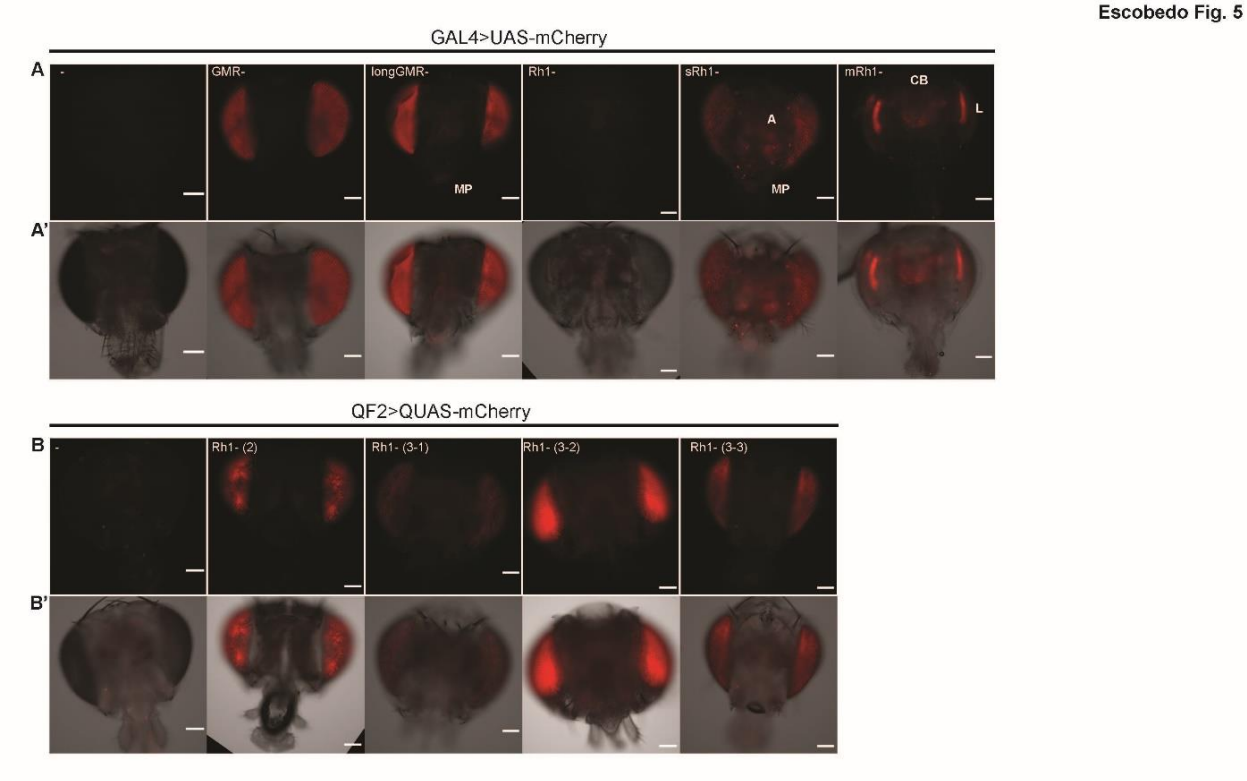

Figure 2-5.*GMR, longGMR* and *Rh1* drivers are expressed eye-specifically, while *sRh1* and *mRh1* are expressed elsewhere in the late stage pupal head and brain. The indicated GAL4 and QF2 driver lines were crossed to *UAS-mCherry* or *QUAS-mCherry* flies, respectively, and fluorescent microscopy was conducted on dissected late stage pupal heads. (A, B) mCherry and (A', B') merged mCherry and transmitted light (TL) images for (A, A') *GMR-Gal4*, *longGMR-Gal4*, *sRh1-Gal4*, *mRh1-Gal4, Rh1-Gal4*, *UAS-mCherry* control, and (B, B') *Rh1-QF2* drivers and *QUAS-mCherry* control. Abbreviations for labeled tissues are as follows: (CB) central brain; (L) lamina; (A) antenna; (MP) mouth parts. Scale bar, 100 µm.

2.3.4 Characterization of driver expression levels in the adult head

We next sought to characterize the relative expression level of each of the newly generated drivers in the adult eye, as compared with the currently available eye specific drivers. To do this, we crossed the Gal4 and QF2 driver lines with *UAS-Luc* and Q*UAS-Luc* respectively and performed luciferase assays on whole head extracts of 10-day old male flies. Because we used whole head extracts for these quantitative luciferase assays, these data represent the sum of expression in all cell types within the adult head including both the eye and brain. Using this approach, *GMR-Gal4* and *longGMR-Gal4* showed the highest luciferase activity of all the eye drivers (Figure 6A). Our *sRh1-Gal4* and *mRh1-Gal4* resulted in a 5- and 20-fold higher luciferase

activity than the full length *Rh1-Gal4* driver, respectively (Figure 6B). Since we observed expression of the *sRh1-Gal4* and *mRh1-Gal4* drivers elsewhere in the adult head, these data cannot be compared directly with *Rh1-Gal4* to determine relative photoreceptor expression. However, all three of these drivers were expressed at least an order of magnitude lower than *GMR-Gal4* and *longGMR-Gal4* (see y axis scale differences between Figure 6A and Figure 6B-C). We note that the insertion site of *Rh1-Gal4* is approximately 5 kb from the nearest gene, suggesting that position effects could account for the lower levels of driver activity than expected relative to the *sRh1-Gal4* and *mRh1-Gal4* drivers, which were generated by ΦC31 integrase-mediated transformation. We also characterized multiple independently transformed *Rh1-QF2* lines (different integration sites on chromosomes 2 and 3), all of which resulted in similar luciferase activity (Figure 6C). Unexpectedly, the expression levels of these drivers are nearly 30-fold higher than the *Rh1-Gal4* driver, suggesting that the *Rh1-QF2* driver provides a robust tool for inducing high levels of transgene expression specifically in the outer photoreceptors of the adult eye. This *Rh1-QF2* driver contains additional 3' regulatory elements (see Figure 1), which might also increase the expression of this driver relative to *Rh1-Gal4*.

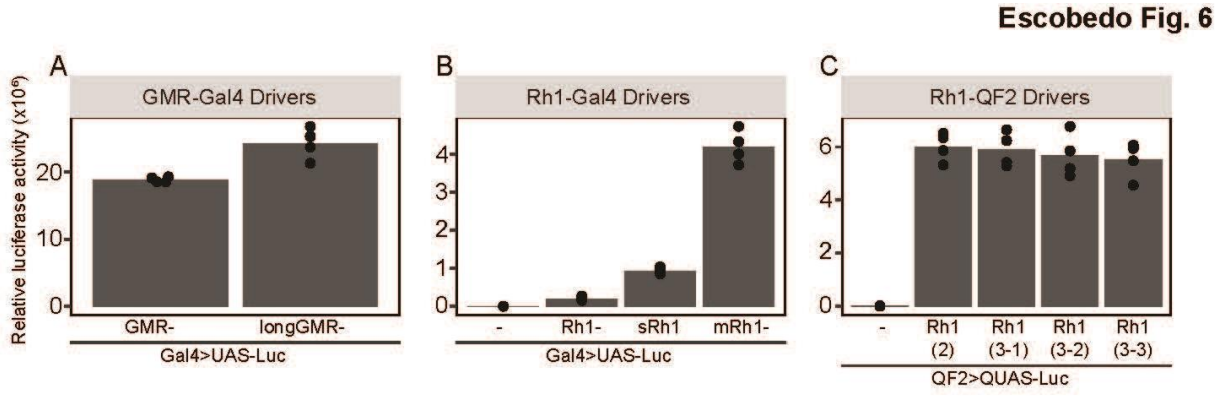

Figure 2-6.Gal4 drivers expressed in multiple cell types induce higher expression levels relative to photoreceptor-specific Gal4 or QF2 drivers. The indicated eye- or photoreceptor-specific driver lines were crossed to flies containing *UAS-Luc* (Q*UAS-Luc* for QF2 drivers), and luciferase activity was assayed in heads from adult male progeny expressing *UAS-Luc* under control of the indicated driver at 10 days post-eclosion. Data are shown as bar plots of means with individual biological replicates overlaid as dots (n = 4, 2 heads/experiment). Luciferase activity for the (A) *GMR-Gal4*, *longGMR-Gal4*; (B) *Rh1-Gal4*, *sRh1-Gal4*, and *mRh1-Gal4* compared to *UAS-Luc* alone; (C) photoreceptor-specific *Rh1-QF2* drivers on chromosomes 2 or 3, compared to *QUAS-Luc* alone.

Last, to characterize the expression levels of our GSGal4 drivers we first established the drug feeding conditions for maximal transgene induction. To do this we crossed *GMR-GSGal4* with *UAS-Luc* flies and fed seven-day old adult progeny for either 24, 48 or 72 hours and then performed luciferase activity assays from head extracts. We observed maximum luciferase activity at 24 hours, with a slight decrease in luciferase activity after longer duration feedings (Figure 7A). We next compared the *GMR-GSGal4* driver with our *Rh1-GSGal4* driver. Both drivers were crossed to *UAS-Luc* and nine-day old adult progeny were fed drug for 24 hours followed by luciferase activity assays. Although all GSGal4 driver lines had statistically significant induction when treated with drug compared to vehicle control, luciferase activity in the *Rh1-GSGal4* lines was 7- to 8-fold lower than that of the *GMR-GSGal4* line, which itself is approximately 3-fold lower than *Rh1-Gal4,* and more than 300-fold lower than either *GMR-Gal4* or *longGMR-Gal4* (Figure 7B).

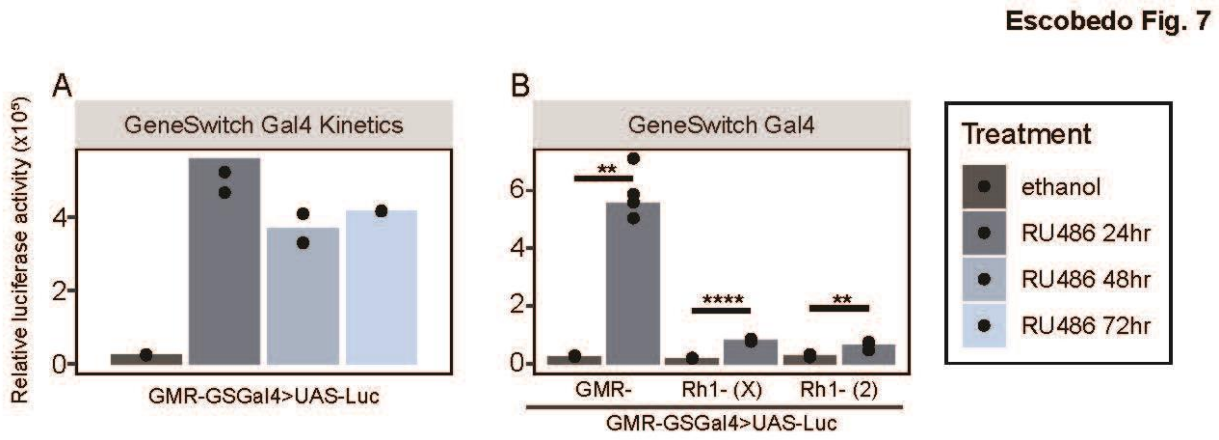

Figure 2-7.Gene Switch drivers induce gene expression weakly in the adult eye. (A) *GMR-GSGal4* flies were crossed to *UAS-Luc* flies and seven-day old adult progeny were fed food supplemented with RU486 or vehicle only for 24, 48, 72 hours followed by luciferase activity assays on heads to establish maximum GSGal4 induction. Data are shown as bar plots of means with individual biological replicates overlaid as dots (n = 2, 2 heads/experiment) (B) *GMR-GSGAL4* and *Rh1-GSGal4* flies crossed to *UAS-Luc* flies and resulting nine-day old progeny were fed food supplemented with RU486 for 24 hours or vehicle only followed by luciferase activity assays on heads. Data are shown as bar plots of means with individual biological replicates overlaid as dots (n = 4, 2 heads/experiment). *p*-value (**<0.005, ****<0.00005), Students *t*-test.

2.4 Discussion

In this study, we characterized the expression and cell specificity of both previously available and newly created *Drosophila* eye- and photoreceptor-specific drivers with the goal of assembling a binary expression toolkit for adult *Drosophila* eye expression. We compared several of the available Gal4 drivers from the BDSC for expression in the eye (*GMR-Gal4*, *Long-GMR-Gal4* and *Rh1-Gal4*), with Gal4 drivers generated by our lab (*sRh1-Gal4*, *mRh1-Gal4*, *Rh1-QF2*). Although many of these drivers have been best characterized in terms of their expression patterns in the developing and/or adult eye, all, except for *Rh1-Gal4* and *Rh1-QF2*, had expression in additional cell types. Specifically, *GMR-Gal4* expression was detected in the embryo Bolwig's organ and ring gland, as well as the trachea of third instar larvae. To our knowledge, we are the first to identify *GMR-Gal4* expression in the late embryo ring gland, while previous reports have also noted the expression in the Bolwig's organ and larval trachea[13]. Interestingly, we did not detect the previously described expression of *GMR-Gal4* in the central nervous system of larvae[13] or in the wing and leg imaginal discs[26].This may be due to the limitations of our imaging technique, where the high mCherry fluorescence in specific tissues masks the weaker mCherry fluorescence in more lowly expressing tissues. Intriguingly, a previous report also showed that two *GMR-Gal4* lines with different integration sites have slight differences in expression pattern[13], suggesting that the local chromatin landscape or the expression level of *GMR-Gal4* may also play a role in its expression pattern. Similar to *GMR-Gal4*, *longGMR-Gal4* resulted in high levels of expression in all cells of the adult eye. As the initial report noted, the expression of *longGMR-Gal4* appears to be more photoreceptor specific as seen by the higher relative mCherry expression in the R cells of this driver when compared to other cells in the eye[30]. Unlike *GMR-Gal4*, *longGMR-Gal4* lacks characterization for expression outside of the adult eye. We report broad developmental expression similar to *GMR-Gal4* with some marked differences; *longGMR-Gal4* lacked the larval trachea expression of *GMR-Gal4* but showed strong expression in larval salivary glands and mouth parts as well as in the central nervous system of embryos. However, due to the strong mCherry expression driven by *longGMR-Gal4* in salivary glands, expression in the eye-antennal imaginal disc is likely masked in our imaging of the whole larvae. Future dissections of *GMR-Gal4* and *longGMR-Gal4* larvae could further characterize the developmental expression pattern of these drivers using this strong mCherry reporter. Thus, while *GMR-Gal4* and *longGMR-Gal4* provide

suitable tools for expressing transgenes broadly throughout the adult eye, caution should be used in attributing their effects to expression in particular cell types.

Because we also observed broad expression patterns for *sRh1-Gal4* and *mRh1-Gal4* drivers in the adult eye, pupal head and other larval and embryonic tissues, while *Rh1-Gal4* is specific to the R1-R6 cells in the adult eye, we suspect that a complex group of regulatory elements in the *ninaE* promoter contribute to its outer photoreceptor specific expression. Both the *sRh1-Gal4* and *mRh1-Gal4* include the TATA box and another short regulatory element named the Rhodopsin Conserved Sequence I (RCSI). This element has been shown to bind the Pax6 proteins eyeless (ey) and twin of eyeless (toy)[39,40], as well as the homeodomain protein Pph13[41]. Together, these two sequence elements have been shown to be necessary for the general photoreceptor specificity of all *rh* genes[34,42,43]. Therefore, we were surprised to find much broader expression profiles for the *sRh1-Gal4* and *mRh1-Gal4* drivers than expected. Moreover, *sRh1-Gal4* and *mRh1-Gal4* have multiple differences in expression throughout development and in the adult head and eye. For example, *mRh1-Gal4* has more obvious photoreceptor expression in the adult eye compared to *sRh1-Gal4*. This and other expression differences likely result from the 300 nucleotides of additional upstream *ninaE* enhancer contained within *mRh1-Gal4* , which also includes the entirety of the *gl* binding site. Multiple conserved elements in the *ninaE* promoter remain uncharacterized[40], which upon additional testing may yield promising eye and photoreceptor specific drivers of various expression levels. Further, neither *sRh1-Gal4* nor *mRh1-Gal4* results in obvious rough eye phenotypes in homozygous flies. This is unlike the more highly expressed *GMR-Gal4* driver, which has a rough eye phenotype in homozygous flies or in heterozygous flies reared in temperatures exceeding 25ºC[44], making these drivers appealing alternatives for expressing transgenes broadly in the adult eye.

In this study, we incorporated the Q-system into our expanding toolkit of eye drivers. *Rh1-QF2* to our knowledge is the first characterized photoreceptor-specific QF2 driver. Surprisingly, *Rh1-QF2* activates photoreceptor specific expression nearly 30-fold higher than that of the currently available *Rh1-Gal4* driver. While *Rh1-Gal4* uses a 3 kb fragment of the *ninaE* promoter as its regulatory element, *Rh1-QF2* includes both the 5’ and 3' regulatory elements, suggesting that the 3' regulatory element may be important for high expression level. *Rh1-QF2* opens the door to an exciting alternative to the currently available Gal4/UAS based expression systems because of the many advantages the Q-system offers. Additional optimization of the temporal regulation of

eye-specific QF2 drivers as well as the integration of both Gal4 and QF2 drivers will further expand the utility of these systems for complex eye specific expression.

To allow for inducible photoreceptor-specific expression we created a *Rh1-GSGal4* driver and compared its temporal induction in adult eyes with that of a currently available *GMR-GSGal4* driver. We showed that both *Rh1-GSGal4* and *GMR-GSGal4* induced significant expression of the luciferase reporter upon RU feeding. However, *Rh1-GSGal4* driven expression of our mCherry reporter assay was under the detection limit of our microscopy analysis, and while drug induced *GMR-GSGal4* resulted in mCherry fluorescence, mCherry was also detected in the vehicle only control. Therefore, while we and others have reported *GMR-GSGal4* induced expression in the adult eye, it appears that limitations may exist for robust GSGal4 activation in particular cell types in this tissue, such as photoreceptors.

In this study, we have systematically characterized various binary expression system drivers. We have summarized our findings for the expression patterns of these drivers throughout development (Figure 8A) as well as their expression patterns in the adult eye and expression levels in the adult head (Figure 8B). This allows for the straightforward comparison of each driver's relative expression and cell specificity. Together, these fly stocks represent a useful binary expression toolkit for adult *Drosophila* eye expression.

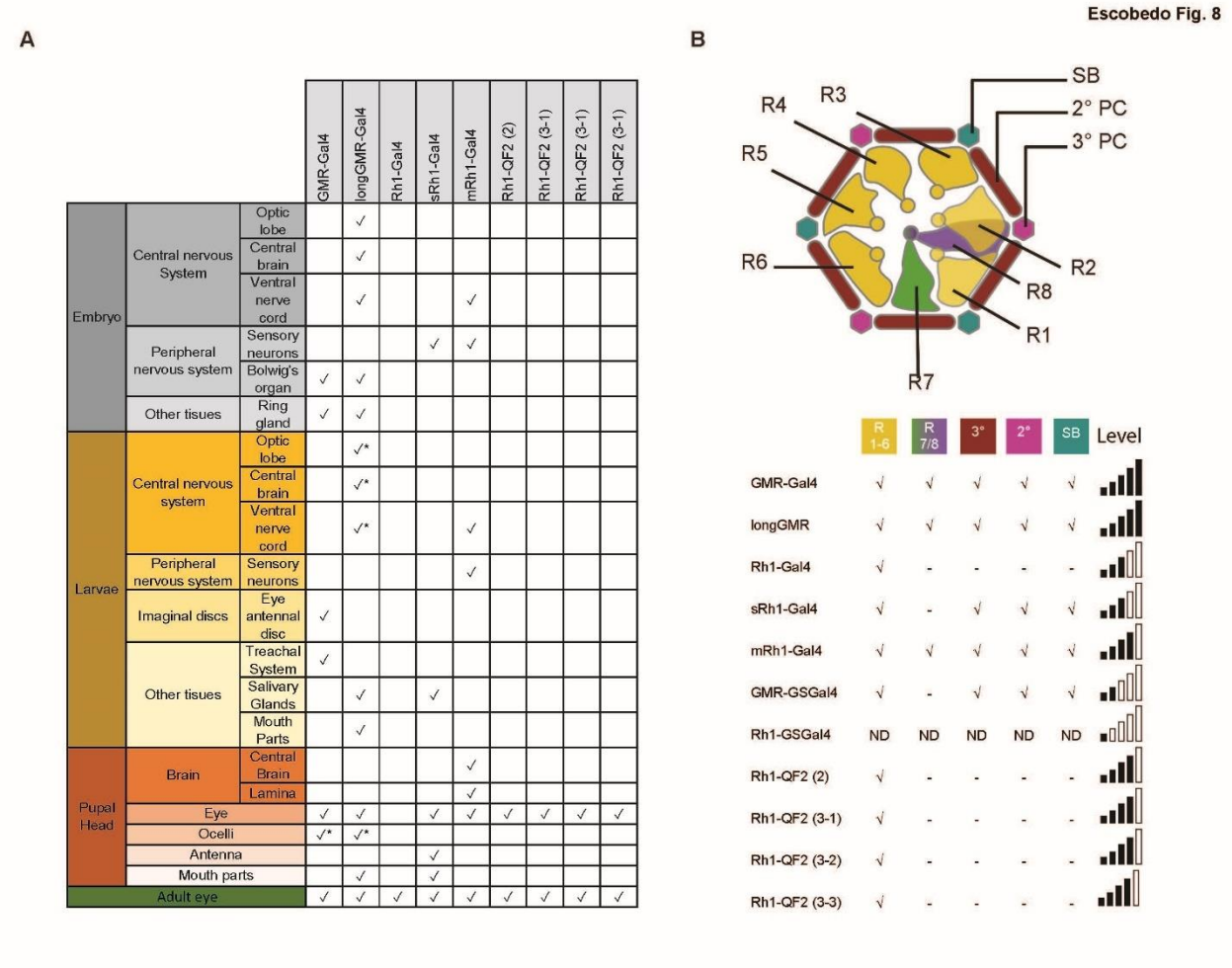

Figure 2-8.Overview of Drosophila Gal4 and QF2 drivers for fine-tuned eye- and photoreceptor-specific expression. (A) Summary table describing each driver's expression pattern in embryo, wandering third instar larvae, pupal heads, and adult eyes. (√*) indicates expression patterns from data not shown in the figures of this manuscript but acquired in these data sets publicly available from the associated Purdue University Research Repository (PURR) website (see Data Availability). (B) Schematic of an adult *Drosophila* ommatidium cross section color coded by cell type; yellow, R1 – R6 photoreceptor cells; green, R7 photoreceptor cell; purple, R8 photoreceptor cell; red, secondary pigment cells; pink, tertiary pigment cells; blue, sensory bristles. The key displays each driver's cell-specific expression and is defined as follows: (√), expression; (-), no expression; (ND), not defined. The relative expression between drivers assessed by luciferase activity from head extracts is shown to the right using a scale of one (low) to five (high) bars.

CHAPTER 3. AGING AND LIGHT STRESS RESULT IN OVERLAPPING AND UNIQUE GENE EXPRESSION CHANGES IN PHOTORECEPTORS

Declaration of collaborative work
The work described in this chapter was the collaborative effort of Spencer Escobedo, Sarah Stanhope, Ziyu Dong and Dr. Vikki Weake. Sarah Stanhope contributed to glutathione ratio analysis. Ziyu Dong assisted in fly aging and collection. All other experiments were performed by Spencer Escobedo. Spencer Escobedo and Dr. Vikki Weake wrote the manuscript with editorial feedback from the other authors.

3.1 Introduction

Aging is characterized by a decline in organismal function. The free radical theory of aging[45], and more broadly characterized damage-based theories[46], suggest that the accumulation of oxidative damage, in combination with other sources, culminate in the decline of function and ultimate demise of an organism with advanced age. In the eye, visual function decreases with age in both humans and in model organisms such as *Drosophila melanogaster*[47–49]. This decrease in function is associated with physiological changes in multiple different cell types and structures in the eye, including the cornea[50], vitreous[51] and retina[52–54]. In addition, age is a major risk-factor for many eye-associated diseases, such as cataract, age-related macular degeneration, glaucoma, and retinopathy[55]. There is also a strong environmental risk component to age-associated eye disease with factors such as diet, smoking, and sunlight exposure contributing to higher risk[56–58]. Understanding how aging and environmental stress impact specific cell types in the eye will help provide insight into how these factors interact and lead to onset of age-associated ocular disease.

Although light is essential for vision, it also represents a considerable stress to cells in the eye. Photoreceptors, the primary light-sensing neurons in the eye, respond to light through the absorption of a photon by the molecule retinal contained within the G-coupled protein receptor Rhodopsin[59,60]. This process is highly conserved between *Drosophila* and humans, with rhodopsin activating the G-protein transducin, which leads to the downstream phototransduction cascade[59]. In flies, but not in vertebrates, Rhodopsin can be directly converted back to its inactive state within a single photoreceptor cell[61,62]. In outer photoreceptors (R1 – R6 cells), blue light activates Rhodopsin 1 (Rh1) forming metaRhodopsin 1 (mRh1), which can be converted back to Rh1 through the absorption of orange light present in the spectra of normal white light[62,63]. Thus, in

flies, prolonged exposure to blue light in the absence of other wavelengths results in constitutive activation of the phototransduction pathway. This overactivation of the phototransduction cascade results in excessive endocytosis of mRh1 and prolonged calcium influx into the photoreceptor that eventually results in its death[64–68]. We previously showed that the retinal degeneration caused by blue light exposure in *Drosophila* is caused by an increase in oxidative stress, particularly lipid peroxidation, that results from calcium excitotoxicity[64]. In aging flies, blue light exposure also increases markers of oxidative stress and decreases lifespan[69]. Thus, in *Drosophila*, blue light exposure provides a unique model in which to assess the impact of oxidative stress on the eye, with potential implications for aging within the organism.

During aging, there are changes in gene expression that lead to defined transcriptomic signatures that include aspects unique to particular tissues[70]. For example, distinct age-associated transcriptional signatures are present in specific cell types in the eye including the human retina[71,72] and *Drosophila* photoreceptors[48]. In addition, we previously profiled the photoreceptor transcriptome of young flies exposed to blue light[73]. These studies identified some similarities in the functional categories of genes that were differentially regulated during aging or under blue light stress, but the different ages, genotypes, and eye color of the flies used confounded direct comparison of these datasets. Here, we determine the photoreceptor transcriptome in a single white eyed fly strain during aging or after blue light exposure, allowing us to directly compare the gene expression changes upon either condition. We identify common gene expression signatures between light stress and aging suggesting that light stress is a major contributor to the aging photoreceptor transcriptome. However, we also observe unique gene expression signatures in aging photoreceptors, indicating that other factors also contribute to the transcriptional changes that occur in these aging cells independent of light. Unexpectedly, we also identify overexpression of an enzyme that counteracts oxidative stress in the white eyed flies used in this study. We find that this genetic background is protected against retinal degeneration induced by blue light or aging, suggesting that increasing oxidative stress is the primary cause of photoreceptor degeneration under both conditions.

3.2 Materials and Methods

3.2.1 Fly stocks, husbandry, and blue light stress

All experiments were conducted with male *Rh1-GFP^{KASH}* flies in a *cn bw* background to deplete eye pigment[74]; these flies have white eyes. Two independent lines were used: *w^{1118}; cn bw; P{w^{+mC}=Rh1-GFP-Msp300KASH}3-1* or *w^{1118}; cn bw; P{w^{+mC}=Rh1-GFP-Msp300KASH}3-2*. To generate these fly stocks, the GFP-Msp300KASH cassette was excised from the pUASTattB-GFP-Msp300KASH vector[75] (Addgene #170806) using EcoRI and XbaI, and directionally cloned into pCaSpeR-ninaEp-GeneswitchGal4[76] digested with the same enzymes to remove the GeneswitchGal4 cassette. Transgenic flies carrying Rh1-GFP^{KASH} were generated by *P*-element mediated transformation into the *w^{1118}* strain. The chromosomal insertion site for *Rh1-GFP^{KASH}* flies on chromosome 3 (line 3-1) was mapped using inverse PCR to 3L: 18,822,623, in the 5' untranslated region (UTR) of the gene *Catalase*. Flies were raised on cornmeal agar food (6.07 g agar type 2, 32 g sugar, 50 g yeast, 50 g cornmeal, 3.2 g methyl paraben for preservation in 1.3L water) at 25ºC and 65-75% humidity under a 12:12 light:dark cycle. The wavelength spectrum in the incubator was measured using a BLACK-Comet UV-VIS Spectrometer (StellarNet model #BLK-C) (Figure S1). Age-matched flies were collected on the first day after eclosion (day one; D1), and aged as described, transferring to fresh food every 2-3 days. All blue light experiments were conducted during the light cycle using a custom designed light stimulator[64]. Vials containing up to 50 day five (D5) flies were exposed to blue light ($\lambda = 465$ nm) at 8000 lux (2 mW/cm^2) for either three, five, or eight hours (h). For RNA-seq, flies were immediately flash frozen in liquid nitrogen post exposure. For phalloidin staining, flies were moved to a dark box in a 25ºC incubator and aged for seven days prior to processing.

3.2.2 Retina staining and analysis

Fly eyes were cut using microdissection scissors in phosphate buffered saline (PBS) with added detergent and fixative (0.3% Triton-X 100, 4% formaldehyde), leaving the corneal lens attached. Dissected eyes were then trimmed to remove excess brain tissue and cuticle, and fixed for a total of 20 minutes. Eyes were rinsed in PBST (0.1% Triton X-100) briefly, then transferred to 200 µL of PBST (0.1% Triton X-100,) containing 1:50 Phalloidin 598 (ThermoFisher, #A12381) in a 0.5 ml microcentrifuge tube and incubated with rocking overnight at 4ºC. Following this, eyes

were washed three times for five minutes each in 200 µL of PBST (0.1% Triton X-100). Eyes were then equilibrated in VectaShield (Vector Laboratories, #H100010) for 15 minutes and mounted lens side up on bridged slides using two #0 coverslips as bridges with a #1.5 coverslip. Samples were stored in the dark at 4ºC for up to 1 week prior to imaging. Confocal fluorescence microscopy was conducted with a Zeiss LSM780 confocal microscope using a Zeiss Plan-Apochromat 20x/.8 objective. Five biological replicates were imaged per condition. To quantify rhabdomere degeneration, all in-focus ommatidia in a single focal plane were scored for the presence of all seven visible rhabdomeres. Scores are shown as a percentage of intact rhabdomeres.

3.2.3 Nuclei immunoprecipitation and RNA-seq

R1-R6 photoreceptor-specific, GFP-labeled nuclei immunoprecipitation was conducted as previously described[77]. Between 150 and 250 male flies were used per sample, and three biological replicates were conducted for all RNA-seq experiments. Following nuclei immunoprecipitation, bead-bound nuclei were lysed in 300 µl of TRIzol (Zymo, Cat # R2050) and RNA was extracted using the Direct-zol RNA MicroPrep kit (Zymo, Cat # R2050) with DNase I treatment. RNA-seq libraries were constructed using the Universal RNA-Seq Library Preparation Kit with *Drosophila* specific rRNA depletion (Tecan Genomics, Cat# 0520-A01) using 10 ng of RNA to generate each library. Libraries were sequenced (150 bp, PE) using the Illumina HiSeq 4000 platform (Novogene). Between 40-80 million reads were obtained per sample.

3.2.4 Bioinformatics

RNA-seq reads were trimmed using Trimmomatic[78] (v0.39) to remove low quality reads >36 bp. High quality paired and unpaired reads were then aligned to the *Drosophila* genome (*Drosophila_melanogaster.BDGP6.28*) using HISAT2[79] (v2.1.0). BAM files were generated and sorted using Samtools[80] (v1.8), and count files obtained using HTseq[81](v0.13.5). Counts were filtered to remove lowly expressed genes (counts per million (cpm) > 10 in all samples), and normalized using the RUVs approach (k=2) from RUVSeq[82](v1.24.0), to obtain normalized cpms for 7929 expressed genes. Differential gene expression was performed using edgeR[83] (v3.32.1). Heatmaps of normalized expression (cpm) were generated using pheatmap[84] (v1.0.12). Enriched GO terms were identified and compared between samples using ClusterProfiler[85,86] (v3.18.1).

Hypergeometric testing (Fisher's exact tests) of significant pairwise intersections was conducted using SuperExactTest[87] (v1.0.7). Cnetplots were generated using ClusterProfiler. All plots were generated using R (v. 4.0.5) using custom scripts.

3.2.5 RT-qPCR from whole heads

Whole heads were dissected from five adult male flies, and RNA was extracted using Trizol, followed by Zymoprep Direct-zol RNA MicroPrep kit (Zymo Research) with DNAase I treatment. cDNA was generated from 100 ng of RNA using Episcript Reverse Transcriptase (Epicentre) and random hexamer primers. RT-qPCR was conducted as pre-viously described44. Catalase gene expression was normalized to the geometric mean of two reference genes (RpL32, eIF1a). Primers are listed in Table S5. Statistical significance was determined using Student's T-test.

3.2.6 Glutathione redox ratios in dissected eyes

Oxidized (GSSG) and reduced (GSH) glutathione levels were quantified in 25 dissected eyes per sample as described previously[88].

3.3 Results

3.3.1 Age and blue light exposure induce global changes in the photoreceptor transcriptome

We previously showed that prolonged exposure to blue light (8h) induces retinal de-generation in young (day six, D6) white-eyed flies46. Retinal degeneration in flies is first apparent through the loss of the photoreceptor rhabdomere, which in most cases is followed by the degeneration of the remainder of the neuron47. Because other studies have also observed premature retinal degeneration in white-eyed flies (w1118) that were not ex-posed to any light stress48, we sought to compare gene expression changes in flies exposed to light stress with flies undergoing normal aging. To examine the photoreceptor transcriptome, we used flies that express GFPKASH, which localizes to the outer nuclear mem-brane enabling immunoprecipitation of tagged nuclei31,33. GFPKASH was expressed directly under control of the ninaE (Rh1) regulatory

elements, which target expression specifically in the adult outer photoreceptors R1 – R6. To generate white-eyed flies, which are sensitized to blue light stress49, we crossed Rh1-GFPKASH into a cn bw background, which depletes eye pigment30.

Next, we examined the photoreceptor transcriptome of flies exposed to light stress and compared this with normal aging. To do this, we exposed young D5 flies to blue light of varying durations (3, 5, or 8h), or aged flies under standard 12:12 light:dark conditions to D5, D15, or D30, and isolated photoreceptor nuclei for RNA-seq under each condition (Figure 1A). We note that nuclear RNA provides a snapshot of actively transcribed RNA, rather than the steady-state mRNA levels in the cell that are measured using other RNA-seq approaches. To examine the differences between each condition, we performed principal component analysis (PCA) on the normalized counts (Figure 1B). The three bio-logical replicates grouped together for each condition by PCA, separating by age along PC1 (28.07% variation), and by blue light exposure along both the PC1 and PC2 axes. These data suggest that there are both overlapping and distinct changes in gene expression in response to blue light or during aging. We note that PC1 and PC2 only explain approximately 50% of the variation, and there is additional variation present particularly between the aging samples, which is more apparent when the relative gene expression is plotted for each sample (Figure 1C and 1D).

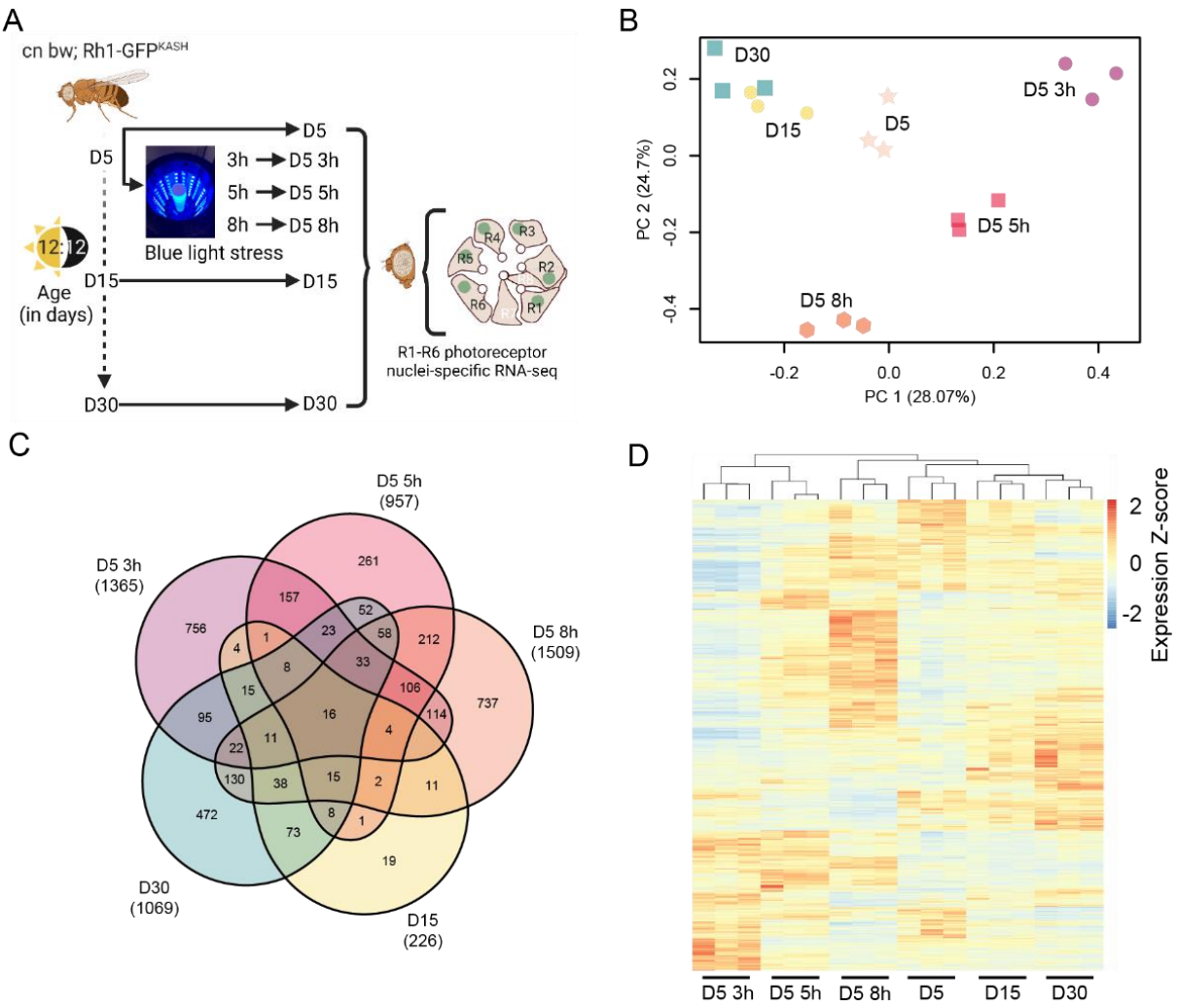

Figure 3-1.Global gene expression changes in white eyed flies with age or blue light exposure. (A) Overview of the experimental design for photoreceptor nuclei-specific RNA-seq from blue light exposed or aged flies. Male white eyed Rh1-GFPKASH flies at D5, D15 or D30, and D5 flies exposed to 3, 5, or 8h of blue light were collected and photoreceptor nuclei-specific RNA-seq performed (n=3). (B) PCA analysis of aged or blue light exposed flies. (C) Venn diagram of the differentially expressed genes in aged or blue light exposed flies identified relative to D5 untreated. The total number of significantly differentially expressed genes is shown under each sample name in brackets. (D) Hierarchical clustering of all differentially expressed genes in aged or blue light exposed flies. Normalized expression (Z-scores) were calculated for each gene (row).

To identify the genes with differential expression during aging or blue light exposure, we compared all conditions to the D5 untreated samples. Using this approach, we identified 1365, 957, and 1509 significantly differentially expressed genes (FDR < 0.05) in flies exposed to 3, 5, or 8h blue light, respectively (Table S1). We identified fewer genes that were differentially expressed

during aging at D15 (226 genes), but this number increased to 1069 genes by D30 (Table S1). We then compared differentially expressed gene sets between all the conditions, and found that there were substantial overlapping sets of genes between many of the pair-wise comparisons (Figure 3.1 C). Additionally, we identified 663 genes that were differentially expressed in three or more conditions (Figure 3.1 C), suggesting that light stress and aging have some overlapping effects on the photoreceptor transcriptome. To further compare the global differences in gene expression, we first compiled a list of all 3453 genes that were differentially expressed in at least one condition. We then generated a heatmap showing the relative expression of each gene across all samples, clustering both samples and genes, and normalizing expression by row (gene) to highlight differences between the conditions (Figure 3.1 D). Samples clustered together using this approach, similar to the PCA, and higher order clustering revealed similarities between the aging samples (D15 and D30) and the longest blue light exposure (8h) (Figure 3.1 D). However, there remain substantial differences between blue light and aging even at the longest blue light exposures, suggesting that there are distinct gene expression changes under both conditions. We conclude that shorter durations of exposure to blue light induce gene expression changes that may be more specific to light stress, whereas longer blue light exposure mimics aging.

3.3.2 Stress-response genes are upregulated upon blue light exposure or aging, while behavioral and neuronal-specific genes are downregulated

Next, we examined the functional classes of genes that were differentially expressed during blue light exposure or aging. To do this, we first separated differentially expressed genes into those that were upregulated (increased expression upon blue light exposure or older age) or downregulated (decreased expression in either condition). We then performed Gene Ontology (GO) term analysis, and compared the GO terms identified for each group to identify overlapping or similar functional sets of genes. In Figure 3.2, we show all significantly enriched GO terms (FDR < 0.05) for either upregulated (Figure 3.2 A) or downregulated (Figure 3.2 B) gene sets for each condition using dot plots, highlighting both shared and unique GO terms between blue light and aging conditions. Full annotated lists of all GO terms are provided in Table S2. We did not identify any significantly enriched GO terms in the upregulated genes at 3h blue light. However, there were substantial overlaps between blue light and aging GO terms in the upregulated genes, particularly

upon 8h blue light exposure for functions such as DNA repair, DNA metabolic process, and cell cycle (Figure 3.2 A).

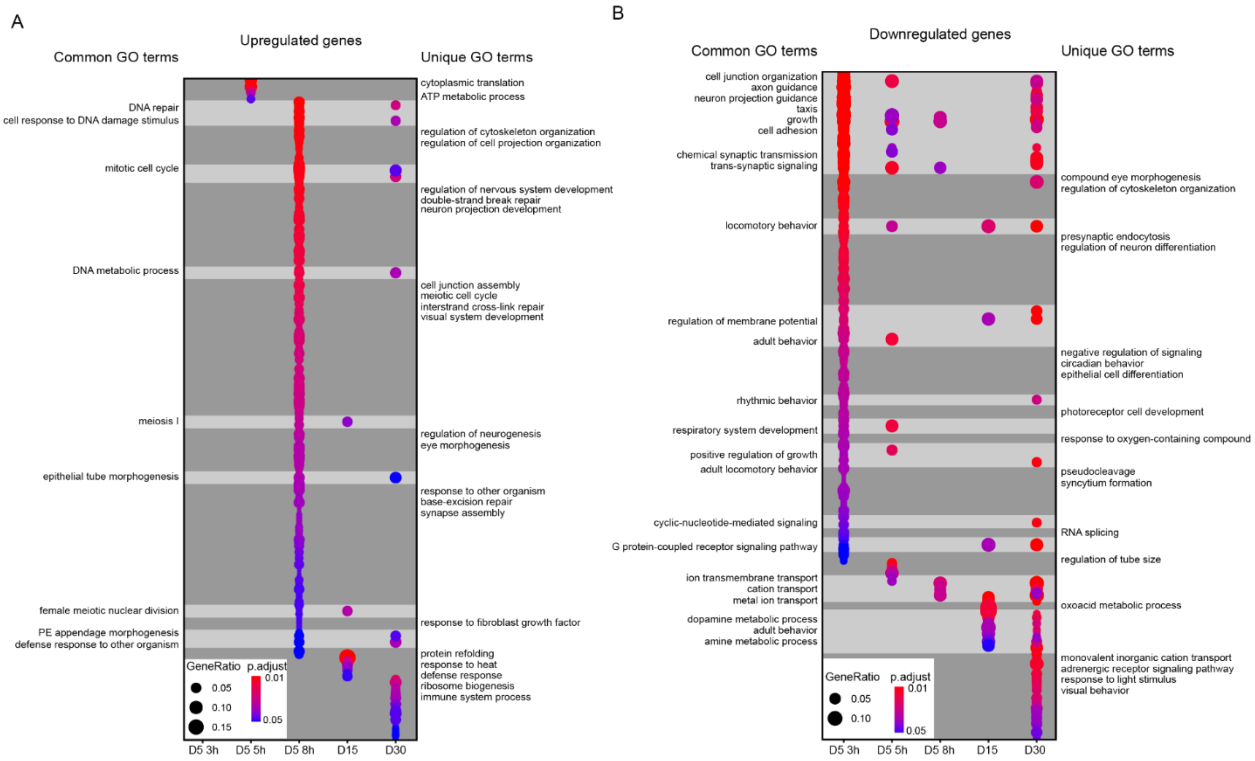

Figure 3-2. Significantly enriched GO terms for upregulated or downregulated genes. Dot plots of all enriched Gene Ontology (GO) terms for upregulated (A) or downregulated (B) genes in aged or blue light exposed flies relative to D5. Plots are shaded to highlight common (light grey) and unique (dark grey) GO terms between samples. Select GO terms of interest are annotated. A full list of GO terms is provided in Table S2.

In contrast, aging samples were uniquely enriched for GO terms such as protein refolding and response to heat, whereas blue light uniquely enriched for GO terms associated with cell organization and development. When we examined the downregulated genes, we observed a larger overlap between blue light and age enriched GO terms compared with the upregulated genes (Figure 3.2 B). GO terms such as axon guidance, trans-synaptic signaling, ion transport, and rhythmic behavior were common between blue light and aging in the downregulated genes. In contrast, blue light samples were uniquely enriched for GO terms such as eye morphogenesis, neuron differentiation and cell differentiation, while aging samples enriched for terms such as

visual behavior and adrenergic receptor signaling. These data suggest that during aging and blue light treatment, photoreceptors induce expression of stress response pathways and metabolic genes, while genes related to neuronal function are downregulated. However, we also observed many unique GO terms in blue light versus aging, again suggesting that there are distinctive gene regulatory pathways specific to each condition.

3.3.3 The flies used in this study are potentially resistant to light stress due to overexpression of Catalase in photoreceptors

We were surprised that there were no significantly enriched GO terms in the genes that were upregulated upon 3h of blue light exposure (Figure 3.2 A) because our previous analysis of gene expression in photoreceptors from similar aged flies exposed to blue light identified substantial enrichment of GO terms associated with stress response[73]. The enrichment of stress-response associated GO terms in Hall, Ma *et al.* 2018 was largely driven by the strong upregulation of *Heat shock* genes, so we directly compared the induction of these genes in both studies (Figure 3.3 A). In this comparison, the $\log_2$ fold change for each gene is determined relative to the appropriate control in each study (3h dark treatment for Hall, Ma *et al.* 2018 versus 0 h exposure in the current study). Unexpectedly, most of the stress response genes were not significantly induced in our study even though these were significantly upregulated in the previous study, despite the similarity in blue light treatment, age, and eye color of the flies used (Figure 3.3 A). Because the EGFP used in the GFP^{KASH} nuclear membrane tag absorbs blue light in the 440-500 nm range with a λ_{max} of 488 nm[89], we initially wondered if the high levels of GFP^{KASH} protein present in the photoreceptors might diminish the negative impact of blue light on photoreceptor survival in the aging white-eyed flies, as well as our blue light exposure, which has a λ_{max} of 465nm[64]. We note that the white LEDs present in the incubator used to raise these flies have a strong peak in the blue wavelengths (Figure S1), which is a common feature of commercially available white LEDs[90–92]. GFP-dependent photoprotection has been observed in reef coral experiencing high light stress[93–95]. However, since both white-eyed fly genotypes express photoreceptor-specific GFP, this is unlikely to underly the difference in sensitivity to blue light induced gene expression changes observed.

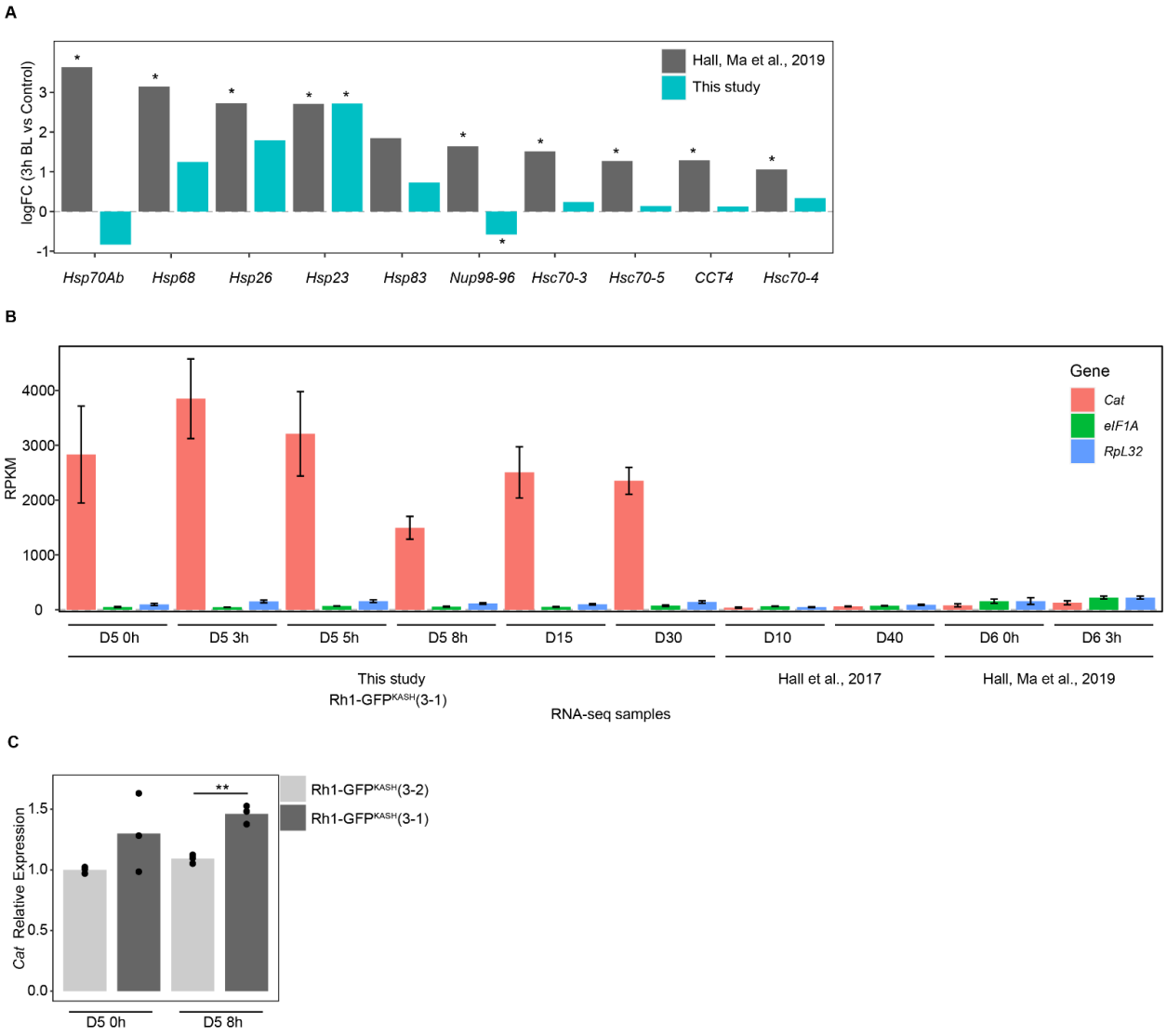

Figure 3-3. Overexpression of *Catalase* in *Rh1-GFP^{KASH}* flies correlates with lower induction of stress-response genes following blue light exposure. (A) $\log_2$ fold-change values for 3h blue light versus control for the indicated genes in Hall, Ma *et al.* 2018 versus this study. *, FDR < 0.05. (B) Relative expression (RPKM) of the indicated genes in samples from this study relative to Hall, Ma et al. 2018 and Hall *et al.* 2017. Panels A and B show nuclear transcript levels based on RNA-seq analysis. Age and/or blue light treatment indicated on *x* axis (D, days; h, blue light exposure time). Bars indicate mean ± SD. (C) Bar plots showing qPCR analysis of *Catalase* mRNA levels from male heads, representing steady-state transcript levels. Bars represent mean expression relative to reference genes with individual replicates overlaid as points.**, p-value < 0.005.

We next examined the genotype of the flies used in each study. In the previous study we used *cn bw; Rh1-Gal4>UAS-GFP^{KASH}* flies[73], but for this study we developed new more efficiently expressed GFP^{KASH} transgenes that were directly under control of Rh1 genomic regulatory elements. These lines were used because they had higher nuclear RNA yields using the nuclei immuno-enrichment approach, and were created by *P*-element mediated transformation, generating insertions on multiple chromosomes to facilitate various genetic experiments. We carefully tested a subset of these lines to ensure that there was no premature age-dependent retinal degeneration in pigmented (red eye) backgrounds because insertion of the transgene could have resulted in mutation of a gene that was necessary for photoreceptor survival (data not shown). When we examined the insertion site of the *Rh1-GFP^{KASH}* transgene used in the current study (referred to hereafter as line 3-1), we found that it was present near the 5' UTR of the *Catalase* gene. *Catalase* encodes an enzyme that reduces hydrogen peroxide (H_2O_2), counteracting oxidative stress, and is protective in aging models[96–98]. Since the *Rh1-GFP^{KASH} 3-1* flies are viable, and homozygous lines do not exhibit premature retinal degeneration, *Catalase* expression is unlikely to be disrupted in these flies. Instead, to our surprise, when we examined the expression level of *Catalase* in the RNA-seq analysis from the current study and compared this with previously published RNA-seq data using *Rh1-Gal4>UAS-GFP^{KASH}* flies, we observed substantially higher levels of *Catalase* expression in all the *Rh1-GFP^{KASH} 3-1* samples relative to *Rh1-Gal4>UAS-GFP^{KASH}* flies[48,73] (Figure 3.3 B). We note that all RNA-seq samples compared in Figure 3B consist of total ribo-depleted nuclear RNA. To examine the steady-state mRNA levels of *Catalase* expression in the *Rh1-GFP^{KASH} 3-1* flies, we performed qRT-PCR analysis in two independent third chromosome insertions of *Rh1-GFP^{KASH}*: lines 3-1 and 3-2, both in a *cn bw* background. We also observed significantly higher *Catalase* expression in line 3-1, which has the insertion in the 5' region of *Catalase*, relative to line 3-2, but not to that same extent as observed in the nuclear RNA measurements. We conclude that insertion of the very strong Rh1 genomic regulatory elements near the 5' UTR of *Catalase* results in potent induction of *Catalase* transcription in photoreceptor nuclei, which contributes to higher steady-state expression of *Catalase* mRNA. Thus, the white-eyed flies used in this study are likely protected against some of the oxidative stress associated with blue light or aging, and should be considered an ameliorated model with regards to reactive oxygen species (ROS) levels. However, stress response genes are induced in the Rh1-GFP^{KASH} flies at older time points (D15, D30) and upon longer blue light

exposures, suggesting that although these flies may be resistant at lower blue light exposures or earlier stages of aging, they do eventually experience the same types of gene expression changes observed in more sensitive models. We note that in some respects, these resistant flies provide advantages for studying gene expression changes associated with light stress versus aging because substantial retinal degeneration could interfere with our ability to obtain sufficient nuclear RNA and compare light stress and aging in the same flies.

3.3.4 Aging and light stress have unique and overlapping effects on gene expression in photoreceptors

To examine the common and distinct pathways regulated by blue light and aging in more detail, we next directly compared the differentially expressed gene sets between each condition for either the upregulated or downregulated genes. We compared these groups separately because we reasoned that the direction of change in expression should be the same under blue light exposure or aging if these genes have a shared biological function in either process. As suggested by the GO term analysis in Figure 3.2, we observed a high overlap between the upregulated genes in both age and blue light (Figure 3.4 A) that was significant for all pairwise comparisons (Figure 3.4 B).

Figure 3-4. Similar stress response genes are induced with age and blue light stress. (A) Venn diagram of the differentially upregulated genes in aged or blue light exposed flies relative to D5. (B) Statistical analysis for all pairwise comparisons of significantly upregulated genes in aging or blue light exposed conditions. Bar height represents the number of genes in each pairwise overlap (green dots). Bars are colored by p-values from fisher's exact test, with the null hypothesis being an overlap no greater than that expected by chance. Cnetplots representing the enriched GO terms and corresponding genes for the intersection between (C) 8h and D30 or (D) D15 and D30 upregulated genes.

Figure 3.4 continued

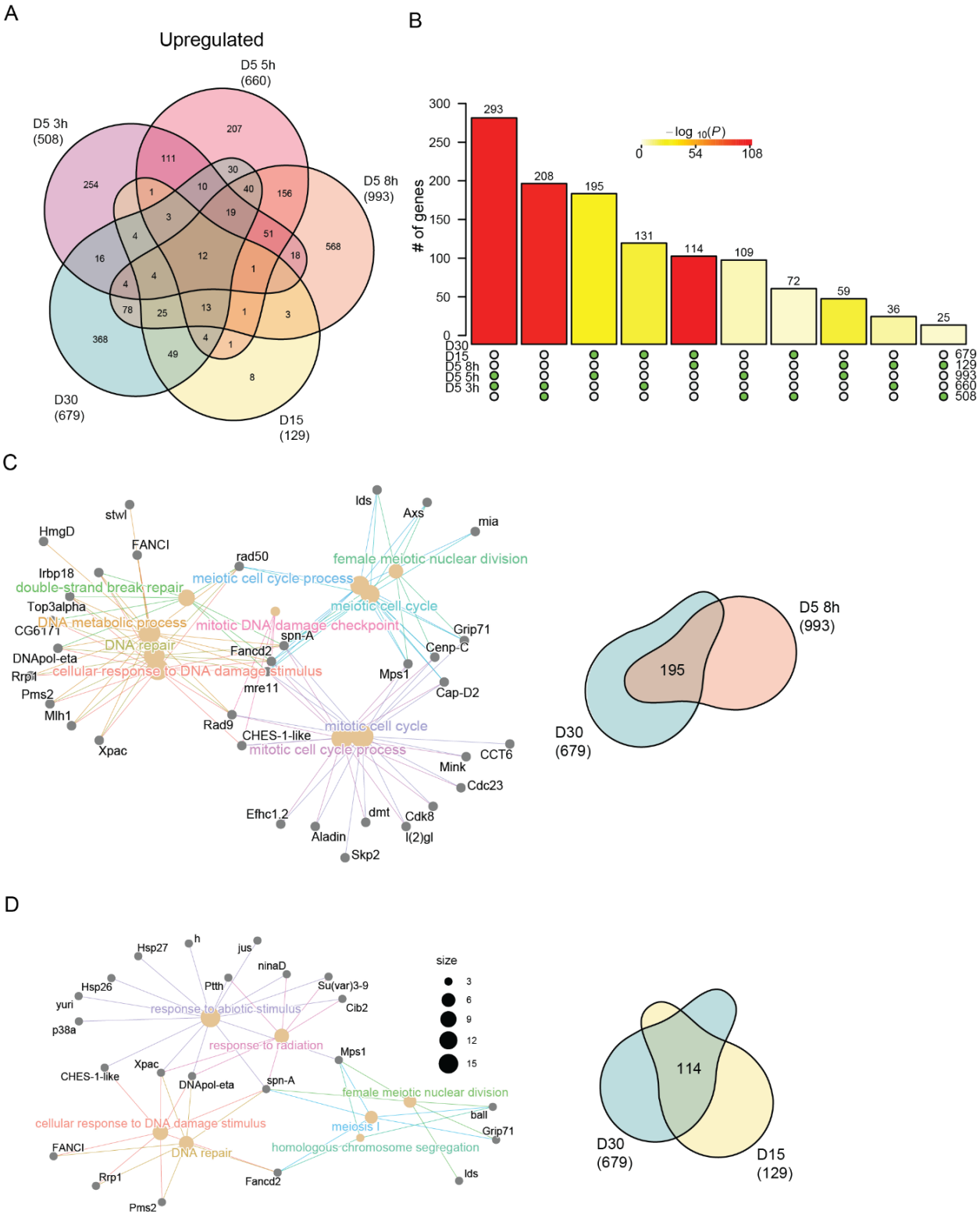

Although the pairwise comparisons between flies exposed to either blue light or during aging showed the most significant overlap (compare 3h vs 5h blue, or D15 vs D30), we also observed a highly significant overlap between 8h blue light and D30. To examine these overlaps in more detail, we generated cnetplots that illustrate the common differentially expressed genes that contribute to each of the enriched GO terms. The cnetplot generated from the commonly upregulated genes identified under 8h blue light and late aging (D30) revealed multiple GO terms related to DNA damage response and repair (Figure 3.4 C). These GO terms were driven by upregulation of genes such as *Xpac* and *Rrp1*, which encode proteins that recognize and catalyze steps in base excision repair. Similarly, *Rad50* and *mre11*, two other genes commonly upregulated in 8h of blue light and D30, encode the components of the DNA damage repair (DDR) complex involved in recognition and repair of double stranded breaks. We also observed GO terms not directly associated with the DNA damage response that were related to the cell cycle. Previous studies have identified the upregulation of cell cycle genes in post-mitotic neurons undergoing programmed cell death in both age related disease[99] or DNA damage models[100–102], suggesting the similar upregulation we observe in aged photoreceptors may also represent a neuronal cell death transcriptional signature. While blue light and aging share common upregulated genes, aging flies at D15 and D30 also exhibited shared upregulation of genes associated with DNA damage and stress response (Figure 3.4 D). Interestingly, many of the same genes commonly upregulated with age (Figure 3.4 D) were also identified in the overlap between 8h and D30 (Figure 3.4 C), suggesting that both blue light and aging induce similar upregulation of genes involved in the DNA damage response. Although a significant number of genes were differentially expressed in both 3h and D30 (85 genes), as well as 5h and D30 (54 genes), no GO terms were significantly enriched in these shared gene sets.

While significant overlaps exist between upregulated genes in aging and blue light exposed flies, many unique gene expression changes also occur under each condition. To explore the differences between age and blue light, we focused on the uniquely upregulated genes in either D30 (368 genes) or 8h blue light (568 genes) samples. GO term analysis of genes that were uniquely upregulated at D30 (age) enriched for processes involved in the defense and immune response, rRNA processing, ribosome biogenesis, and nucleoside metabolism (Table S3). The upregulation of immune and defense response pathways may signal that aging flies have an accumulation of pathogens[103,104], while the increase in ribosome biogenesis indicates a regulatory

feedback loop from the disruption or dysregulation in protein synthesis[105]. In contrast, 8h blue light resulted in the unique upregulation of a large number of genes involved in cellular organization, growth, neuronal projections, nucleotide excision repair (NER), and the negative regulation of response to stimulus (Table S3). For example *PKa-R1* and *Vps33B* are involved in suppressing the light response[106,107], suggest that photoreceptors induce expression of genes to directly counteract the overactivation of the phototransduction signaling cascade caused by blue light exposure, and that this response is not induced during aging.

We also observed a high overlap of downregulated genes between aging and blue light (Figure 3.5 A), which were significant for all pairwise comparisons (Figure 3.5 B). While the most significant pairwise comparisons were between blue light and aging conditions, the most significant overlap between blue light and age was between 8h and D30. The cnetplot of this overlapping gene set revealed genes associated with phototransduction such as *shakB* and *trpl*. (Figure 3.5 C). When we evaluated the overlap between D15 and D30, we identified genes associated with neurotransmitter signaling and behavior (Figure 3.5 D). For example, *Gabat* and *AANAT1* both encode enzymes that modify neurotransmitters involved in the regulation of sleep. Based on this, we conclude that extended blue light exposure (8h) induces similar changes in phototransduction genes as those in old D30 photoreceptors.

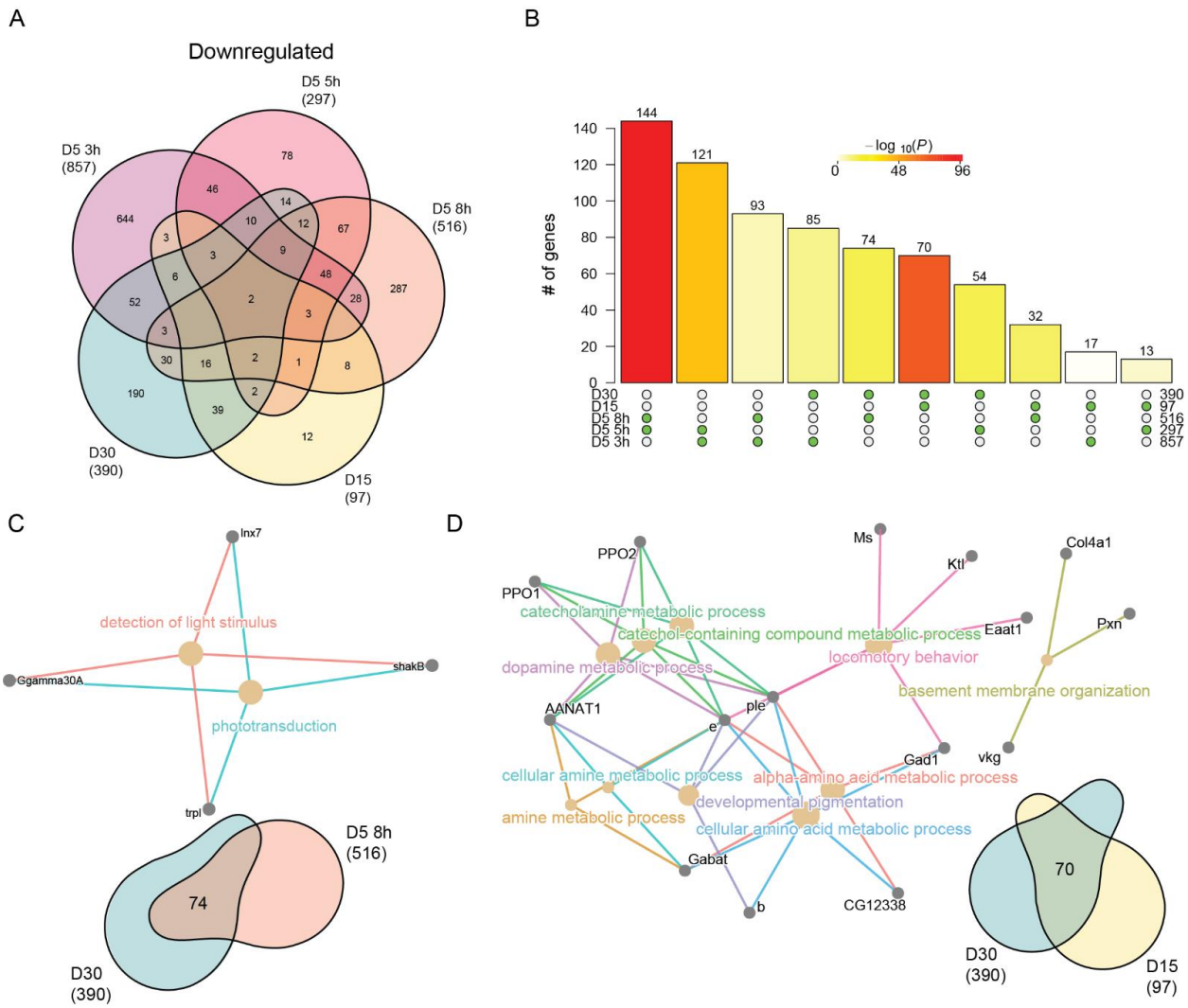

Figure 3-5. Neuronal specific genes are downregulated with age and blue light stress. (A) Venn diagram of the differentially downregulated genes in aged or blue light exposed flies relative to D5. (B) Statistical analysis for all pairwise comparisons of significantly downregulated genes in aging or blue light exposed conditions. Bar height represents the number of genes in each pairwise overlap (green dots). Bars are colored by p-values from fisher's exact test, with the null hypothesis being an overlap no greater than that expected by chance. Cnetplots representing the enriched GO terms and corresponding genes for the intersection between (C) 8h and D30 or (D) D15 and D30, as well as (E) uniquely downregulated genes at D30.

Last, we asked what unique processes were downregulated with age or blue light. We identified 190 and 287 unique downregulated genes in D30 and 8h blue light samples, respectively. Surprisingly, no GO terms were enriched in the uniquely downregulated genes upon 8h of blue light. However, downregulated genes specific to D30 enriched for functions related to cation and transmembrane ion transport (Table S4). Specifically, these genes encode multiple potassium channels, such as *KCNQ*, *kcc*, *CG3078*, and *Ork1*. Potassium transport is an important stabilizer of photoreceptor membrane potential[108,109], and the downregulation of these genes suggests that this process may become dysregulated in aging photoreceptors. Additionally, we observed age-specific downregulation of genes involved in ATP synthesis, such as *ATPsynb*, *blw*, and *VhaM9.7-a*. This suggests that that there might be a decrease in energy production in aging photoreceptors that is independent of light stress.

3.3.5 Catalase overexpression correlates with decreased retinal degeneration and oxidative stress levels

Because the white-eyed *Rh1-GFP^{KASH} 3-1* flies used in the current study exhibited high levels of *Catalase* expression in photoreceptors, and delayed gene expression responses relative to previous studies[73,88], we wondered if these flies would also be protected against the retinal degeneration induced by blue light exposure in white-eyed flies. Prolonged exposure to blue light (8h) induces retinal degeneration in young (day six, D6) white-eyed flies, although there are differences in severity between *w^{1118}* and *cn bw* genotypes[45]. We assessed retinal degeneration in our white-eyed *Rh1-GFP^{KASH} 3-1* flies during aging or light stress (see methods). To do this, we exposed young D5 flies to blue light of varying durations (3, 5, or 8h), or aged flies under standard 12:12 light:dark conditions to time points between D5 and D50 (D5, D15, D30, D50), and assessed retinal degeneration (rhabdomere loss) by staining retinas with phalloidin, which marks the actin-rich rhabdomeres in the photoreceptors (Figure 3.6A). Similar to our previous observations for white-eyed flies expressing GFP^{KASH} [29], shorter durations of blue light exposure (3 – 5h) did not induce substantial retinal degeneration (Figure 6B). Interestingly, prolonged blue light exposure (8h) also did not result in significant rhabdomere loss; however, multiple replicates showed a degeneration phenotype, albeit to a lesser extent than that observed previously in *w^{1118}* or *cn bw* flies that do not express GFP[45]. Moreover, in contrast to observations for *w^{1118}* flies, which show initial signs of retinal degeneration by D5 that progress to substantial rhabdomere loss at D15 and

D30[47], we did not observe significant retinal degeneration with age in the genotype used for this study (Figure 3.6C). However, similar to 8h blue light exposure, multiple D50 replicates of line 3-1 showed a retinal degeneration phenotype.

To test if the overexpression of *Catalase* in the *Rh1-GFP^{KASH} 3-1* flies correlated with protection from blue light-induced retinal degeneration, we assessed blue light-induced retinal degeneration in the *Rh1-GFP^{KASH} 3-2* flies that did not overexpress *Catalase* and in *w^{1118}* flies using an identical approach to that used for the 3-1 line. In contrast to line 3-1, we did observe significant rhabdomere loss in the *Rh1-GFP^{KASH} 3-2* line and in *w^{1118}* flies of the same age exposed to 8h blue light exposure, consistent with previous studies[20,45] (Figure 3.6B). These data indicate that photoreceptor overexpression of *Catalase* in the white-eyed flies used in the current study (line 3-1) correlates with decreased retinal degeneration resulting from prolonged (8h) blue light treatment. Since we did observe early sporadic signs of rhabdomere loss in the flies used for this study both at 8h and at older time points (D50), we predict that retinal degeneration might only be delayed in this genetic background relative to other white-eyed flies.

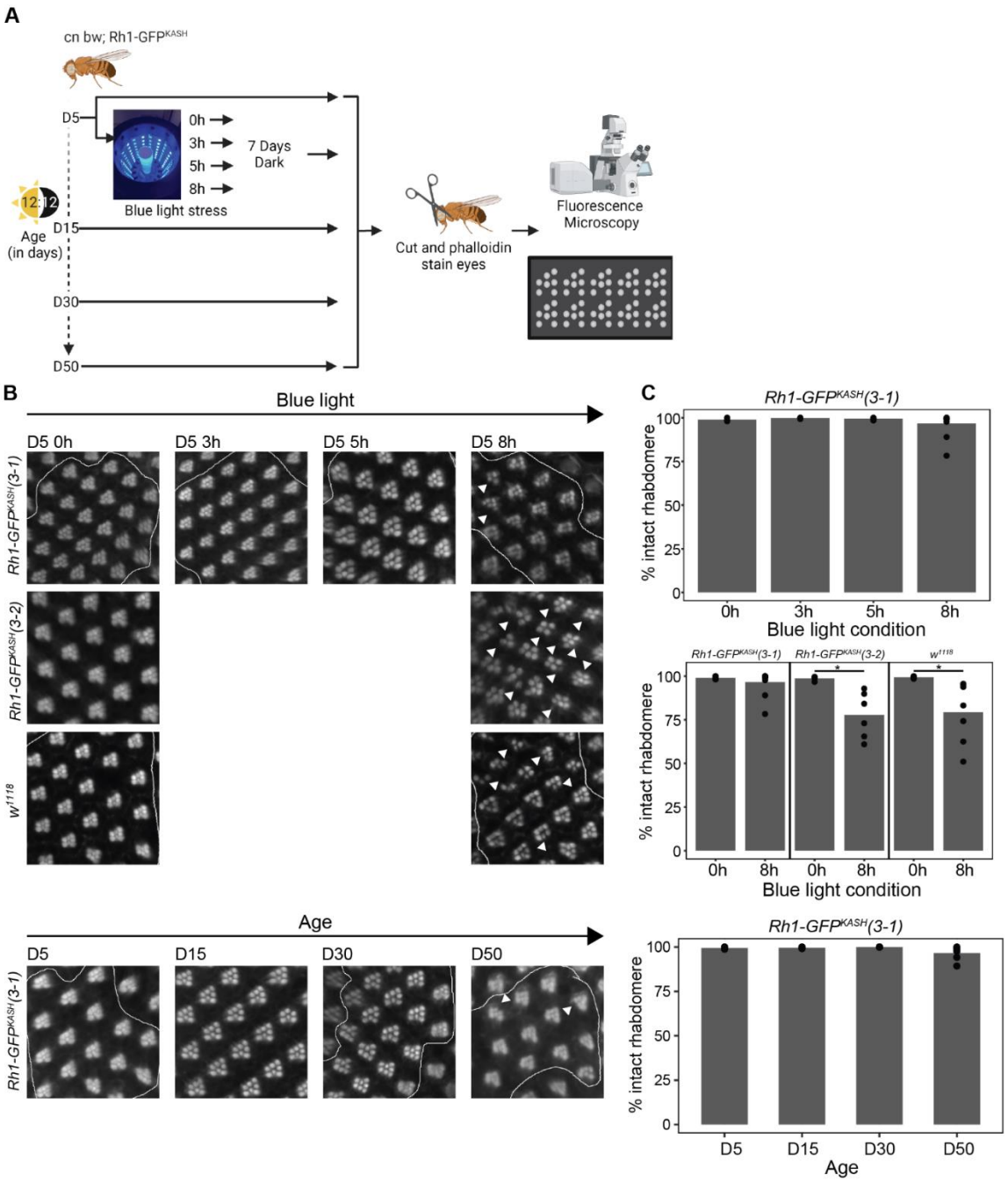

Figure 3-6. *Catalase* overexpression correlates with mild suppression of retinal degeneration in *Rh1-GFP^{KASH}* (3-1) flies. (A) Overview of the experimental design for assessing retinal degeneration in male flies of the indicated genotypes at D5, D15, D30 and D50, or D5 flies exposed to 0, 3, 5 or 8h of blue light. (B) Representative images of dissected and phalloidin (F-actin) stained blue light exposed or aged eyes from the indicated genotypes (*cn bw; Rh1-GFP^{KASH} (3-1), cn bw; Rh1-GFP^{KASH} (3-2)* or *w^{1118}*). Arrow heads point to ommatidia or regions in the eye with degenerated rhabdomeres. (C) Quantification (displayed as percent of intact rhabdomere) of rhabdomere loss in aged or blue light exposed flies from the indicated genotypes ($n \geq 5$). Black circles indicate individual biological replicates (flies), and mean shown by bar height. *p*-value (*<0.05), t-test.

Oxidative stress increases in many tissues during aging[110,111], and we previously showed that blue light increases levels of H_2O_2 and a marker of lipid peroxidation, malondialdehyde, in the eye[112]. To compare oxidative stress induced by aging or blue light exposure in the flies used for this study relative to *w*^{1118}, we examined ratios of reduced and oxidized glutathione (GSH:GSSG) in dissected eyes from flies treated as outlined in Figure 3.6A. Glutathione is an important thiol antioxidant that prevents the accumulation of toxic lipid peroxides[113,114]. The ratio of GSH:GSSG correlates with, and provides an indication of, the relative level of cellular oxidative stress[115,116]. In this assay, a decreased ratio of GSH:GSSG indicates higher levels of the oxidized glutathione pool, correlating with increased oxidative stress. Using this approach, we found a significant increase in oxidative stress in *w*^{1118} flies exposed to 8h blue light but not in *cn bw; Rh1-GFP*^{KASH} *3-1* (Figure 3.7A). However, we did observe a significant increase in oxidative stress in the latter genotype in D30 relative to D5 (Figure 3.7B). Surprisingly, there was a significant increase in the GSH:GSSG ratio in D15 flies relative to untreated D5, indicating that these flies have a more reduced glutathione pool which may infer a higher capacity to respond to oxidative damage than that of D5 flies, potentially correlating with *Catalase* expression, although this has not been tested in the current study. These data suggest that the early changes in aging white-eyed flies by D15 might include an increased antioxidant response, but that this is insufficient to counteract the high levels of oxidative stress present at older ages such as D30. These glutathione pool measurements, together with the retinal degeneration assessment in the fly line used in the current study, support a neuroprotective role for *Catalase* overexpression in photoreceptors in both light stress and aging models.

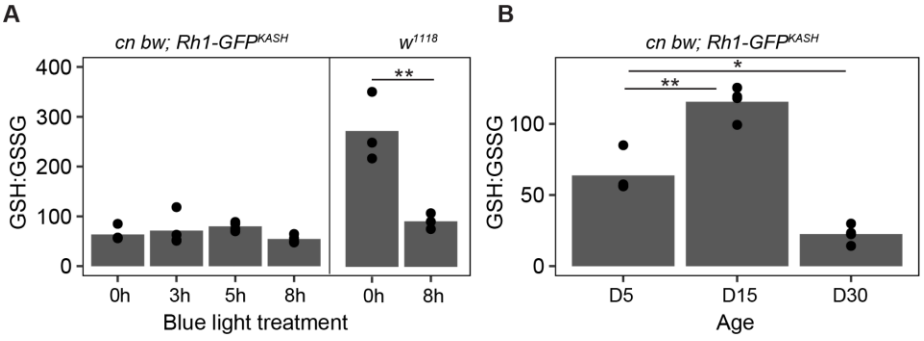

Figure 3-7. Lower levels of glutathione oxidation following blue light exposure in Rh1-GFPKASH flies relative to w1118. (A) GSH:GSSG ratios in male white eyed cn bw Rh1-GFPKASH or w1118 flies eyes exposed to 3, 5 or 8h of blue light at D5 versus untreated control (0h). Black circles indicate individual biological replicates (n ≥ 3; 25 eyes per sample), and mean shown by bar height. p-value (**<0.005,), t-test. (B) GSH:GSSG ratio in male white eyed cn bw Rh1-GFPKASH flies aged to D5, D15, or D30. p-value (*<0.05, **<0.005), ANOVA with post-hoc.

3.4 Discussion:

Here, we directly compare gene expression changes that result from light stress or aging in photoreceptors, allowing us to separate the age-associated changes in gene expression caused by environmental light stress from those caused by other factors. Similar to our previous study in young (D6) white-eyed flies exposed to 3h blue light[73], we also identified similar functional categories of genes that were differentially expressed upon different blue light exposure durations in these flies (D5). In particular, blue light upregulates expression of several stress response genes, indicating that this light exposure causes a substantial stress response in the fly photoreceptors. Other studies have shown that flies exposed to lower intensities of blue light throughout their lifespan exhibit increased expression of heat shock and oxidative stress genes[69]. When we compared blue light and aging, we identified substantial overlaps in gene expression between the longest blue light exposure condition and D30. However, oxidative stress levels as measured by oxidized:reduced glutathione levels were only significantly higher at D30, and not under 8h blue light exposure. We previously observed increased H_2O_2 and malondialdehyde (lipid peroxidation) levels in eyes from w^{1118} flies exposed to 8h blue light[112], indicating that blue light increases oxidative stress levels in the eye. Moreover, both these markers of oxidative stress and retinal degeneration were rescued by overexpression of *Cytochrome-b5*, which suppresses the lipid peroxidation resulting from blue light exposure[112]. We attribute the differences in severity/onset of the retinal degeneration in the flies used in the current study (*Rh1-GFP*^{KASH} 3-1) versus the previous lines used (w^{1118} or *cn bw*) to the high levels of *Catalase* expressed in photoreceptors resulting from the insertion position of the transgene. Recent studies have shown that w^{1118} (null mutation in the gene *white*) flies that lack eye pigment exhibit significant retinal degeneration in 50% of ommatidia by D5, and that retinal degeneration progresses further by D15 and D30[117]. Despite this potential protective effect, the increase in stress response genes observed in our D5 flies exposed to 3, 5, or 8h blue light suggests that they are experiencing oxidative stress, but that the overexpression of *Catalase*, which reduces H_2O_2 and decreases oxidative stress, might be sufficient to prevent global changes in glutathione ratios in the eye. This is particularly striking given that the overexpression of *Catalase* at steady-state level is relatively modest (~30% higher than control), even though *Catalase* nuclear transcript levels were much higher. Similarly, the higher reduced pool of glutathione observed in white-eyed D15 flies suggests that relatively young flies may be able to counteract the early effects of oxidative stress in part by increasing antioxidant

capacity. It is interesting that *Catalase* expression correlates with protection against blue light stress because overexpression of *Superoxide dismutase 1* (*Sod1*) decreases H_2O_2 levels in the eye but does not protect against blue light-induced retinal degeneration[112]. Although the high level of *Catalase* expression in the *Rh1-GFP^{KASH}* 3-1 flies generated in this study was inadvertent, these flies provide an intriguing model for further study to characterize the oxidative stress-dependent transcriptome of aging photoreceptors. The differences in level of *Catalase* expression observed between the photoreceptor nuclear RNA and whole head steady-state mRNA levels are also notable, suggesting that *Catalase* mRNA levels might be tightly regulated in these cells.

Overall, our data indicate that 15 - 25 percent of the gene expression changes observed in aging photoreceptors can likely be attributed to light stress. These light stress-dependent gene expression changes include the upregulation of stress response and DNA repair pathways, as well as a conserved neuronal cell death signature consisting of cell cycle genes. In addition, light stress appears to be responsible for the downregulation of phototransduction genes observed in aging photoreceptors. Although the current studies were performed in white-eyed flies, some similar GO terms were enriched when gene expression changes were analyzed during aging in flies with red eyes (*Rh1-Gal4>UAS-GFP^{KASH}*), albeit at much later time points[48,77]. However, because of the differences in genetic background and nuclei immuno-enrichment technique used, it is not possible to directly compare the data from these studies. Thus, our data suggest that the eye ages more rapidly in white versus red-eyed flies, likely due to an increase in light stress dependent accumulation of damage that is ameliorated by the presence of neuroprotective pigments in red-eyed flies.

Although many pathways were commonly regulated by light stress and aging, we also identified gene expression signatures that were unique to each condition. During aging, genes involved in defense and immune response were upregulated while genes involved in ion transport and ATP synthesis were downregulated. These data indicate that aging photoreceptors might be exposed to other environmental stresses such as cellular damage or pathogens that induce immune response. Moreover, aspects of metabolism may become dysregulated in aging photoreceptors independent of light stress. Recent work by our lab has identified metabolic changes in the aging *Drosophila* eye that include changes to folate, S-adenosyl-methionine (SAM), and glutamate biosynthesis[118]. In contrast, blue light exposure upregulated genes involved in cellular organization and the negative regulation of stimulus, suggesting that blue light exposed photoreceptors induce

gene expression pathways to quench the light response, likely as a neuroprotective mechanism. Since these pathways were not induced in aging photoreceptors, they likely represent a specialized response to light stress in the eye.

Together, our data support a model in which light stress and other factors contribute to the aging transcriptome of photoreceptors. Moreover, we demonstrate that white-eyed flies might provide a suitable model for premature aging in the *Drosophila* eye. Our study helps to define the complicated environmental and intrinsic signals that lead to changes in gene expression within a single cell type, photoreceptor neurons, in an aging organism.

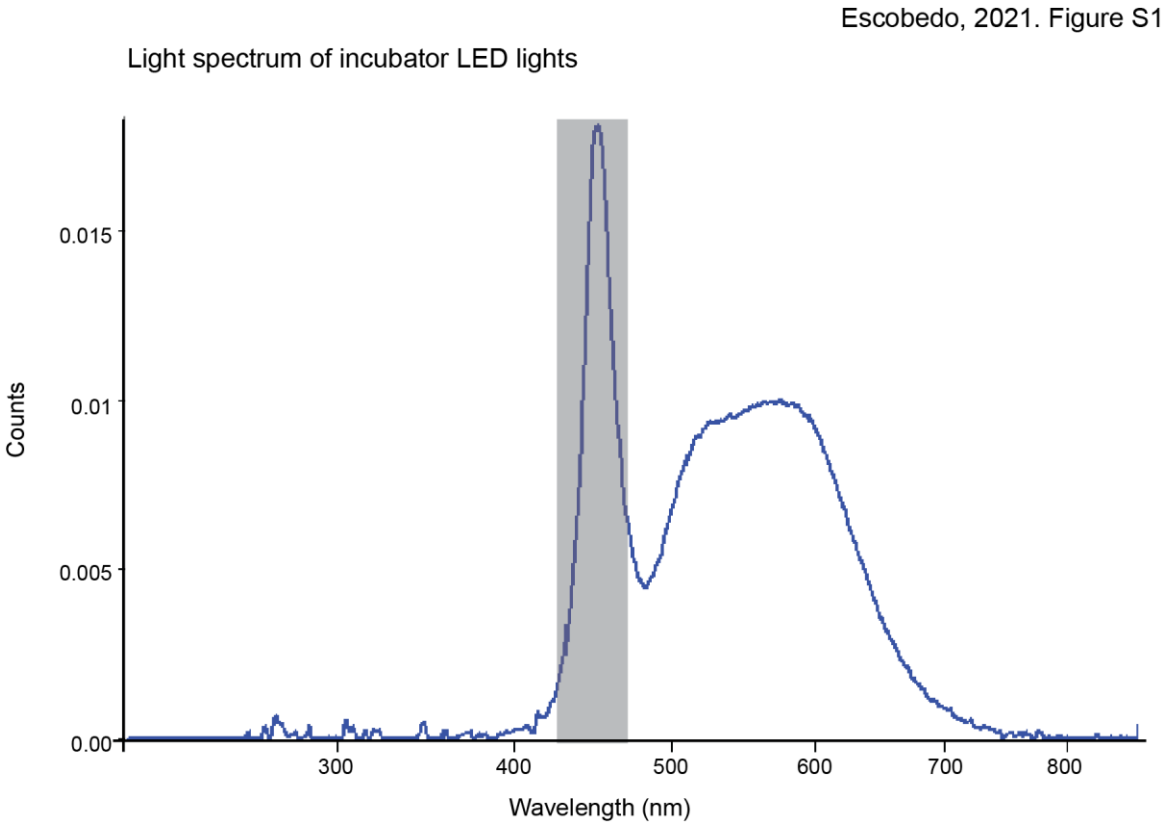

Figure 3-8. Light spectrum of 12:12 *Drosophila* incubator. Visible is the blue light peak, followed by the broad peak in the visible spectrum indicative of white LEDs. Grey shading represents the primary excitation wavelengths of GFP.

CHAPTER 4. KNOCKDOWN OF THE TRANSCRIPTION REGULATORS *SPT5* AND *DOM* IN *DROSOPHILA* PHOTORECEPTORS RESULTS IN PREMATURE RETINAL DEGENERATION AND TRANSCRIPTIONAL SIGNATURE SIMILAR TO OLD FLIES

Declaration of collaborative work

The work described in this chapter was the collaborative effort of Spencer Escobedo, Juan Jauregui-Lozano, Kratika Singhal, Sarah Stanhope, Anik Paul, Ryan Debernardis and Dr. Vikki Weake. Juan Jauregui conducted the aging time course RNAseq, Kratika Singhal, Sarah Stanhope and Anik Paul contributed to knockdown qRT-PCR experiments. Ryan Debernardis assisted in fly aging. All other experiments were performed by Spencer Escobedo. Spencer Escobedo and Dr. Vikki Weake wrote the manuscript.

4.1 Introduction

The risk of ocular disease strongly increases with advanced age, particularly after age 75, leading to increased prevalence of blindness and visual impairment irrespective of race or regional groups [119,120]. Moreover, aging is associated with increased incidence of eye diseases such as cataract, diabetic retinopathy, glaucoma, and age-regulated macular degeneration (AMD) [121]. Although environmental factors such as smoking, diet, and sunlight exposure can modify the risk of developing age-associated eye disease [122], chronological age remains the major factor that influences the likelihood of developing eye disease. We and others have identified reproducible and robust changes in gene expression that occur in aging cells within the eye. In mice, aging rod photoreceptors undergo global changes in gene expression that precede any signs of retinal degeneration [54,123]. Age-regulated genes in rods are involved in morphogenesis, motor axon guidance, neuronal signaling, and regulation of transcription [124]. *Drosophila* photoreceptors, which functionally resemble vertebrate rods, show similar changes in the aging transcriptome, with increased expression of DNA damage response genes and downregulation of genes involved in neuronal function that correlate with decreased visual function [23,88].

In addition to changes in gene expression, there are age-dependent alterations in epigenetic marks including chromatin accessibility, histone marks, and DNA methylation in the eye. For example, changes in chromatin accessibility have been detected at the onset of disease state for AMD [125] and in aging *Drosophila* photoreceptors [77]. Further, changes in DNA methylation are observed in aging mouse rods, particularly near genes involved in energy metabolism[126]. Similar

broad changes in gene expression and chromatin marks are also observed in other aging tissues, suggesting that these transcriptional and epigenetic changes are a common feature of aging [127128129]. The reproducible changes of some epigenetic marks such as DNA methylation in aging tissues has led to its use as an epigenetic clock to estimate the age in specific cell types with chronological age or in various disease states and cancer cell types [130]. While collectively these data suggest that the epigenomic and transcriptional signature of long-lived cells within the retina such as photoreceptors correlates with chronological age, it is unclear whether the age-associated changes in gene expression patterns in the eye directly contribute to the increased risk of ocular disease.

We reasoned that the reproducible epigenetic and transcriptional changes in aging photoreceptors suggested that the activity of specific gene regulatory mechanisms declines with advanced age. If the age-dependent changes in photoreceptor gene expression contribute to increased risk of retinal degeneration, then decreasing the expression of specific transcriptional regulators in adult photoreceptors should result in premature cell death. To test if disrupting specific transcriptional processes could lead to premature retinal degeneration, we performed a targeted RNAi screen in *Drosophila* photoreceptors. Strikingly, we show that knockdown of several epigenetic regulators associated with transcription elongation leads to premature age-dependent retinal degeneration and results in gene expression signatures that resemble much older flies. Our data suggest that the diminished transcription elongation may underly a large proportion of the changes in gene expression observed in aging photoreceptors. Moreover, our findings suggest that the age-dependent changes in gene expression in photoreceptors directly contribute to the increased risk of retinal degeneration.

4.2 Materials and methods

4.2.1 Fly strains, genetics, and aging

Flies were raised in 12h:12h light dark at 25°C on standard fly food. Aging was conducted by collecting flies 3 days after eclosion so that flies were +/- 1 day old. Flies were transferred onto fresh food every 2 - 3 days. Male flies were used for all experiments. Genotypes are listed in Table S4, and all RNAi lines and stock numbers are listed in Table S1. To assess knockdown efficiency, RNAi lines were crossed to *Act5C-Gal4* and third instar larvae collected for analysis. If ubiquitous knockdown led to developmental lethality or if RNAi stocks had balancer chromosomes, RNAi

lines were crossed to *Act5C-Gal4, tub-Gal80^{ts}* flies, progeny raised at 18ºC and shifted to 29ºC for 24 h at D5 post-eclosion, and adult males collected for analysis.

4.2.2 Luciferase assays and Optic Neutralization

Luciferase assays and optic neutralization were performed as previously described [127]. For optic neutralization, scores of 1 to 7 were assigned by severity in degeneration as follows: 1 = no degeneration, 2 = >10% of ommatidia have rhab*dom*ere loss, 3 = 10-20%, …, 7= <50%. All scores for optic neutralization were assigned blindly based on all in-focus ommatidia

4.2.3 qRT-PCR analysis.

RNA extraction, cDNA synthesis, and qRT-PCR were conducted as previously described on single larvae or adult male flies[127]. Three biological replicates were examined for each genotype. Primers are listed in Table S5.

4.2.4 Statistics

A ll statistics were conducted using R or Microsoft Excel. Significant changes in luciferase activity or optic scores were compared between RNAi lines and all four control lines using Dunnett's test. The significance threshold for the initial RNAi lines (sh-RNA #1) was set at a p-value <0.05 for both luciferase and optic, and at p<0.05 and p<0.01 for the second independent RNAi line (sh-RNA #2) for luciferase activity and optic scores, respectively. Statistical analysis for aging time course data (luciferase activity and optic neutralization) were conducted using ANOVA with post hoc Tukey HSD. All other pairwise statistical analyses were conducted by Students T-test with a significance threshold of p-value <0.05.

4.2.5 Photoreceptor specific nuclei-immunoenrichment (NIE)

NIE was conducted as previously described[77]. Each sample was prepared using 150 to 250 D30 male flies. A full step-by-step protocol is available at [131].

4.2.6 RNA-seq and bioinformatics

RNA-seq libraries were constructed and differential gene expression analysis conducted using EdgeR as previously described (Escobedo, et. al. 2021) with the following minor modifications. Counts were filtered to remove lowly expressed genes requiring counts per million (cpm) > 30 in at least 27 of the 29 libraries (10 RNAi lines, n = 3) resulting in 7069 genes used for downstream analysis. We discarded one replicate for *Spt5* due to poor quality. RUV-seq normalization was conducted using a k=4 to account for the variation between the 10 RNAi lines, as well as any variation due to batch effects. All plots were generated in Rstudio (v. 4.0.5) using custom scripts. Gene Ontology (GO) enrichment was conducted using Cluster profiler(v3.18.1) [85]. RNA-seq data for the RNAi screen lines is available at the Gene Expression Omnibus (GEO) repository. The aging RNA-seq data used for comparisons is available at GSE169328 and GSE174515.

4.3 Results

4.3.1 Drosophila undergo age-dependent retinal degeneration.

We sought to perform a targeted RNAi-based candidate screen to identify the transcriptional and epigenetic mechanisms that are required for photoreceptor survival during aging. To do this, we generated flies in which we could express *UAS-shRNA* against various target genes in differentiated, adult photoreceptors using *Rh1-Gal4* in the presence of *UAS-Dcr-2* to enhance knockdown. These flies also express photoreceptor-specific luciferase (*Rh1-ffluc*), enabling us to assess photoreceptor survival throughout aging using two independent assays: *Rh1-ffluc* activity as a proxy for photoreceptor number [127]; and optic neutralization in live flies to assess rhab*dom*ere integrity [132]. To quantify rhab*dom*ere loss by optic neutralization, we scored retinal degeneration from little to no degeneration as a score of 1 to highly degenerated ommatidia with a score of 7 (Fig. 1B). We refer to these *Rh1-ffluc, Rh1-Gal4>UAS-Dcr2* flies hereafter as *Rh1-Gal4* for simplicity.

We then characterized photoreceptor survival throughout aging in *Rh1-Gal4* flies expressing RNAi against mCherry (*sh-mCherry*), which does not target any *Drosophila* gene. These flies show similar lifespans to other wild-type *Drosophila* strains at 25ºC with median survival of 51.5 and 56.5 days for male and female flies, respectively (Fig. 1C). Consistent with

the continued increase in expression of Rh1 (Rhodopsin 1, encoded by the *ninaE* gene) in the first few days following eclosion, we observe a substantial increase in luciferase activity from day one (D1) to D10, followed by maintained levels of luciferase activity that only start to decline around D60 (Fig. 1D). This decrease in luciferase activity at D60 correlates with substantial and significant rhab*dom*ere loss as determined by optic neutralization at this same age (Fig. 1E). In contrast, little to no retinal degeneration is observed by either technique at D30, with intermediate and highly variable rhab*dom*ere loss at D50 (Fig. 1D – E). We conclude that old *Rh1-Gal4* flies, defined as being in the second half of their median lifespan, exhibit significant retinal degeneration that is almost entirely absent from young (D10) or middle-aged flies (D30). We and others have previously shown that red-eyed *Drosophila* show negligible retinal degeneration prior to D40 [23].

Figure 4-1. *Drosophila* undergo age dependent retinal degeneration. A) Schematic describing the techniques used to assess retinal degeneration in aging *Rh1-ffluc, Rh1-Gal4>sh-RNA Drosophila*. B) Survival curve of *Rh1-ffluc, Rh1-Gal4>sh-mCherry* male and female flies (n = 300). C) Optic neutralization images were scored for severity of rhab*dom*ere loss using a scale of 1 to 7, where 7 indicates severe retinal degeneration. D) Luciferase activity in heads of aging flies, p-value<0.005 (**), ANOVA with post-hoc Tukey HSD. E) Optic neutralization at D30, D50, and D60. Scores shown in left panel ($n \geq 8$ independent flies) with representative images shown in the right panel. Arrowheads indicate missing rhab*dom*eres. p-value (***< $5x10^3$, ****<$.5x10^4$), ANOVA with post-hoc Tukey HSD.

Figure 4.1 continued

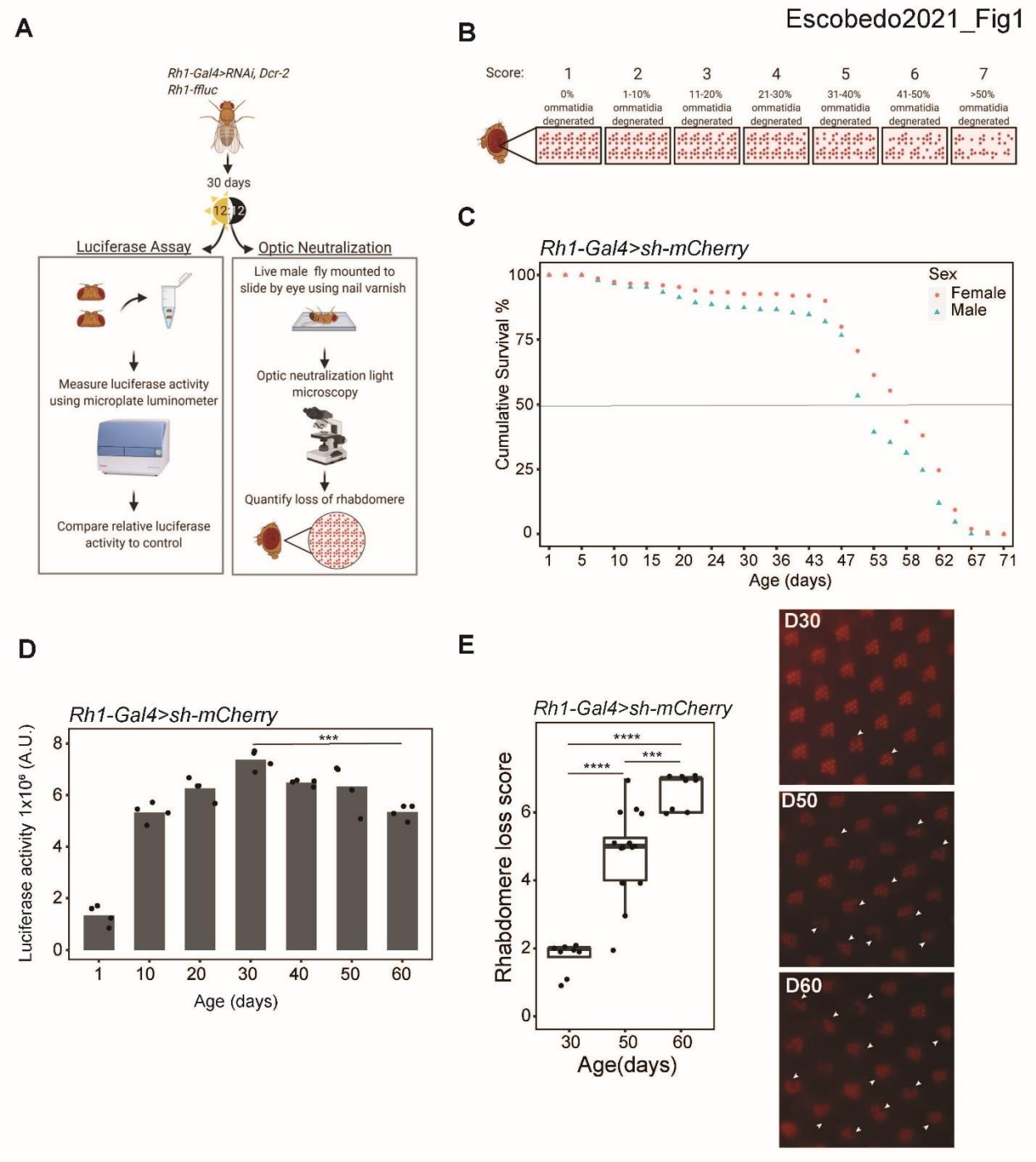

Next, we asked if RNAi expressed in photoreceptors under *Rh1-Gal4* control was effective throughout aging. To do this, we crossed flies expressing either *sh-luciferase* or *sh-mCherry* to *Rh1-Gal4* flies. We then examined luciferase activity in the progeny to test if expression of *sh-luciferase* in photoreceptors lead to efficient knockdown of the *Rh1-ffluc* transgene relative to the *sh-mCherry* negative control. Using this approach, *sh-luciferase* expression significantly reduced luciferase activity relative to *sh-mCherry* control from two days post-eclosion right through until D50 (Supp fig. 1A). In fact, by D15, *sh-luciferase* expressing flies showed 50-fold lower luciferase activity relative to *sh-mCherry*, supporting a robust RNAi in adult photoreceptors using this system. We note that *Rh1-Gal4* does not drive expression of target transgenes until 75% through pupal development, after the cells in the adult eye are fully differentiated (Supp fig. 1B) [76]. Supporting the late activity of *Rh1-Gal4*, we do not observe significant decreases in luciferase activity until D2. Together, these data show that *Rh1-Gal4* flies can be used for robust RNAi-mediated knockdown of target gene expression in adult photoreceptors, with little impact on development of the eye.

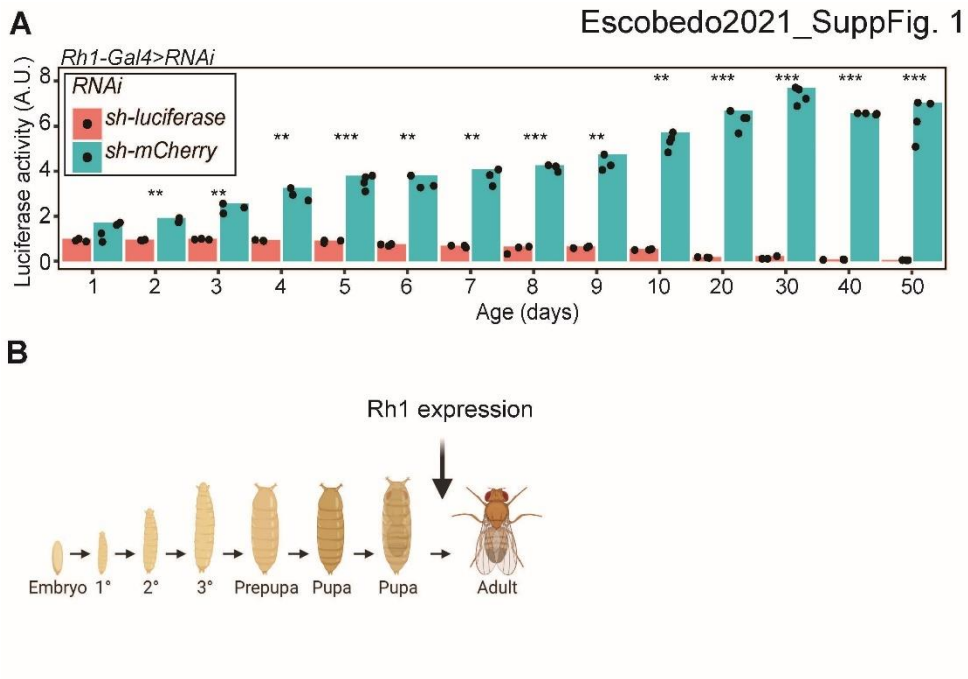

Figure 4-2.Photoreceptor-specific shRNA leads to knockdown by 2 days post-eclosion and remains effective throughout aging. A) Luciferase activity was examined in head extracts from Rh1-ffluc, Rh1-Gal4 flies expressing either sh-luciferase or sh-mCherry at the indicated ages (n = 4). p-value (***< $5x10^{3}$, ****< $5x10^{4}$), Students T-test. B) Schematic showing the developmental stage at which the *ninaE* (*Rh1*) transcript is first detected.

4.3.2 Photoreceptor-specific targeted RNAi screen reveals transcription elongation factors are necessary for age-dependent photoreceptor survival.

Next, we crossed lines expressing RNAi against a variety of transcriptional regulators with the *Rh1-Gal4* flies, and assessed photoreceptor health by luciferase assays and optic neutralization at D30, when control flies exhibit little to no retinal degeneration (Fig. 2A). We initially used RNAi lines that targeted 155 unique genes representing a diverse group of gene regulatory factors. 94 of these RNAi lines included histone modifiers, chromatin remodelers, and factors that regulate specific aspects of the transcription cycle (Fig. 2B, Table S1). We also targeted 61 transcription factors that were previously identified as having enriched binding motifs in the promoters of genes that were differentially expressed in aging photoreceptors (Fig. 2B). In addition, we used 5 independent RNAi lines that target genes not expressed in *Drosophila* as negative controls: mCherry, GFP #1, GFP #2, lexA #1, lexA #2.

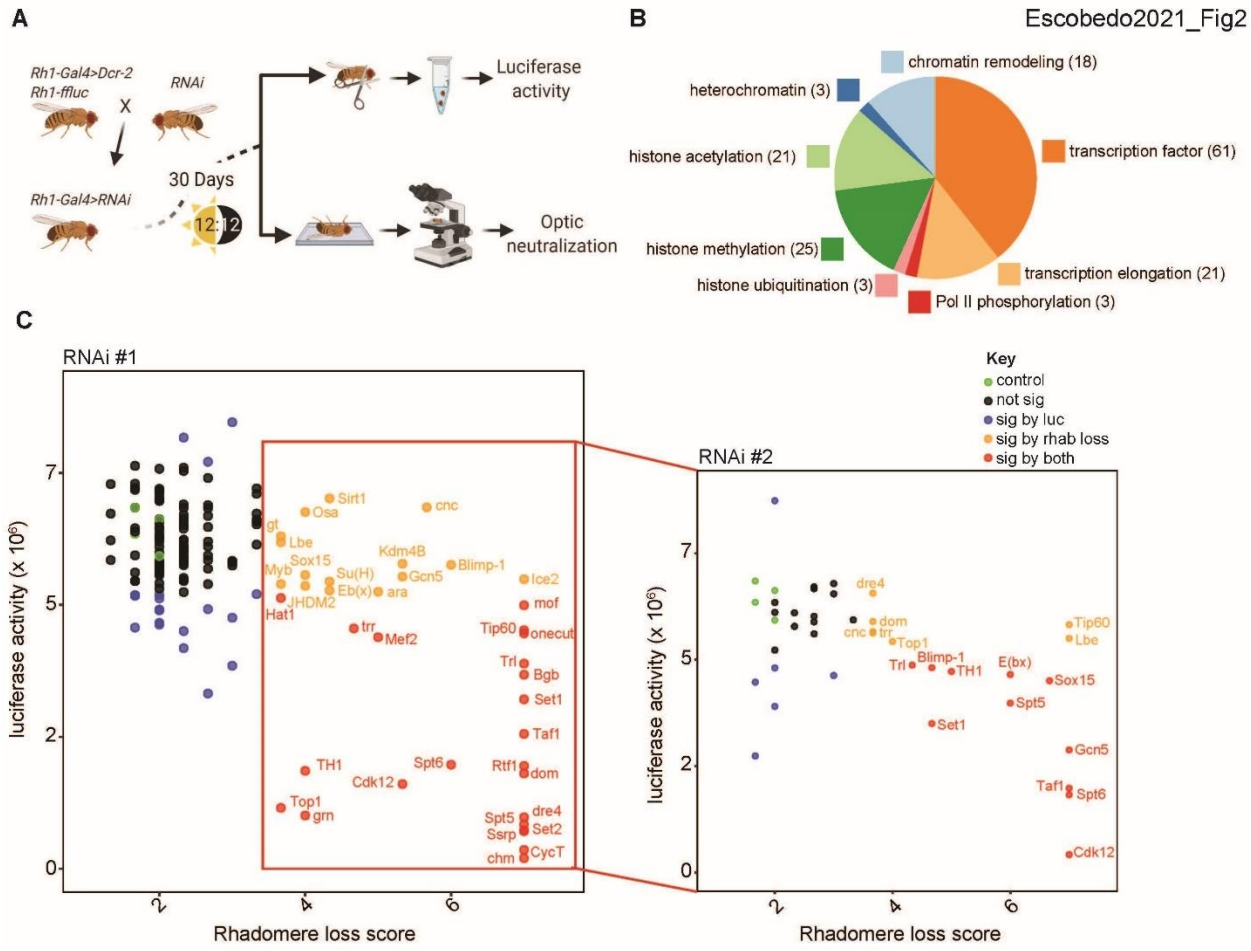

Figure 4-3. Targeted RNAi screen identifies 18 transcriptional regulators that are necessary for survival of aging photoreceptors. A) Schematic describing the targeted RNAi screen to identify factors that are necessary in adult photoreceptors for cell survival. B) Pie chart showing the gene functions of the 155 unique genes tested in the targeted RNAi screen. C) Scatter plot showing the mean luciferase activity versus optic neutralization score for each of the initial (*sh-RNA#1*, left panel) or secondary (*sh-RNA#2*, right panel) RNAi lines targeted (n = 3). Each point represents a single *sh-RNA* line and is colored as described in the legend (green, control; black, non-significant; blue, significant change in luciferase activity; orange, significant change in optic score; red, significant change in luciferase activity and optic score).

We primarily selected VALIUM20 lines from the Transgenic RNAi Project (TRiP) collection, but used TRiP VALIUM1/10 or Vienna Drosophila Stock Center (VDRC) KK RNAi collections if VALIUM20 lines were not available for the target gene[133]. Whereas the VALIUM20 lines are *sh-RNA* transgenes that utilize the *mir-1* scaffold for efficient and specific knockdown of the target gene [134,135], the VALIUM1/10 and KK RNAi lines utilize long dsRNA hairpins [136], which have an increased likelihood of off target effects [137]. As expected from the *sh-mCherry* analysis in Figure 1, we did not observe retinal degeneration in four of the five control RNAi lines at D30 using luciferase assays or optic neutralization (Fig. 2C, green circles). However, surprisingly one of the *sh-GFP* lines (GFP #2) had substantial rhab*dom*ere loss by optic and a significant decrease in luciferase activity, presumably due to off-target effects; we therefore excluded this line as a control (Table S1).

We separately compared luciferase activity and optic scores between each of the 155 target gene RNAi lines and the remaining four controls, and identified RNAi lines that showed significant changes in both luciferase activity and optic scores ($p < 0.05$, Dunnett's test; 22 genes; red circles, Fig. 2C left panel). We also identified RNAi lines with significant changes only in luciferase activity (18 genes; blue circles) or optic scores (14 genes; yellow circles). We reasoned that changes in luciferase activity that were not accompanied by rhab*dom*ere loss most likely represent altered expression of the *Rh1-ffluc* transgene; thus, we focused on the 36 *RNAi* #1 targets with significant changes in optic scores for validation. To decrease the likelihood of false positives due to off-target effects, we tested an additional independent RNAi line for each of the 36 genes targeted by these lines (*RNAi* #2, right panel Fig. 2C). Only 18 of these 36 independent RNAi lines resulted in significant degeneration phenotypes (red and yellow circles, RNAi #2, right panel Fig. 2C); these 18 genes represent high confidence targets for factors that are necessary to prevent retinal degeneration in adult photoreceptors.

Table 4.1. Gene regulatory factors whose photoreceptor-specific knockdown results in premature, age-dependent retinal degeneration

Screen hit groups		**Gene**	**Gene function**	**Complex**
Transcription Elongation	GAGA Factor	*Trl*	GAGA factor. Regulates gene expression through its role as both a transcription factor and chromatin regulator.	None
	Chromatin remodeler	*E(bx)*	Regulator of homeotic and heat shock gene expression, ISWI chromatin remodeling complex member.	NURF
	Pausing Factors	*Spt5*	One of the two proteins that make up the dimeric DSIF complex. Regulates promoter proximal pausing and inducible gene expression.	DSIF
		TH1	One of the four subunits of the NELF complex. Involved in inducible gene expression and Pol II promoter proximal pausing.	NELF
	CTD phosphorylase	*Cdk12*	Phosphorylates Serine 2 of Pol II CTD. for Pol II elongation. Shown to regulate Nrf2 (Cnc) target genes in Drosophila.	None
	Histone Chaperone	*Spt6*	Elongation factor involved in nucleosome reassembly behind elongating Pol II	None
		dre4	Histone chaperone like complex member, maintains promoter proximal paused Pol II.	FACT
Transcription activation	Histone Acetyltransferase	*Tip60*	Histone acetyltransferase involved in H4 acetylation. for DNA damage and stress response.	NuA4
		Gcn5	Histone acetyltransferase of the SAGA and ATAC complexes. cofactor for RNA Pol II transcription	SAGA/ATAC
	Histone Methyltransferase	*Set1*	Histone methyltransferase responsible for HeK4me2/3. Activates gene expression through modifications made at gene promoters.	Compass
		trr	Histone methyltransferase responsible for H3K4me1.Regulates enhancer elements.	Compass like/ MLR
	RNA Pol II Cofactor	*Taf1*	Largest complex member of the TFIID complex. Targets TFIID to promoter. Mutations in humans associated with intellectual disabilities.	TFIID
	Chromatin remodeler	*dom*	ATP-dependent chromatin remodeler involved in incorporating H2A.V. Recruited to sites of DNA damage Also involved in H4 acetylation. Involved in Notch signaling	SWR1 and NuA4
Topoisomerase		*Top1*	DNA topoisomerase. Relieves topological stress from DNA during replication and transcription.	None
Transcription Factors	Stress response	*cnc*	Nrf2 homolog. Activates oxidative stress/inducible gene expression.	None
	Development	*Blimp-1*	Prdm1 homolog. C2H2 TF. Involved in cellular response to ecdysone, as well as neuronal development in human cells.	None
		lbe	NK-like Homeobox TF. Roles in muscle and heart development	None
		Sox15	HMGB TF. Maintains cell stemness.	None

To test if the retinal degeneration observed at D30 for each of these 18 factors was due to expression of the respective RNAi, we performed optic neutralization in each of these RNAi lines outcrossed to *Rh1-ffluc* in the absence of the *Rh1-Gal4* driver (Fig. 3A, no driver). We did not observe substantial retinal degeneration in either the first or second RNAi line targeting the 18 high confidence targets in these no driver controls, indicating that photoreceptor-specific knockdown of the respective target gene indeed underlies the observed decrease in photoreceptor survival. Although the lack of phenotype in 14 of the second RNAi lines tested for the initial 36 genes identified by our screen is most likely due to off-target effects in the initial RNAi line, it is also possible that the second RNAi line did not efficiently knockdown expression of the target gene. To test this, and provide some measure of knockdown efficiency within the 36 initial RNAi #1 targets identified, we examined knockdown of target transcripts using qRT-PCR. Because *Rh1-Gal4* is only expressed in adult photoreceptors making it difficult to examine knockdown efficiency in the mixed cell population present in eyes, we instead assessed knockdown efficiency in whole animals using the ubiquitous *Act5C-Gal4* driver (Supp fig. 3A). Unsurprisingly, ubiquitous knockdown of many of these important transcriptional regulators lead to developmental lethality (Table S2); knockdown efficiency was assessed in those lines, or for RNAi lines that contained balancer chromosomes, using *Act5C-Gal4* with temporal restriction by *tub-Gal80^{ts}* (Table S2). Using this approach, we observed that (#PENDING) of the 36 targets showed significant decrease in levels of the target gene transcript by qRT-PCR relative to the *sh-mCherry* control for at least one of the RNAi lines used. Moreover, knockdown efficiency correlated with severity of the phenotype for several of the 18 high confidence hits (*eg Tip60*, *Top1*), but did not account for lack of phenotype in many of the other RNAi #2 lines (*eg CycT*, *ara*). These data suggest that the majority of the RNAi lines effectively knockdown expression of the target gene; however, there might be differences in protein expression that were not examined in this study.

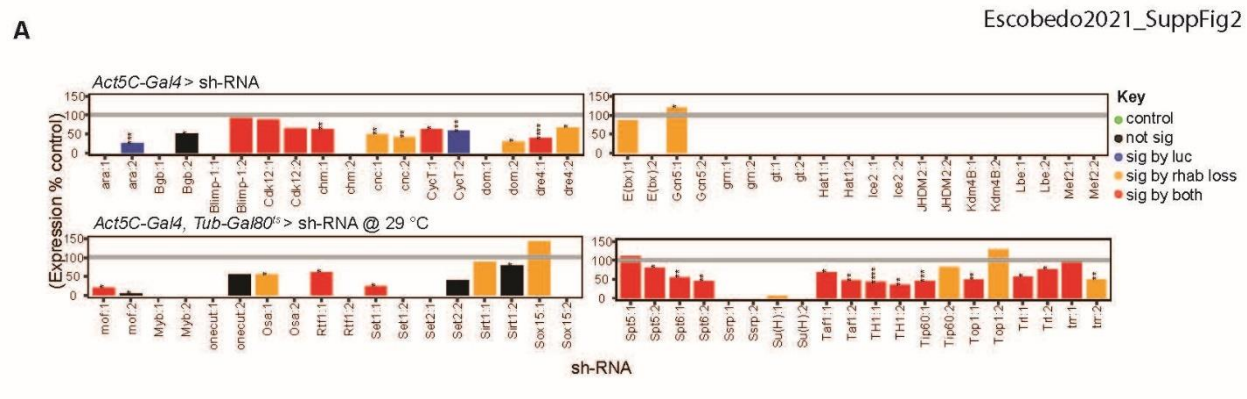

Figure 4-4. Knockdown efficiency of selected sh-RNA lines. Summary of the knockdown efficiency of both independent *sh-RNA* lines for the 36 factors with a significant optic neutralization score in the initial screen (*sh-RNA #1*). Bar plot shows mean relative expression for each target gene assessed by qRT-PCR compared to *sh-mCherry* control; expression values for target genes were normalized to the geometric mean of *Rpl32* and *eiF1a*. Knockdown efficiency was determined in larvae (*Act5C-Gal4>sh-RNA*, left panel) or in adults (*tub-Gal80^{ts}*, *Act5C-Gal4>sh-RNA* at 29°C, right panel), as indicated by panel labels. The color of each bar corresponds to the retinal degeneration phenotype of the line as described in Figure 2C (green, control; black, non-significant; blue, significant change in luciferase activity; orange, significant change in optic score; red, significant change in luciferase activity and optic score). P-value(*<0.05, **< 5x10^{3}, ***< 5x10*4*), Students T-test.

Next, we asked if the retinal degeneration induced by photoreceptor-specific RNAi against these 18 high confidence targets was progressive with increasing age by comparing optic scores in flies at D10 and D30. Surprisingly, we found that the majority of the RNAi lines exhibit a retinal degeneration phenotype that becomes progressively worse with age (Fig. 3B). Although the delayed manifestation of the retinal degeneration phenotype might be due to differences in knockdown efficiency for some RNAi lines, such as *Spt5* and *Cdk12*, we showed that *Rh1*-Gal4 mediated knockdown is efficient as early as D2 (Fig. S1). Thus, our data suggest that the proper expression of these 18 factors becomes increasingly important for regulating gene expression pathways that promote survival in old photoreceptors. In summary, our screen has identified 18 genes whose normal expression is necessary for photoreceptor survival in aging flies (Table 1).

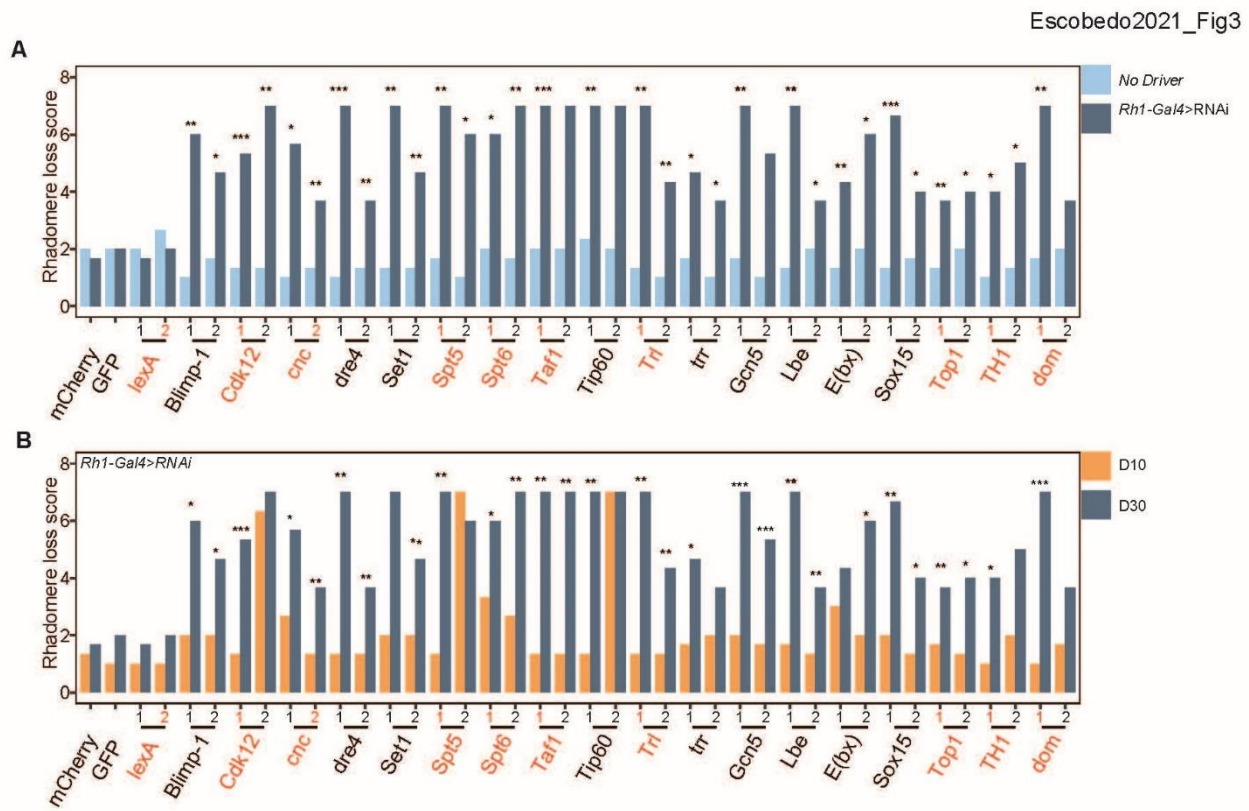

Figure 4-5.Retinal degeneration induced by knockdown of the 18 factors is progressive and requires Gal4 expression. A) Bar plot showing mean optic neutralization scores in D30 flies for each *UAS-shRNA* line in the presence or absence of *Rh1-Gal4* (n = 3). #1, #2 correspond to initial and secondary RNAi lines tested in the original screen. p-value (*<0.05, **<0.005, ***<0.0005), Students one-tailed T-test.B) Bar plot showing mean optic neutralization scores in D10 versus D30 flies expressing *Rh1-Gal4>shRNA* against indicated targets. P-value as in panel A.

We observed a striking enrichment for factors that are involved in transcription elongation and release of the paused RNA polymerase II (Pol II) (7 of 18 factors). First, we identified both the *Drosophila* GAGA factor (GAF) *Trl* and the Nucleosome Remodeling Factor (NURF) subunit *E(bx)*, which together are important for nucleosome depletion in gene promoters [138,139], recruiting RNA Pol II [140], and regulating promoter proximal pause release further downstream [138]. We also identified the DRB Sensitivity Inducing Factor (DSIF) *Spt5* and the Negative elongation Factor (NELF) subunit *TH1*, both of which are important regulators of promoter proximal pausing [141–143]. In addition, we identified the RNA Pol II CTD Ser2 phosphorylase *Cdk12,* and the histone chaperones *Spt6* and Facilitates Chromatin Transactions (FACT) complex subunit *dre4*, which all promote productive transcription elongation by RNA Pol II [141,144,145]. The next largest group of

factors identified by our screen can be broadly characterized as regulators of transcription activation. These included the histone acetyltransferases (HAT) *Tip60* and *Gcn5* of the NuA4/Tip60 and SAGA/ATAC complexes, respectively. Interestingly, our screen also identified the chromatin remodeler *dom*, which encodes two splice isoforms that are either incorporated into the NuA4/Tip60 or SWR1 like complex [146,147]. We also identified two of the three H3K4 methyltransferases in flies (*Set1* and *trr*) as well as the TFIID subunit *Taf1* and the topoisomerase *Top1*. Interestingly, although transcription factors were overrepresented in the target screen (61/155 factors), these are underrepresented in the targets identified by our screen (Table 1). Only four transcription factors were identified as being necessary for age-dependent photoreceptor survival: *cnc, Blimp-1, Lbe,* and *Sox15*. *Blimp-1* is the ortholog of mammalian *Prdm1*, which plays an important role in determining photoreceptor identity in the mouse retina[148,149]. *Cnc* is the ortholog of mammalian *Nrf2*, the master regulator of anti-oxidative and detoxification response [150].

4.3.3 Loss of dom results in transcriptional changes that significantly overlap those seen in aging

We previously showed that there is a correlation between increasing gene length and decreasing age-dependent gene expression in photoreceptors [23,151], suggesting that transcription elongation might become less effective with advanced age. If so, we would expect that knockdown of those factors involved in transcription elongation in photoreceptors would mimic the gene expression changes observed in aging photoreceptors. To test this, we examined gene expression in photoreceptors from D30 flies expressing *sh-RNA* against nine of the identified factors involved in different stages of transcription including elongation: *Cnc, Cdk12, dom, Spt5, Spt6, Taf1, TH1, Top1, Trl* (RNAi lines used for RNA-seq highlighted in red in Fig. 4A – B). As a control, we expressed *sh-lexA #2 (*lexA*)*, which did not exhibit any retinal degeneration by D30. We used our previously described photoreceptor nuclei-immunoenrichment (NIE) approach to isolate nuclear RNA from photoreceptors in *Rh1-GFP^{KASH}, Rh1-Gal4>sh-RNA* flies (n = 3; Fig. 5A). We note that all RNAi lines selected for RNA-seq were *sh-RNA* VALIUM20 lines, so we did not express Dcr-2 in these flies. Because NIE is based on immunoenrichment of nuclei that are tagged with GFP^{KASH}, this approach should enrich nuclei from photoreceptors that have not yet degenerated, enabling us to identify the changes in gene expression in these cells.

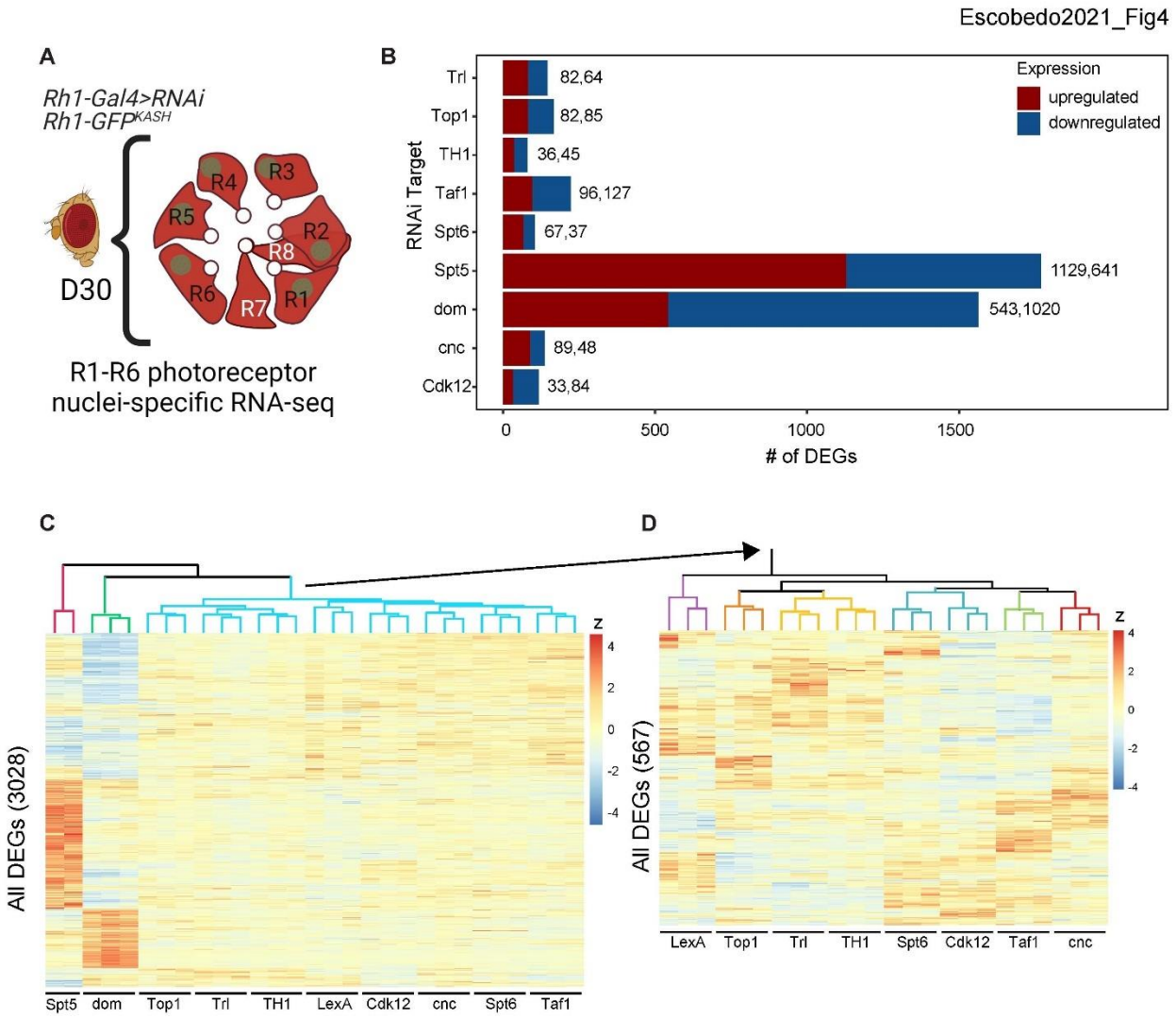

Figure 4-6. Knockdown of the factors required for photoreceptor survival leads to distinct and overlapping changes in gene expression in photoreceptors. A) Photoreceptor nuclear RNA-seq was performed in D30 flies expressing *sh-RNA* against 9 of the unique targets identified as being necessary for photoreceptor survival. B) Bar plot showing the number of significantly differentially expressed genes (DEGs, FDR < 0.05) identified for each *sh-RNA* target relative to the *sh-LexA* control. Up- and down-regulated genes are indicated in red and blue, respectively. C) Heatmap depicting the relative expression (z-score) across all samples for all 3028 DEGs identified in any *sh-RNA* line versus control, clustered by genes (rows) and samples (columns). Sample dendrogram is colored to show major groups. D) Heatmap showing the relative expression of the 567 DEGs identified in the blue cluster in panel C.

Next, we identified differentially expressed genes (DEGs, FDR < 0.05) in each RNAi line relative to the lexA control. Surprisingly, we only identified a relatively small number of DEGs (<250) in many of the RNAi lines (*Trl, Top1, TH1, Taf1, Spt6, Cnc, Cdk12*), while knockdown of *dom* and *Spt5* had much more widespread effects on gene expression with 1563 and 1129 DEGs, respectively. When we clustered the samples based on their relative expression (z score) for all DEGs, we found that both *Spt5* (red cluster) and *dom* (green cluster) samples were distinct from one another, and grouped separately from all other samples (Fig. 4C). When we repeated this clustering without *Spt5* and *dom* to examine the relationship between the other samples more closely, we found that several factors showed similar changes in gene expression such as Tr1 and *TH1* (yellow), or *Spt6* and *Cdk12* (blue), suggesting that these factors might regulate common sets of genes.

We next asked how the gene expression changes resulting from knockdown of these factors compared with those observed during normal aging in photoreceptors. To do this, we performed functional enrichment analysis on the DEGs identified upon knockdown of the 9 lines tested at D30, and compared this with age-dependent DEG sets previously identified in D50 and D60 photoreceptors relative to D10 [88]. We first separated DEGs into up- or down-regulated genes, and then identified enriched Gene Ontology terms (GO, FDR < 0.05) for each DEG set and compared these between gene sets using dot plots (Fig. 5A – B, complete list of enriched GO terms in Table S3). We did not identify any enriched GO terms in the DEGs for *Trl*, *TH1* or *cnc*, likely due to the relatively low number of DEGs in these samples. As suggested by the gene expression heatmaps, we observed similar GO terms enriched for *Cdk12*, *Spt6*, and *Taf1* downregulated DEGs, or *Spt6*, *Taf1*, and *Top1* upregulated genes that overlapped modestly with the age-regulated genes at D50 or D60 (Fig. 5A – B). Strikingly, *Spt5* and *dom* showed much stronger overlaps with the GO terms from the aging DEGs for both down- and up-regulated genes (Fig. 5A – B). Whereas *Spt5* and *dom* knockdown mimicked the aging DEGs for functional categories such as synapse activity, negative regulation of signaling, and growth, *dom* knockdown resembled aging even more extensively with commonly enriched GO terms including nervous system development, rhythmic processes, and responses to abiotic stress and regulation of the immune system. These data suggested that decreased levels of *Spt5* and *dom* resulted in similar gene expression changes at D30 to those observed in much older flies at D50 or D60. To test this, we directly compared the up- and downregulated DEGs identified upon *Spt5* or *dom* knockdown with the aging DEGs

identified at D60. We observed significant overlap of up- (Fig 6A-B) and downregulated (Fig. 6C-D) genes at D60 with both *Spt5* and *dom* knockdown at D30. Strikingly, more than half of all differentially expressed genes in *dom* RNAi were similarly differentially expressed in D60 flies (322/541 upregulated, 496/1014 downregulated). Although *Spt5* and Dom knockdown resembled D60 gene expression changes more than they did each other, there were also significant overlaps between all three sets of DEGs (Fig. 6; 66 up, $p = 6.62x10^{-28}$; 122 down-regulated genes, $p = 4.84x10^{-72}$).

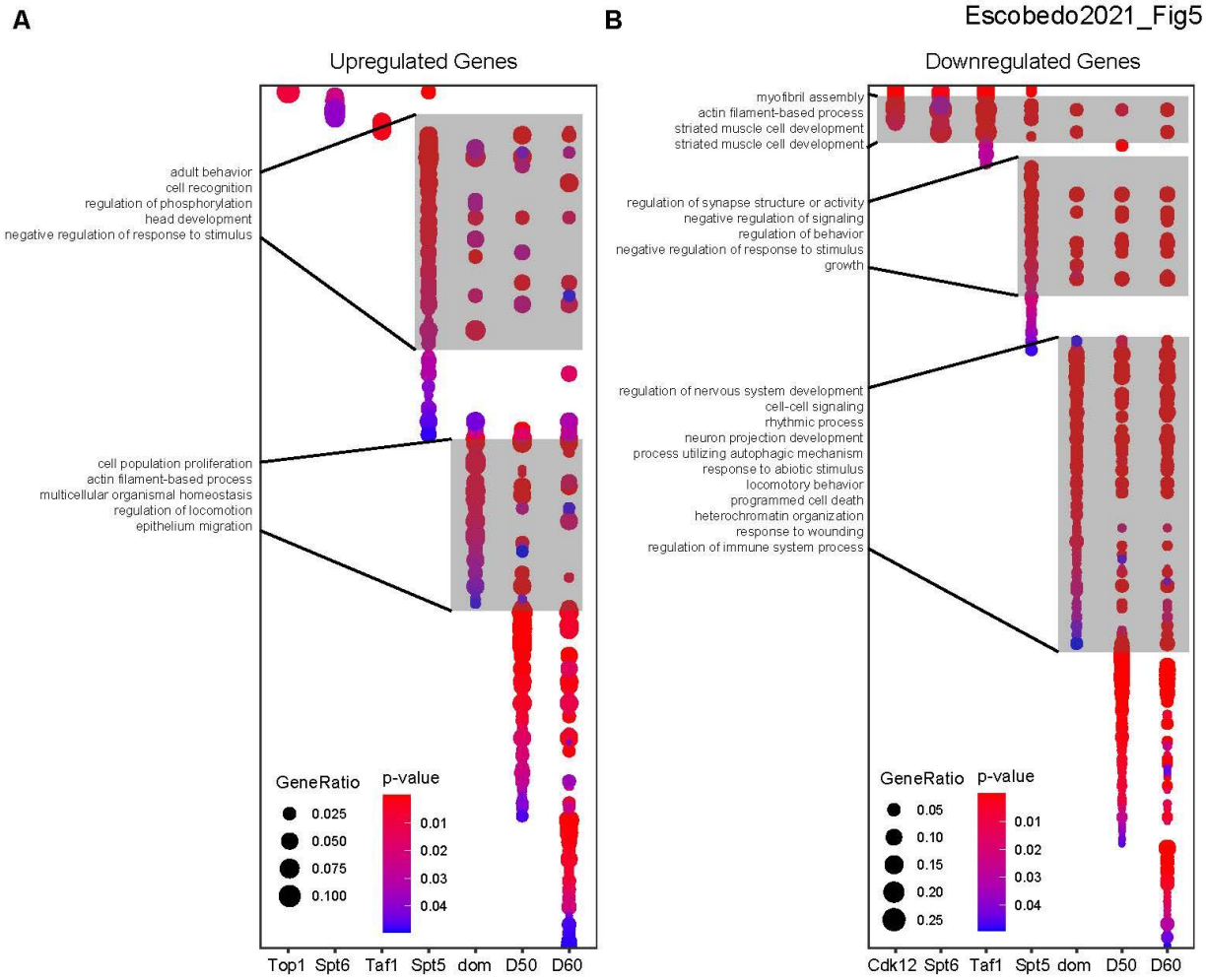

Figure 4-7. Knockdown of *Spt5* and *dom* results in gene expression changes that resemble those observed in aging photoreceptors. Dot plot depicting significantly enriched GO terms from up- (A) or down- (B) regulated genes identified in the indicated *sh-RNA* lines were compared with age-dependent changes in gene expression in photoreceptors between D10 and D30, D50, or D60. Selected GO term labels are shown, and a full list of all GO terms identified is provided in Table Sx.

To examine these common sets of genes more closely, we generated cnet plots, which display the DEGs that contribute to the enriched GO terms (Fig. 6A – B). Intriguingly, these cnet plots show that many of the neuronal-specific processes that we previously showed are downregulated with age in photoreceptors [23] require *dom* and *Spt5*, such as response to light, regulation of intracellular protein transport. Surprisingly, genes involved in circadian rhythm were also highly enriched in this common set of genes; we recently showed that disruption of the circadian clock in photoreceptors by expression of *dom*inant-negative Clock transcription factor results in altered chromatin accessibility, decreased expression of phototransduction genes, and retinal degeneration [88]. The unexpected finding that *dom* and *Spt5* knockdown also decreases expression of circadian genes, similar to the pattern observed in old photoreceptors, suggests a potential role for these transcription regulatory factors in this process. Together, these data suggest the loss of *Spt5* and *dom* mimic the gene expression changes seen in older D60 flies, resulting in a premature aging transcriptional signature.

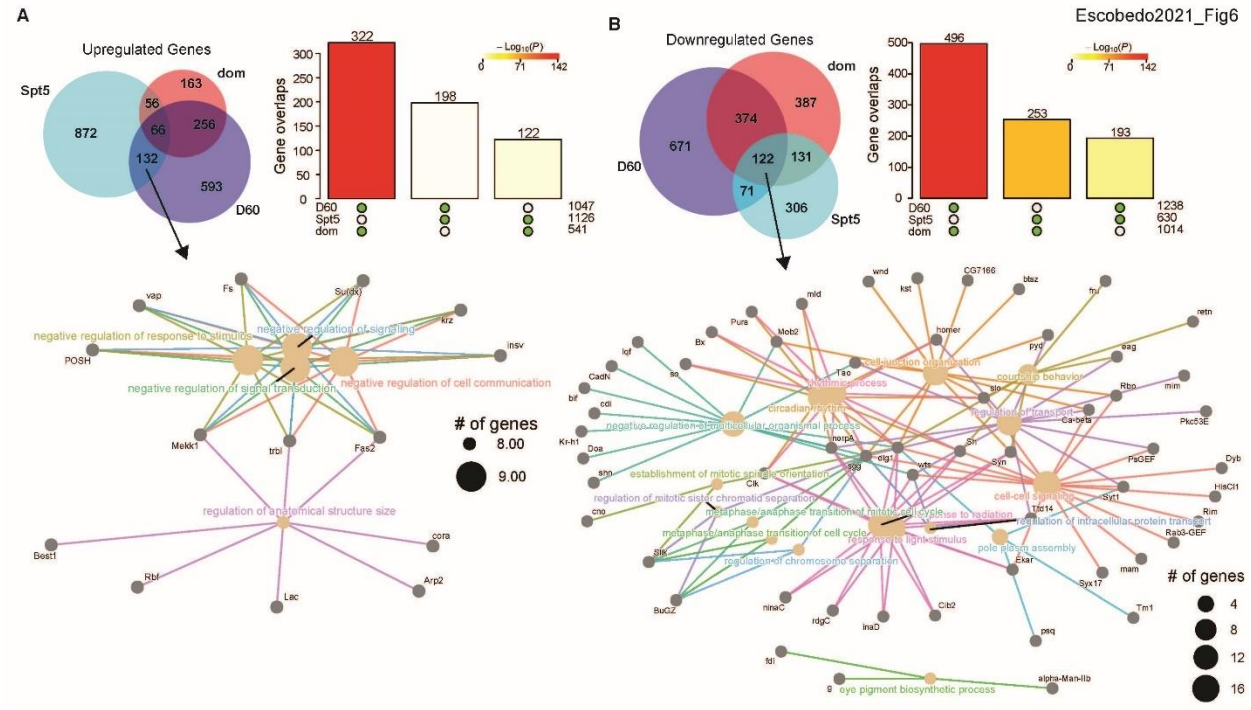

Figure 4-8. DEGs in photoreceptors with knockdown of *Spt5* and *dom* significantly overlap age-dependent DEGs in old flies. Venn diagrams of the overlap between up-(A) or down-(C) regulated gene sets upon knockdown of *Spt5* or *dom* or in old D60 photoreceptors. Significance of pairwise overlaps (bars) between gene sets were determined by Fishers exact test and colored by p-value. Green dots bellow bars indicate the gene sets for each pairwise overlap.

4.4 Discussion

Here, we show knockdown of factors that regulate the expression of age-dependent genes in photoreceptors results in premature retinal degeneration. These data suggest that maintaining proper gene expression programs is critical for the survival of aging photoreceptors. Although transcriptional regulators that are involved in gene repression were well represented in our intial set of 155 RNAi lines, no epigenetic factors involved in repression were identified in our 18 factors that are necessary for age-dependent photoreceptor survival. We do note, however, since we used the *Rh1-ffluc* reporter as a proxy for photoreceptor number in the RNAi screen, our data may also provide information on potential transcriptional regulators of Rh1 expression in adult photoreceptors. For example, we identified the transcription factors *cyc*, *CtBP* and *Utx* with increased luciferase activity relative to control, suggesting a potential role for these factors in repressing Rh1 (*ninaE*) transcription (Table S1). These data suggest that old photoreceptors, and potentially other neurons, might be most sensitive to decreased activity of the transcriptional mechanisms that promote, rather than repress, gene expression. Supporting this idea, there is a global decrease in chromatin accessibility in aging *Drosophila* photoreceptors [77], and two histone marks associated with active transcription show global genome-wide decreases in aging fly heads [152,153]. While our screen has broadly identified activators of transcription, previous studies in mouse IPSC's [154,155] and models of rapid aging disorders [156] show that the de-repression of heterochromatin may be a driving force of aging. *Drosophila* neurons also have increased activity of transposable elements [157] which have also been implicated in various human neurodegenerative diseases [158] This suggests that the loss of heterochromatin with age may lead to de-repression of these elements [159], and their ensuing activity may lead to increased genomic instability detrimental to aging neurons.

Knockdown of two factors, *Spt5* and *dom*, resulted in gene expression changes that resembled those in old photoreceptors, and in premature retinal degeneration. Spt5, one half of the highly conserved DSIF complex [160], is involved in stabilizing promoter proximally paused RNA Pol II [141,161]. Recent findings have shown that Spt5 prevents paused Pol II ubiquitination and degradation [162,163], and temporal knockdown in human cells results in decreased activation of target genes, and alterations in chromatin state. The *dom* gene encodes the only SWR1 like ATP dependent chromatin remodeler ortholog in flies. Recent findings have shown that the two isoforms of *dom* result in distinct multi-subunit complexes, DOM-A.C and DOM-B.C. While

DOM-B.C resembles the yeast SWR1 complex [164], incorporating H2AV genome wide [147,165], DOM-A.C includes the histone acetyltransferase and human *KAT5* ortholog *Tip60* [166], forming the NuA4 like complex [147,167]. Intriguingly, our RNAi screen also identified that knockdown of *Tip60* results in premature, age-dependent retinal degeneration in photoreceptors. *Tip60* regulated genes are commonly dysregulated with the onset of age-dependent neurological disease such as Alzheimer's [168–170], suggesting that *Tip60*, and specifically the activity of NuA4.C, may be responsible for some of the gene expression changes observed in aging photoreceptors. Our data suggest that neither *Spt5*, *dom nor Tip60* are downregulated at least at the transcript levels in aging photoreceptors (Fig. S3); we did not observe a significant decrease in expression for any of the 18 genes identified in our screen. Also, none of these genes with detectible protein levels in *Drosophila* heads or eyes have age-dependent changes in abundance [171]. Therefore, we propose that the activity of these proteins in their respective complexes decreases with age; however, the mechanisms that underly such a decrease in activity remain to be determined.

When we looked at significantly enriched GO terms in in the DEG sets for all 9 of our RNA-seq lines we observed common enrichment of pathways involved in actin- and myosin assembly and muscle cell development in the genes that were downregulated for *Cdk12, Spt6,Taf1, Spt5* and *dom*. These pathways were also downregulated in old photoreceptors. Age-dependent changes in the cytoskeleton have been identified in several model organisms [172] and has been identified as an important modulator of neurodegenerative disease [173–175]. 50% of the DEGs in *Spt5* and *dom* were also differentially expressed in old photoreceptors, with significant overlaps between all three DEG sets. These common up- and downregulated genes were enriched for functions involved in the negative regulation of signaling, response to light, circadian rhythm, and regulation of cellular transport. Intriguingly, DOM-A.C activity has been shown to regulate circadian genes in specialized neurons in the brain [176]. These data, together with previous findings from our lab and others suggest that the *Drosophila* NuA4 complex may be important for the regulation of circadian genes in aging neurons.

REFERENCES

(1) Cagan, R. Principles of Drosophila Eye Differentiation. *Curr Top Dev Biol* **2009**, *89*, 115–135. https://doi.org/10.1016/S0070-2153(09)89005-4.

(2) Ugur, B.; Chen, K.; Bellen, H. J. Drosophila Tools and Assays for the Study of Human Diseases. *Disease Models & Mechanisms* **2016**, *9* (3), 235–244. https://doi.org/10.1242/dmm.023762.

(3) McGurk, L.; Berson, A.; Bonini, N. M. Drosophila as an In Vivo Model for Human Neurodegenerative Disease. *Genetics* **2015**, *201* (2), 377–402. https://doi.org/10.1534/genetics.115.179457.

(4) Newsome, T. P.; Asling, B.; Dickson, B. J. Analysis of Drosophila Photoreceptor Axon Guidance in Eye-Specific Mosaics. *Development* **2000**, *127* (4), 851–860.

(5) Viktorinová, I.; Wimmer, E. A. Comparative Analysis of Binary Expression Systems for Directed Gene Expression in Transgenic Insects. *Insect Biochemistry and Molecular Biology* **2007**, *37* (3), 246–254. https://doi.org/10.1016/j.ibmb.2006.11.010.

(6) Webster, N.; Jin, J. R.; Green, S.; Hollis, M.; Chambon, P. The Yeast UASG Is a Transcriptional Enhancer in Human Hela Cells in the Presence of the GAL4 Trans-Activator. *Cell* **1988**, *52* (2), 169–178. https://doi.org/10.1016/0092-8674(88)90505-3.

(7) Duffy, J. B. GAL4 System in Drosophila: A Fly Geneticist's Swiss Army Knife. *Genesis* **2002**, *34* (1–2), 1–15. https://doi.org/10.1002/gene.10150.

(8) McGuire, S. E.; Le, P. T.; Osborn, A. J.; Matsumoto, K.; Davis, R. L. Spatiotemporal Rescue of Memory Dysfunction in Drosophila. *Science* **2003**, *302* (5651), 1765–1768. https://doi.org/10.1126/science.1089035.

(9) Osterwalder, T.; Yoon, K. S.; White, B. H.; Keshishian, H. A Conditional Tissue-Specific Transgene Expression System Using Inducible GAL4. *PNAS* **2001**, *98* (22), 12596–12601. https://doi.org/10.1073/pnas.221303298.

(10) Potter, C. J.; Tasic, B.; Russler, E. V.; Liang, L.; Luo, L. The Q System: A Repressible Binary System for Transgene Expression, Lineage Tracing, and Mosaic Analysis. *Cell* **2010**, *141* (3), 536–548. https://doi.org/10.1016/j.cell.2010.02.025.

(11) Dillon, M. E.; Wang, G.; Garrity, P. A.; Huey, R. B. Review: Thermal Preference in Drosophila. *J Therm Biol* **2009**, *34* (3), 109–119. https://doi.org/10.1016/j.jtherbio.2008.11.007.

(12) Ready, D. F.; Hanson, T. E.; Benzer, S. Development of the Drosophila Retina, a Neurocrystalline Lattice. *Developmental Biology* **1976**, *53* (2), 217–240. https://doi.org/10.1016/0012-1606(76)90225-6.

(13) RAY, M.; LAKHOTIA, S. C. The Commonly Used Eye-Specific Sev-GAL4 and GMR-GAL4 Drivers in Drosophila Melanogaster Are Expressed in Tissues Other than Eyes Also. *J Genet* **2015**, *94* (3), 407–416. https://doi.org/10.1007/s12041-015-0535-8.

(14) Kramer, J. M.; Staveley, B. E. GAL4 Causes Developmental Defects and Apoptosis When Expressed in the Developing Eye of Drosophila Melanogaster. *Genet. Mol. Res.* **2003**, *2* (1), 43–47.

(15) Huang, A. M.; Rehm, E. J.; Rubin, G. M. Recovery of DNA Sequences Flanking P-Element Insertions in Drosophila: Inverse PCR and Plasmid Rescue. *Cold Spring Harb Protoc* **2009**, *2009* (4), pdb.prot5199. https://doi.org/10.1101/pdb.prot5199.

(16) Riabinina, O.; Luginbuhl, D.; Marr, E.; Liu, S.; Wu, M. N.; Luo, L.; Potter, C. J. Improved and Expanded Q-System Reagents for Genetic Manipulations. *Nature Methods* **2015**, *12* (3), 219–222. https://doi.org/10.1038/nmeth.3250.

(17) Roman, G.; Endo, K.; Zong, L.; Davis, R. L. P{Switch}, a System for Spatial and Temporal Control of Gene Expression in Drosophila Melanogaster. *PNAS* **2001**, *98* (22), 12602–12607. https://doi.org/10.1073/pnas.221303998.

(18) Rister, J.; Razzaq, A.; Boodram, P.; Desai, N.; Tsanis, C.; Chen, H.; Jukam, D.; Desplan, C. Single–Base Pair Differences in a Shared Motif Determine Differential Rhodopsin Expression. *Science* **2015**, *350* (6265), 1258–1261. https://doi.org/10.1126/science.aab3417.

(19) Gohl, D. M.; Silies, M. A.; Gao, X. J.; Bhalerao, S.; Luongo, F. J.; Lin, C.-C.; Potter, C. J.; Clandinin, T. R. A Versatile in Vivo System for Directed Dissection of Gene Expression Patterns. *Nat. Methods* **2011**, *8* (3), 231–237. https://doi.org/10.1038/nmeth.1561.

(20) Rothwell, W. F.; Sullivan, W. Fixation of Drosophila Embryos. *CSH Protoc* **2007**, *2007*, pdb.prot4827. https://doi.org/10.1101/pdb.prot4827.

(21) O'Tousa, J. E.; Baehr, W.; Martin, R. L.; Hirsh, J.; Pak, W. L.; Applebury, M. L. The Drosophila NinaE Gene Encodes an Opsin. *Cell* **1985**, *40* (4), 839–850. https://doi.org/10.1016/0092-8674(85)90343-5.

(22) Kumar, J. P.; Ready, D. F. Rhodopsin Plays an Essential Structural Role in Drosophila Photoreceptor Development. *Development* **1995**, *121* (12), 4359–4370.

(23) Hall, H.; Medina, P.; Cooper, D. A.; Escobedo, S. E.; Rounds, J.; Brennan, K. J.; Vincent, C.; Miura, P.; Doerge, R.; Weake, V. M. Transcriptome Profiling of Aging Drosophila Photoreceptors Reveals Gene Expression Trends That Correlate with Visual Senescence. *BMC Genomics* **2017**, *18* (1), 894. https://doi.org/10.1186/s12864-017-4304-3.

(24) Ellis, M. C.; O'Neill, E. M.; Rubin, G. M. Expression of Drosophila Glass Protein and Evidence for Negative Regulation of Its Activity in Non-Neuronal Cells by Another DNA-Binding Protein. *Development* **1993**, *119* (3), 855–865.

(25) Freeman, M. Reiterative Use of the EGF Receptor Triggers Differentiation of All Cell Types in the Drosophila Eye. *Cell* **1996**, *87* (4), 651–660. https://doi.org/10.1016/S0092-8674(00)81385-9.

(26) Li, W.-Z.; Li, S.-L.; Zheng, H. Y.; Zhang, S.-P.; Xue, L. A Broad Expression Profile of the GMR-GAL4 Driver in Drosophila Melanogaster. *Genet. Mol. Res.* **2012**, *11* (3), 1997–2002. https://doi.org/10.4238/2012.August.6.4.

(27) Cherbas, L.; Hu, X.; Zhimulev, I.; Belyaeva, E.; Cherbas, P. EcR Isoforms in Drosophila: Testing Tissue-Specific Requirements by Targeted Blockade and Rescue. *Development* **2003**, *130* (2), 271–284. https://doi.org/10.1242/dev.00205.

(28) Hrdlicka, L.; Gibson, M.; Kiger, A.; Micchelli, C.; Schober, M.; Schöck, F.; Perrimon, N. Analysis of Twenty-Four Gal4 Lines in Drosophila Melanogaster. *Genesis* **2002**, *34* (1–2), 51–57. https://doi.org/10.1002/gene.10125.

(29) Freeman, M. Cell Determination Strategies in the Drosophila Eye. *Development* **1997**, *124* (2), 261–270.

(30) Wernet, M. F.; Labhart, T.; Baumann, F.; Mazzoni, E. O.; Pichaud, F.; Desplan, C. Homothorax Switches Function of Drosophila Photoreceptors from Color to Polarized Light Sensors. *Cell* **2003**, *115* (3), 267–279. https://doi.org/10.1016/S0092-8674(03)00848-1.

(31) Mazzoni, E. O.; Celik, A.; Wernet, M. F.; Vasiliauskas, D.; Johnston, R. J.; Cook, T. A.; Pichaud, F.; Desplan, C. Iroquois Complex Genes Induce Co-Expression of Rhodopsins in Drosophila. *PLoS Biol.* **2008**, *6* (4), e97. https://doi.org/10.1371/journal.pbio.0060097.

(32) Pollock, J. A.; Benzer, S. Transcript Localization of Four Opsin Genes in the Three Visual Organs of Drosophila ; RH2 Is Ocellus Specific. *Nature* **1988**, *333* (6175), 779–782. https://doi.org/10.1038/333779a0.

(33) Mollereau, B.; Wernet, M. F.; Beaufils, P.; Killian, D.; Pichaud, F.; Kühnlein, R.; Desplan, C. A Green Fluorescent Protein Enhancer Trap Screen in Drosophila Photoreceptor Cells. *Mechanisms of Development* **2000**, *93* (1), 151–160. https://doi.org/10.1016/S0925-4773(00)00287-2.

(34) Mismer, D.; Rubin, G. M. Analysis of the Promoter of the NinaE Opsin Gene in Drosophila Melanogaster. *Genetics* **1987**, *116* (4), 565–578.

(35) Riabinina, O.; Potter, C. J. The Q-System: A Versatile Expression System for Drosophila. *Methods Mol. Biol.* **2016**, *1478*, 53–78. https://doi.org/10.1007/978-1-4939-6371-3_3.

(36) Roman, G.; Davis, R. L. Conditional Expression of UAS-Transgenes in the Adult Eye with a New Gene-Switch Vector System. *genesis* **2002**, *34* (1–2), 127–131. https://doi.org/10.1002/gene.10133.

(37) Wang, Y.; O'Malley, B. W.; Tsai, S. Y.; O'Malley, B. W. A Regulatory System for Use in Gene Transfer. *Proc. Natl. Acad. Sci. U.S.A.* **1994**, *91* (17), 8180–8184. https://doi.org/10.1073/pnas.91.17.8180.

(38) Bateman, J. R.; Lee, A. M.; Wu, C. -ting. Site-Specific Transformation of Drosophila via ΦC31 Integrase-Mediated Cassette Exchange. *Genetics* **2006**, *173* (2), 769–777. https://doi.org/10.1534/genetics.106.056945.

(39) Sheng, G.; Thouvenot, E.; Schmucker, D.; Wilson, D. S.; Desplan, C. Direct Regulation of Rhodopsin 1 by Pax-6/Eyeless in Drosophila: Evidence for a Conserved Function in Photoreceptors. *Genes Dev.* **1997**, *11* (9), 1122–1131. https://doi.org/10.1101/gad.11.9.1122.

(40) Papatsenko, D.; Nazina, A.; Desplan, C. A Conserved Regulatory Element Present in All Drosophila Rhodopsin Genes Mediates Pax6 Functions and Participates in the Fine-Tuning of Cell-Specific Expression. *Mech Dev* **2001**, *101* (1–2), 143–153. https://doi.org/10.1016/s0925-4773(00)00581-5.

(41) Mishra, M.; Oke, A.; Lebel, C.; McDonald, E. C.; Plummer, Z.; Cook, T. A.; Zelhof, A. C. Pph13 and Orthodenticle Define a Dual Regulatory Pathway for Photoreceptor Cell Morphogenesis and Function. *Development* **2010**, *137* (17), 2895–2904. https://doi.org/10.1242/dev.051722.

(42) Mismer, D.; Rubin, G. M. Definition of Cis-Acting Elements Regulating Expression of the Drosophila Melanogaster Ninae Opsin Gene by Oligonucleotide-Directed Mutagenesis. *Genetics* **1989**, *121* (1), 77–87.

(43) Fortini, M. E.; Rubin, G. M. Analysis of Cis-Acting Requirements of the Rh3 and Rh4 Genes Reveals a Bipartite Organization to Rhodopsin Promoters in Drosophila Melanogaster. *Genes & Development* **1990**, *4* (3), 444–463. https://doi.org/10.1101/gad.4.3.444.

(44) FlyBase Reference Report: Freeman, 1996.10.3, GMR-GAL4. http://flybase.org/reports/FBrf0089999.html#reference (accessed 2021 -03 -14).

(45) Harman, D. Aging: A Theory Based on Free Radical and Radiation Chemistry. *J Gerontol* **1956**, *11* (3), 298–300. https://doi.org/10.1093/geronj/11.3.298.

(46) The Hallmarks of Aging https://www.ncbi.nlm.nih.gov/pmc/articles/PMC3836174/ (accessed 2020 -11 -13).

(47) Andersen, G. J. Aging and Vision: Changes in Function and Performance from Optics to Perception. *Wiley Interdiscip Rev Cogn Sci* **2012**, *3* (3), 403–410. https://doi.org/10.1002/wcs.1167.

(48) Hall, H.; Medina, P.; Cooper, D. A.; Escobedo, S. E.; Rounds, J.; Brennan, K. J.; Vincent, C.; Miura, P.; Doerge, R.; Weake, V. M. Transcriptome Profiling of Aging Drosophila Photoreceptors Reveals Gene Expression Trends That Correlate with Visual Senescence. *BMC Genomics* **2017**, *18*. https://doi.org/10.1186/s12864-017-4304-3.

(49) Carbone, M. A.; Yamamoto, A.; Huang, W.; Lyman, R. A.; Meadors, T. B.; Yamamoto, R.; Anholt, R. R. H.; Mackay, T. F. C. Genetic Architecture of Natural Variation in Visual Senescence in Drosophila. *PNAS* **2016**, *113* (43), E6620–E6629. https://doi.org/10.1073/pnas.1613833113.

(50) Gipson, I. K. Age-Related Changes and Diseases of the Ocular Surface and Cornea. *Investigative Ophthalmology & Visual Science* **2013**, *54* (14), ORSF48–ORSF53. https://doi.org/10.1167/iovs.13-12840.

(51) Spitzer, M. S.; Januschowski, K. Gesunder Glaskörper und seine Alterung. *Ophthalmologe* **2015**, *112* (7), 552–558. https://doi.org/10.1007/s00347-015-0031-9.

(52) Curcio, C. A.; Millican, C. L.; Allen, K. A.; Kalina, R. E. Aging of the Human Photoreceptor Mosaic: Evidence for Selective Vulnerability of Rods in Central Retina. *Invest Ophthalmol Vis Sci* **1993**, *34* (12), 3278–3296.

(53) Jackson, G. R.; Owsley, C.; Curcio, C. A. Photoreceptor Degeneration and Dysfunction in Aging and Age-Related Maculopathy. *Ageing Res Rev* **2002**, *1* (3), 381–396. https://doi.org/10.1016/s1568-1637(02)00007-7.

(54) Campello, L.; Singh, N.; Advani, J.; Mondal, A. K.; Corso-Díaz, X.; Swaroop, A. Aging of the Retina: Molecular and Metabolic Turbulences and Potential Interventions. *Annu. Rev. Vis. Sci.* **2021**, *7* (1), 633–664. https://doi.org/10.1146/annurev-vision-100419-114940.

(55) Maylahn, C.; Gohdes, D. M.; Balamurugan, A.; Larsen, B. A. Age-Related Eye Diseases: An Emerging Challenge for Public Health Professionals. *Prev Chronic Dis* **2005**, *2* (3), A17.

(56) Velilla, S.; García-Medina, J. J.; García-Layana, A.; Dolz-Marco, R.; Pons-Vázquez, S.; Pinazo-Durán, M. D.; Gómez-Ulla, F.; Arévalo, J. F.; Díaz-Llopis, M.; Gallego-Pinazo, R. Smoking and Age-Related Macular Degeneration: Review and Update. *J Ophthalmol* **2013**, *2013*, 895147. https://doi.org/10.1155/2013/895147.

(57) Capurso, C.; Bellanti, F.; Lo Buglio, A.; Vendemiale, G. The Mediterranean Diet Slows Down the Progression of Aging and Helps to Prevent the Onset of Frailty: A Narrative Review. *Nutrients* **2019**, *12* (1), E35. https://doi.org/10.3390/nu12010035.

(58) Rittié, L.; Fisher, G. J. Natural and Sun-Induced Aging of Human Skin. *Cold Spring Harb Perspect Med* **2015**, *5* (1), a015370. https://doi.org/10.1101/cshperspect.a015370.

(59) Arshavsky, V. Y.; Lamb, T. D.; Pugh, E. N. G Proteins and Phototransduction. *Annu Rev Physiol* **2002**, *64*, 153–187. https://doi.org/10.1146/annurev.physiol.64.082701.102229.

(60) Wang, T.; Montell, C. Phototransduction and Retinal Degeneration in Drosophila. *Pflugers Arch - Eur J Physiol* **2007**, *454* (5), 821–847. https://doi.org/10.1007/s00424-007-0251-1.

(61) Katz, B.; Minke, B. Drosophila Photoreceptors and Signaling Mechanisms. *Front Cell Neurosci* **2009**, *3*, 2. https://doi.org/10.3389/neuro.03.002.2009.

(62) Hillman, P.; Hochstein, S.; Minke, B. A Visual Pigment with Two Physiologically Active Stable States. *Science* **1972**, *175* (4029), 1486–1488. https://doi.org/10.1126/science.175.4029.1486.

(63) White, R. H. Insect Visual Pigments. In *Advances in Insect Physiology*; Treherne, J. E., Berridge, M. J., Wigglesworth, V. B., Eds.; Academic Press, 1978; Vol. 13, pp 35–67. https://doi.org/10.1016/S0065-2806(08)60264-7.

(64) Chen, X.; Leon-Salas, W. D.; Zigon, T.; Ready, D. F.; Weake, V. M. A Programmable Optical Stimulator for the Drosophila Eye. *HardwareX* **2017**, *2*, 13–33. https://doi.org/10.1016/j.ohx.2017.07.001.

(65) Weiss, S.; Kohn, E.; Dadon, D.; Katz, B.; Peters, M.; Lebendiker, M.; Kosloff, M.; Colley, N. J.; Minke, B. Compartmentalization and Ca2+ Buffering Are Essential for Prevention of Light-Induced Retinal Degeneration. *J Neurosci* **2012**, *32* (42), 14696–14708. https://doi.org/10.1523/JNEUROSCI.2456-12.2012.

(66) Weiss, S.; Minke, B. A New Genetic Model for Calcium Induced Autophagy and ER-Stress in Drosophila Photoreceptor Cells. *Channels (Austin)* **2015**, *9* (1), 14–20. https://doi.org/10.4161/19336950.2014.981439.

(67) Satoh, A. K.; Ready, D. F. Arrestin1 Mediates Light-Dependent Rhodopsin Endocytosis and Cell Survival. *Current Biology* **2005**, *15* (19), 1722–1733. https://doi.org/10.1016/j.cub.2005.08.064.

(68) Kiselev, A.; Socolich, M.; Vinós, J.; Hardy, R. W.; Zuker, C. S.; Ranganathan, R. A Molecular Pathway for Light-Dependent Photoreceptor Apoptosis in Drosophila. *Neuron* **2000**, *28* (1), 139–152. https://doi.org/10.1016/s0896-6273(00)00092-1.

(69) Nash, T. R.; Chow, E. S.; Law, A. D.; Fu, S. D.; Fuszara, E.; Bilska, A.; Bebas, P.; Kretzschmar, D.; Giebultowicz, J. M. Daily Blue-Light Exposure Shortens Lifespan and Causes Brain Neurodegeneration in Drosophila. *npj Aging Mech Dis* **2019**, *5* (1), 1–8. https://doi.org/10.1038/s41514-019-0038-6.

(70) Stegeman, R.; Weake, V. M. Transcriptional Signatures of Aging. *J Mol Biol* **2017**, *429* (16), 2427–2437. https://doi.org/10.1016/j.jmb.2017.06.019.

(71) Ratnapriya, R.; Sosina, O. A.; Starostik, M. R.; Kwicklis, M.; Kapphahn, R. J.; Fritsche, L. G.; Walton, A.; Arvanitis, M.; Gieser, L.; Pietraszkiewicz, A.; Montezuma, S. R.; Chew, E. Y.; Battle, A.; Abecasis, G. R.; Ferrington, D. A.; Chatterjee, N.; Swaroop, A. Retinal Transcriptome and EQTL Analyses Identify Genes Associated with Age-Related Macular Degeneration. *Nat Genet* **2019**, *51* (4), 606–610. https://doi.org/10.1038/s41588-019-0351-9.

(72) Liang, Q.; Dharmat, R.; Owen, L.; Shakoor, A.; Li, Y.; Kim, S.; Vitale, A.; Kim, I.; Morgan, D.; Liang, S.; Wu, N.; Chen, K.; DeAngelis, M. M.; Chen, R. Single-Nuclei RNA-Seq on Human Retinal Tissue Provides Improved Transcriptome Profiling. *Nat Commun* **2019**, *10* (1), 5743. https://doi.org/10.1038/s41467-019-12917-9.

(73) Hall, H.; Ma, J.; Shekhar, S.; Leon-Salas, W. D.; Weake, V. M. Blue Light Induces a Neuroprotective Gene Expression Program in Drosophila Photoreceptors. *BMC Neurosci* **2018**, *19*. https://doi.org/10.1186/s12868-018-0443-y.

(74) Tearle, R. Tissue Specific Effects of Ommochrome Pathway Mutations in Drosophila Melanogaster. *Genetics Research* **1991**, *57* (3), 257–266. https://doi.org/10.1017/S0016672300029402.

(75) Ma, J.; Weake, V. M. Affinity-Based Isolation of Tagged Nuclei from Drosophila Tissues for Gene Expression Analysis. *JoVE (Journal of Visualized Experiments)* **2014**, No. 85, e51418. https://doi.org/10.3791/51418.

(76) Escobedo, S. E.; Shah, A.; Easton, A. N.; Hall, H.; Weake, V. M. Characterizing a Gene Expression Toolkit for Eye- and Photoreceptor-Specific Expression in Drosophila. *Fly* **2021**, *15* (1), 73–88. https://doi.org/10.1080/19336934.2021.1915683.

(77) Jauregui-Lozano, J.; Bakhle, K.; Weake, V. M. In Vivo Tissue-Specific Chromatin Profiling in Drosophila Melanogaster Using GFP-Tagged Nuclei. *Genetics* **2021**, *218* (3). https://doi.org/10.1093/genetics/iyab079.

(78) Trimmomatic: a flexible trimmer for Illumina sequence data | Bioinformatics | Oxford Academic https://academic.oup.com/bioinformatics/article/30/15/2114/2390096 (accessed 2021 -09 -15).

(79) Kim, D.; Paggi, J. M.; Park, C.; Bennett, C.; Salzberg, S. L. Graph-Based Genome Alignment and Genotyping with HISAT2 and HISAT-Genotype. *Nat Biotechnol* **2019**, *37* (8), 907–915. https://doi.org/10.1038/s41587-019-0201-4.

(80) Sequence Alignment/Map format and SAMtools | Bioinformatics | Oxford Academic https://academic.oup.com/bioinformatics/article/25/16/2078/204688 (accessed 2021 -09 -15).

(81) Anders, S.; Pyl, P. T.; Huber, W. HTSeq—a Python Framework to Work with High-Throughput Sequencing Data. *Bioinformatics* **2015**, *31* (2), 166–169. https://doi.org/10.1093/bioinformatics/btu638.

(82) Normalization of RNA-seq data using factor analysis of control genes or samples | Nature Biotechnology https://www.nature.com/articles/nbt.2931 (accessed 2021 -09 -15).

(83) Robinson, M. D.; McCarthy, D. J.; Smyth, G. K. EdgeR: A Bioconductor Package for Differential Expression Analysis of Digital Gene Expression Data. *Bioinformatics* **2010**, *26* (1), 139–140. https://doi.org/10.1093/bioinformatics/btp616.

(84) Kolde, R. *Pheatmap: Pretty Heatmaps*; 2019.

(85) Yu, G.; Wang, L.-G.; Han, Y.; He, Q.-Y. ClusterProfiler: An R Package for Comparing Biological Themes Among Gene Clusters. *OMICS: A Journal of Integrative Biology* **2012**, *16* (5), 284–287. https://doi.org/10.1089/omi.2011.0118.

(86) clusterProfiler 4.0: A universal enrichment tool for interpreting omics data: The Innovation https://www.cell.com/the-innovation/fulltext/S2666-6758(21)00066-7?_returnURL=https%3A%2F%2Flinkinghub.elsevier.com%2Fretrieve%2Fpii%2FS2666675821000667%3Fshowall%3Dtrue (accessed 2021 -09 -15).

(87) Wang, M.; Zhao, Y.; Zhang, B. Efficient Test and Visualization of Multi-Set Intersections. *Sci Rep* **2015**, *5* (1), 16923. https://doi.org/10.1038/srep16923.

(88) Jauregui-Lozano, J.; Hall, H.; Stanhope, S. C.; Bakhle, K. M.; Marlin, M. N.; Weake, V. M. *The Clock:Cycle Complex Is a Major Transcriptional Regulator of Drosophila Photoreceptors That Protects the Eye from Retinal Degeneration and Oxidative Stress*. https://doi.org/10.1101/2021.09.27.461946.

(89) Santos, N. V. dos; Saponi, C. F.; Greaves, T. L.; Pereira, J. F. B. Revealing a New Fluorescence Peak of the Enhanced Green Fluorescent Protein Using Three-Dimensional Fluorescence Spectroscopy. *RSC Adv.* **2019**, *9* (40), 22853–22858. https://doi.org/10.1039/C9RA02567G.

(90) Hye Oh, J.; Ji Yang, S.; Rag Do, Y. Healthy, Natural, Efficient and Tunable Lighting: Four-Package White LEDs for Optimizing the Circadian Effect, Color Quality and Vision Performance. *Light Sci Appl* **2014**, *3* (2), e141–e141. https://doi.org/10.1038/lsa.2014.22.

(91) Pust, P.; Schmidt, P. J.; Schnick, W. A Revolution in Lighting. *Nat Mater* **2015**, *14* (5), 454–458. https://doi.org/10.1038/nmat4270.

(92) Pust, P.; Weiler, V.; Hecht, C.; Tücks, A.; Wochnik, A. S.; Henß, A.-K.; Wiechert, D.; Scheu, C.; Schmidt, P. J.; Schnick, W. Narrow-Band Red-Emitting $Sr[LiAl_3N_4]:Eu^{2+}$ as a next-Generation LED-Phosphor Material. *Nat Mater* **2014**, *13* (9), 891–896. https://doi.org/10.1038/nmat4012.

(93) Salih, A.; Larkum, A.; Cox, G.; Kühl, M.; Hoegh-Guldberg, O. Fluorescent Pigments in Corals Are Photoprotective. *Nature* **2000**, *408* (6814), 850–853. https://doi.org/10.1038/35048564.

(94) Smith, E. G.; D'Angelo, C.; Salih, A.; Wiedenmann, J. Screening by Coral Green Fluorescent Protein (GFP)-like Chromoproteins Supports a Role in Photoprotection of Zooxanthellae. *Coral Reefs* **2013**, *32* (2), 463–474. https://doi.org/10.1007/s00338-012-0994-9.

(95) Quick, C.; D'Angelo, C.; Wiedenmann, J. Trade-Offs Associated with Photoprotective Green Fluorescent Protein Expression as Potential Drivers of Balancing Selection for Color Polymorphism in Reef Corals. *Frontiers in Marine Science* **2018**, *5*, 11. https://doi.org/10.3389/fmars.2018.00011.

(96) Schriner, S. E.; Linford, N. J. Extension of Mouse Lifespan by Overexpression of Catalase. *Age (Dordr)* **2006**, *28* (2), 209–218. https://doi.org/10.1007/s11357-006-9010-z.

(97) Selvaratnam, J.; Robaire, B. Overexpression of Catalase in Mice Reduces Age-Related Oxidative Stress and Maintains Sperm Production. *Exp Gerontol* **2016**, *84*, 12–20. https://doi.org/10.1016/j.exger.2016.08.012.

(98) Nandi, A.; Yan, L.-J.; Jana, C. K.; Das, N. Role of Catalase in Oxidative Stress- and Age-Associated Degenerative Diseases. *Oxidative Medicine and Cellular Longevity* **2019**, *2019*, e9613090. https://doi.org/10.1155/2019/9613090.

(99) Frade, J. M.; Ovejero-Benito, M. C. Neuronal Cell Cycle: The Neuron Itself and Its Circumstances. *Cell Cycle* **2015**, *14* (5), 712–720. https://doi.org/10.1080/15384101.2015.1004937.

(100) Freeman, R. S.; Estus, S.; Johnson, E. M. Analysis of Cell Cycle-Related Gene Expression in Postmitotic Neurons: Selective Induction of Cyclin D1 during Programmed Cell Death. *Neuron* **1994**, *12* (2), 343–355. https://doi.org/10.1016/0896-6273(94)90276-3.

(101) Herrup, K.; Neve, R.; Ackerman, S. L.; Copani, A. Divide and Die: Cell Cycle Events as Triggers of Nerve Cell Death. *J. Neurosci.* **2004**, *24* (42), 9232–9239. https://doi.org/10.1523/JNEUROSCI.3347-04.2004.

(102) Kruman, I. I. Why Do Neurons Enter the Cell Cycle? *Cell Cycle* **2004**, *3* (6), 767–771. https://doi.org/10.4161/cc.3.6.901.

(103) Zerofsky, M.; Harel, E.; Silverman, N.; Tatar, M. Aging of the Innate Immune Response in Drosophila Melanogaster. *Aging Cell* **2005**, *4* (2), 103–108. https://doi.org/10.1111/j.1474-9728.2005.00147.x.

(104) Garschall, K.; Flatt, T. The Interplay between Immunity and Aging in Drosophila. *F1000Res* **2018**, *7*, 160. https://doi.org/10.12688/f1000research.13117.1.

(105) Turi, Z.; Lacey, M.; Mistrik, M.; Moudry, P. Impaired Ribosome Biogenesis: Mechanisms and Relevance to Cancer and Aging. *Aging (Albany NY)* **2019**, *11* (8), 2512–2540. https://doi.org/10.18632/aging.101922.

(106) Chyb, S.; Hevers, W.; Forte, M.; Wolfgang, W. J.; Selinger, Z.; Hardie, R. C. Modulation of the Light Response by CAMP InDrosophila Photoreceptors. *J Neurosci* **1999**, *19* (20), 8799–8807. https://doi.org/10.1523/JNEUROSCI.19-20-08799.1999.

(107) Midorikawa, R.; Yamamoto-Hino, M.; Awano, W.; Hinohara, Y.; Suzuki, E.; Ueda, R.; Goto, S. Autophagy-Dependent Rhodopsin Degradation Prevents Retinal Degeneration in Drosophila. *J Neurosci* **2010**, *30* (32), 10703–10719. https://doi.org/10.1523/JNEUROSCI.2061-10.2010.

(108) Zhang, X.; Yang, D.; Hughes, B. A. KCNQ5/Kv7.5 Potassium Channel Expression and Subcellular Localization in Primate Retinal Pigment Epithelium and Neural Retina. *Am J Physiol Cell Physiol* **2011**, *301* (5), C1017–C1026. https://doi.org/10.1152/ajpcell.00185.2011.

(109) Abdul Kadir, L.; Stacey, M.; Barrett-Jolley, R. Emerging Roles of the Membrane Potential: Action Beyond the Action Potential. *Frontiers in Physiology* **2018**, *9*, 1661. https://doi.org/10.3389/fphys.2018.01661.

(110) Liguori, I.; Russo, G.; Curcio, F.; Bulli, G.; Aran, L.; Della-Morte, D.; Gargiulo, G.; Testa, G.; Cacciatore, F.; Bonaduce, D.; Abete, P. Oxidative Stress, Aging, and Diseases. *Clin Interv Aging* **2018**, *13*, 757–772. https://doi.org/10.2147/CIA.S158513.

(111) Tan, B. L.; Norhaizan, M. E.; Liew, W.-P.-P.; Sulaiman Rahman, H. Antioxidant and Oxidative Stress: A Mutual Interplay in Age-Related Diseases. *Frontiers in Pharmacology* **2018**, *9*, 1162. https://doi.org/10.3389/fphar.2018.01162.

(112) Chen, X.; Hall, H.; Simpson, J. P.; Leon-Salas, W. D.; Ready, D. F.; Weake, V. M. Cytochrome B5 Protects Photoreceptors from Light Stress-Induced Lipid Peroxidation and Retinal Degeneration. *npj Aging and Mechanisms of Disease* **2017**, *3* (1), 1–9. https://doi.org/10.1038/s41514-017-0019-6.

(113) Maher, P. The Effects of Stress and Aging on Glutathione Metabolism. *Ageing Res Rev* **2005**, *4* (2), 288–314. https://doi.org/10.1016/j.arr.2005.02.005.

(114) McCay, P. B.; Gibson, D. D.; Kuo-Lan, F.; K. Roger, H. Effect of Glutathione Peroxidase Activity on Lipid Peroxidation in Biological Membranes. *Biochimica et Biophysica Acta (BBA) - Lipids and Lipid Metabolism* **1976**, *431* (3), 459–468. https://doi.org/10.1016/0005-2760(76)90212-5.

(115) Jones, D. P.; Carlson, J. L.; Mody, V. C.; Cai, J.; Lynn, M. J.; Sternberg, P. Redox State of Glutathione in Human Plasma. *Free Radical Biology and Medicine* **2000**, *28* (4), 625–635. https://doi.org/10.1016/S0891-5849(99)00275-0.

(116) Florholmen-Kjær, Å.; Lysså, R. A.; Fuskevåg, O.-M.; Goll, R.; Revhaug, A.; Mortensen, K. E. A Sensitive Method for the Analysis of Glutathione in Porcine Hepatocytes. *Scandinavian Journal of Gastroenterology* **2014**, *49* (11), 1359–1366. https://doi.org/10.3109/00365521.2014.964757.

(117) Ferreiro, M. J.; Pérez, C.; Marchesano, M.; Ruiz, S.; Caputi, A.; Aguilera, P.; Barrio, R.; Cantera, R. Drosophila Melanogaster White Mutant W1118 Undergo Retinal Degeneration. *Front Neurosci* **2018**, *11*, 732. https://doi.org/10.3389/fnins.2017.00732.

(118) Hall, H.; Cooper, B. R.; Qi, G.; Wijeratne, A. B.; Mosley, A. L.; Weake, V. M. Quantitative Proteomic and Metabolomic Profiling Reveals Altered Mitochondrial Metabolism and Folate Biosynthesis Pathways in the Aging Drosophila Eye. *Mol Cell Proteomics* **2021**, *20*, 100127. https://doi.org/10.1016/j.mcpro.2021.100127.

(119) Klaver, C. C. W.; Wolfs, R. C. W.; Vingerling, J. R.; Hofman, A.; de Jong, P. T. V. M. Age-Specific Prevalence and Causes of Blindness and Visual Impairment in an Older Population: The Rotterdam Study. *Archives of Ophthalmology* **1998**, *116* (5), 653–658. https://doi.org/10.1001/archopht.116.5.653.

(120) Klein, R.; Klein, B. E. K. The Prevalence of Age-Related Eye Diseases and Visual Impairment in Aging: Current Estimates. *Investigative Ophthalmology & Visual Science* **2013**, *54* (14), ORSF5–ORSF13. https://doi.org/10.1167/iovs.13-12789.

(121) Coleman, H. R.; Chan, C.-C.; Ferris, F. L.; Chew, E. Y. Age-Related Macular Degeneration. *Lancet* **2008**, *372* (9652), 1835–1845. https://doi.org/10.1016/S0140-6736(08)61759-6.

(122) Ng Yin Ling, C.; Lim, S. C.; Jonas, J. B.; Sabanayagam, C. Obesity and Risk of Age-Related Eye Diseases: A Systematic Review of Prospective Population-Based Studies. *Int J Obes* **2021**, *45* (9), 1863–1885. https://doi.org/10.1038/s41366-021-00829-y.

(123) Swaroop, A.; Kim, D.; Forrest, D. Transcriptional Regulation of Photoreceptor Development and Homeostasis in the Mammalian Retina. *Nat Rev Neurosci* **2010**, *11* (8), 563–576. https://doi.org/10.1038/nrn2880.

(124) Parapuram, S. K.; Cojocaru, R. I.; Chang, J. R.; Khanna, R.; Brooks, M.; Othman, M.; Zareparsi, S.; Khan, N. W.; Gotoh, N.; Cogliati, T.; Swaroop, A. Distinct Signature of Altered Homeostasis in Aging Rod Photoreceptors: Implications for Retinal Diseases. *PLoS One* **2010**, *5* (11), e13885. https://doi.org/10.1371/journal.pone.0013885.

(125) Wang, J.; Zibetti, C.; Shang, P.; Sripathi, S. R.; Zhang, P.; Cano, M.; Hoang, T.; Xia, S.; Ji, H.; Merbs, S. L.; Zack, D. J.; Handa, J. T.; Sinha, D.; Blackshaw, S.; Qian, J. ATAC-Seq Analysis Reveals a Widespread Decrease of Chromatin Accessibility in Age-Related Macular Degeneration. *Nat Commun* **2018**, *9* (1), 1364. https://doi.org/10.1038/s41467-018-03856-y.

(126) Corso-Díaz, X.; Gentry, J.; Rebernick, R.; Jaeger, C.; Brooks, M. J.; van Asten, F.; Kooragayala, K.; Gieser, L.; Nellissery, J.; Covian, R.; Cogliati, T.; Mondal, A. K.; Jiang, K.; Swaroop, A. Genome-Wide Profiling Identifies DNA Methylation Signatures of Aging in Rod Photoreceptors Associated with Alterations in Energy Metabolism. *Cell Reports* **2020**, *31* (3), 107525. https://doi.org/10.1016/j.celrep.2020.107525.

(127) Stegeman, R.; Hall, H.; Escobedo, S. E.; Chang, H. C.; Weake, V. M. Proper Splicing Contributes to Visual Function in the Aging *Drosophila* Eye. *Aging Cell* **2018**, *17* (5), e12817. https://doi.org/10.1111/acel.12817.

(128) Horvath, S. DNA Methylation Age of Human Tissues and Cell Types. *Genome Biol* **2013**, *14* (10), R115. https://doi.org/10.1186/gb-2013-14-10-r115.

(129) Pal, S.; Tyler, J. K. Epigenetics and Aging. *Sci Adv* **2016**, *2* (7), e1600584. https://doi.org/10.1126/sciadv.1600584.

(130) Horvath, S.; Raj, K. DNA Methylation-Based Biomarkers and the Epigenetic Clock Theory of Ageing. *Nat Rev Genet* **2018**, *19* (6), 371–384. https://doi.org/10.1038/s41576-018-0004-3.

(131) Weake, V. M.; Jauregui-Lozano, J. P. In vivo tissue-specific chromatin profiling in Drosophila https://www.protocols.io/view/in-vivo-tissue-specific-chromatin-profiling-in-dro-buiqnudw (accessed 2021 -12 -02).

(132) Franceschini, N.; Kirschfeld, K. Les phénomènes de pseudopupille dans l'œil composé deDrosophila. *Kybernetik* **1971**, *9* (5), 159–182. https://doi.org/10.1007/BF02215177.

(133) Dietzl, G.; Chen, D.; Schnorrer, F.; Su, K.-C.; Barinova, Y.; Fellner, M.; Gasser, B.; Kinsey, K.; Oppel, S.; Scheiblauer, S.; Couto, A.; Marra, V.; Keleman, K.; Dickson, B. J. A Genome-Wide Transgenic RNAi Library for Conditional Gene Inactivation in Drosophila. *Nature* **2007**, *448* (7150), 151–156. https://doi.org/10.1038/nature05954.

(134) Ni, J.-Q.; Zhou, R.; Czech, B.; Liu, L.-P.; Holderbaum, L.; Yang-Zhou, D.; Shim, H.-S.; Tao, R.; Handler, D.; Karpowicz, P.; Binari, R.; Booker, M.; Brennecke, J.; Perkins, L. A.; Hannon, G. J.; Perrimon, N. A Genome-Scale ShRNA Resource for Transgenic RNAi in Drosophila. *Nat Methods* **2011**, *8* (5), 405–407. https://doi.org/10.1038/nmeth.1592.

(135) Perkins, L. A.; Holderbaum, L.; Tao, R.; Hu, Y.; Sopko, R.; McCall, K.; Yang-Zhou, D.; Flockhart, I.; Binari, R.; Shim, H.-S.; Miller, A.; Housden, A.; Foos, M.; Randkelv, S.; Kelley, C.; Namgyal, P.; Villalta, C.; Liu, L.-P.; Jiang, X.; Huan-Huan, Q.; Wang, X.; Fujiyama, A.; Toyoda, A.; Ayers, K.; Blum, A.; Czech, B.; Neumuller, R.; Yan, D.; Cavallaro, A.; Hibbard, K.; Hall, D.; Cooley, L.; Hannon, G. J.; Lehmann, R.; Parks, A.; Mohr, S. E.; Ueda, R.; Kondo, S.; Ni, J.-Q.; Perrimon, N. The Transgenic RNAi Project at Harvard Medical School: Resources and Validation. *Genetics* **2015**, *201* (3), 843–852. https://doi.org/10.1534/genetics.115.180208.

(136) Ni, J.-Q.; Markstein, M.; Binari, R.; Pfeiffer, B.; Liu, L.-P.; Villalta, C.; Booker, M.; Perkins, L.; Perrimon, N. Vector and Parameters for Targeted Transgenic RNA Interference in Drosophila Melanogaster. *Nat Methods* **2008**, *5* (1), 49–51. https://doi.org/10.1038/nmeth1146.

(137) Kulkarni, M.; Booker, M.; Silver, S.; Friedman, A.; Hong, P.; Perrimon, N.; Mathey-Prevot, B. Evidence of Off-Target Effects Associated with Long DsRNAs in Drosophila Melanogaster Cell-Based Assays. *Nat Methods* **2006**, *3* (10). https://doi.org/10.1038/nmeth935.

(138) Fuda, N. J.; Guertin, M. J.; Sharma, S.; Danko, C. G.; Martins, A. L.; Siepel, A.; Lis, J. T. GAGA Factor Maintains Nucleosome-Free Regions and Has a Role in RNA Polymerase II Recruitment to Promoters. *PLoS Genet* **2015**, *11* (3), e1005108. https://doi.org/10.1371/journal.pgen.1005108.

(139) Tsai, S.-Y.; Chang, Y.-L.; Swamy, K. B. S.; Chiang, R.-L.; Huang, D.-H. GAGA Factor, a Positive Regulator of Global Gene Expression, Modulates Transcriptional Pausing and Organization of Upstream Nucleosomes. *Epigenetics & Chromatin* **2016**, *9* (1), 32. https://doi.org/10.1186/s13072-016-0082-4.

(140) Judd, J.; Duarte, F. M.; Lis, J. T. Pioneer-like Factor GAF Cooperates with PBAP (SWI/SNF) and NURF (ISWI) to Regulate Transcription. *Genes Dev.* **2020**. https://doi.org/10.1101/gad.341768.120.

(141) Andrulis, E. D.; Guzmán, E.; Döring, P.; Werner, J.; Lis, J. T. High-Resolution Localization of Drosophila Spt5 and Spt6 at Heat Shock Genes in Vivo: Roles in Promoter Proximal Pausing and Transcription Elongation. *Genes Dev.* **2000**, *14* (20), 2635–2649. https://doi.org/10.1101/gad.844200.

(142) Wu, C.-H.; Yamaguchi, Y.; Benjamin, L. R.; Horvat-Gordon, M.; Washinsky, J.; Enerly, E.; Larsson, J.; Lambertsson, A.; Handa, H.; Gilmour, D. NELF and DSIF Cause Promoter Proximal Pausing on the Hsp70 Promoter in Drosophila. *Genes Dev.* **2003**, *17* (11), 1402–1414. https://doi.org/10.1101/gad.1091403.

(143) Aoi, Y.; Smith, E. R.; Shah, A. P.; Rendleman, E. J.; Marshall, S. A.; Woodfin, A. R.; Chen, F. X.; Shiekhattar, R.; Shilatifard, A. NELF Regulates a Promoter-Proximal Step Distinct from RNA Pol II Pause-Release. *Molecular Cell* **2020**, *78* (2), 261-274.e5. https://doi.org/10.1016/j.molcel.2020.02.014.

(144) Orphanides, G.; LeRoy, G.; Chang, C. H.; Luse, D. S.; Reinberg, D. FACT, a Factor That Facilitates Transcript Elongation through Nucleosomes. *Cell* **1998**, *92* (1), 105–116. https://doi.org/10.1016/s0092-8674(00)80903-4.

(145) Tellier, M.; Zaborowska, J.; Caizzi, L.; Mohammad, E.; Velychko, T.; Schwalb, B.; Ferrer-Vicens, I.; Blears, D.; Nojima, T.; Cramer, P.; Murphy, S. CDK12 Globally Stimulates RNA Polymerase II Transcription Elongation and Carboxyl-Terminal Domain Phosphorylation. *Nucleic Acids Research* **2020**, *48* (14), 7712–7727. https://doi.org/10.1093/nar/gkaa514.

(146) Squatrito, M.; Gorrini, C.; Amati, B. Tip60 in DNA Damage Response and Growth Control: Many Tricks in One HAT. *Trends in Cell Biology* **2006**, *16* (9), 433–442. https://doi.org/10.1016/j.tcb.2006.07.007.

(147) Scacchetti, A.; Schauer, T.; Reim, A.; Apostolou, Z.; Campos Sparr, A.; Krause, S.; Heun, P.; Wierer, M.; Becker, P. B. Drosophila SWR1 and NuA4 Complexes Are Defined by DOMINO Isoforms. *eLife* **2020**, *9*, e56325. https://doi.org/10.7554/eLife.56325.

(148) Brzezinski, J. A.; Lamba, D. A.; Reh, T. A. Blimp1 Controls Photoreceptor versus Bipolar Cell Fate Choice during Retinal Development. *Development* **2010**, *137* (4), 619–629. https://doi.org/10.1242/dev.043968.

(149) Brzezinski, J. A.; Uoon Park, K.; Reh, T. A. Blimp1 (Prdm1) Prevents Re-Specification of Photoreceptors into Retinal Bipolar Cells by Restricting Competence. *Developmental Biology* **2013**, *384* (2), 194–204. https://doi.org/10.1016/j.ydbio.2013.10.006.

(150) Vomund, S.; Schäfer, A.; Parnham, M. J.; Brüne, B.; von Knethen, A. Nrf2, the Master Regulator of Anti-Oxidative Responses. *Int J Mol Sci* **2017**, *18* (12). https://doi.org/10.3390/ijms18122772.

(151) Jauregui-Lozano, J.; Easton, A.; Escobedo, S.; Lanman, N. A.; Weake, V. M.; Hall, H. *Proper Control of R-Loop Homeostasis Is Required for Maintenance of Gene Expression and Neuronal Function during Aging*; 2021; p 2021.06.29.450380. https://doi.org/10.1101/2021.06.29.450380.

(152) Wood, J. G.; Hillenmeyer, S.; Lawrence, C.; Chang, C.; Hosier, S.; Lightfoot, W.; Mukherjee, E.; Jiang, N.; Schorl, C.; Brodsky, A. S.; Neretti, N.; Helfand, S. L. Chromatin Remodeling in the Aging Genome of Drosophila. *Aging Cell* **2010**, *9* (6), 971–978. https://doi.org/10.1111/j.1474-9726.2010.00624.x.

(153) Wood, J.; Helfand, S. Chromatin Structure and Transposable Elements in Organismal Aging. *Frontiers in Genetics* **2013**, *4*, 274. https://doi.org/10.3389/fgene.2013.00274.

(154) Liu, G.-H.; Barkho, B. Z.; Ruiz, S.; Diep, D.; Qu, J.; Yang, S.-L.; Panopoulos, A. D.; Suzuki, K.; Kurian, L.; Walsh, C.; Thompson, J.; Boue, S.; Fung, H. L.; Sancho-Martinez, I.; Zhang, K.; Yates, J.; Belmonte, J. C. I. Recapitulation of Premature Aging with IPSCs from Hutchinson-Gilford Progeria Syndrome. *Nature* **2011**, *472* (7342), 221–225. https://doi.org/10.1038/nature09879.

(155) Miller, J. D.; Ganat, Y. M.; Kishinevsky, S.; Bowman, R. L.; Liu, B.; Tu, E. Y.; Mandal, P.; Vera, E.; Shim, J.; Kriks, S.; Taldone, T.; Fusaki, N.; Tomishima, M. J.; Krainc, D.; Milner, T. A.; Rossi, D. J.; Studer, L. Human IPSC-Based Modeling of Late-Onset Disease via Progerin-Induced Aging. *Cell Stem Cell* **2013**, *13* (6), 691–705. https://doi.org/10.1016/j.stem.2013.11.006.

(156) Zhang, W.; Li, J.; Suzuki, K.; Qu, J.; Wang, P.; Zhou, J.; Liu, X.; Ren, R.; Xu, X.; Ocampo, A.; Yuan, T.; Yang, J.; Li, Y.; Shi, L.; Guan, D.; Pan, H.; Duan, S.; Ding, Z.; Li, M.; Yi, F.; Bai, R.; Wang, Y.; Chen, C.; Yang, F.; Li, X.; Wang, Z.; Aizawa, E.; Goebl, A.; Soligalla, R. D.; Reddy, P.; Esteban, C. R.; Tang, F.; Liu, G.-H.; Belmonte, J. C. I. A Werner Syndrome Stem Cell Model Unveils Heterochromatin Alterations as a Driver of Human Aging. *Science* **2015**, *348* (6239), 1160–1163. https://doi.org/10.1126/science.aaa1356.

(157) Li, W.; Prazak, L.; Chatterjee, N.; Grüninger, S.; Krug, L.; Theodorou, D.; Dubnau, J. Activation of Transposable Elements during Aging and Neuronal Decline in Drosophila. *Nat Neurosci* **2013**, *16* (5), 529–531. https://doi.org/10.1038/nn.3368.

(158) Li, W.; Jin, Y.; Prazak, L.; Hammell, M.; Dubnau, J. Transposable Elements in TDP-43-Mediated Neurodegenerative Disorders. *PLoS One* **2012**, *7* (9), e44099. https://doi.org/10.1371/journal.pone.0044099.

(159) Andrenacci, D.; Cavaliere, V.; Lattanzi, G. The Role of Transposable Elements Activity in Aging and Their Possible Involvement in Laminopathic Diseases. *Ageing Research Reviews* **2020**, *57*, 100995. https://doi.org/10.1016/j.arr.2019.100995.

(160) Wada, T.; Takagi, T.; Yamaguchi, Y.; Ferdous, A.; Imai, T.; Hirose, S.; Sugimoto, S.; Yano, K.; Hartzog, G. A.; Winston, F.; Buratowski, S.; Handa, H. DSIF, a Novel Transcription Elongation Factor That Regulates RNA Polymerase II Processivity, Is Composed of Human Spt4 and Spt5 Homologs. *Genes Dev* **1998**, *12* (3), 343–356. https://doi.org/10.1101/gad.12.3.343.

(161) Moorefield, B. SPT5 Roles in Transcriptional Elongation. *Nat Struct Mol Biol* **2021**, *28* (10), 778–778. https://doi.org/10.1038/s41594-021-00673-8.

(162) Aoi, Y.; Takahashi, Y.-H.; Shah, A. P.; Iwanaszko, M.; Rendleman, E. J.; Khan, N. H.; Cho, B.-K.; Goo, Y. A.; Ganesan, S.; Kelleher, N. L.; Shilatifard, A. SPT5 Stabilization of Promoter-Proximal RNA Polymerase II. *Mol Cell* **2021**, *81* (21), 4413-4424.e5. https://doi.org/10.1016/j.molcel.2021.08.006.

(163) Hu, S.; Peng, L.; Xu, C.; Wang, Z.; Song, A.; Chen, F. X. SPT5 Stabilizes RNA Polymerase II, Orchestrates Transcription Cycles, and Maintains the Enhancer Landscape. *Molecular Cell* **2021**, *81* (21), 4425-4439.e6. https://doi.org/10.1016/j.molcel.2021.08.029.

(164) Börner, K.; Becker, P. B. Splice Variants of the SWR1-Type Nucleosome Remodeling Factor Domino Have Distinct Functions during Drosophila Melanogaster Oogenesis. *Development* **2016**, *143* (17), 3154–3167. https://doi.org/10.1242/dev.139634.

(165) Mizuguchi, G.; Shen, X.; Landry, J.; Wu, W.-H.; Sen, S.; Wu, C. ATP-Driven Exchange of Histone H2AZ Variant Catalyzed by SWR1 Chromatin Remodeling Complex. *Science* **2004**, *303* (5656), 343–348. https://doi.org/10.1126/science.1090701.

(166) Sapountzi, V.; Logan, I. R.; Robson, C. N. Cellular Functions of TIP60. *Int J Biochem Cell Biol* **2006**, *38* (9), 1496–1509. https://doi.org/10.1016/j.biocel.2006.03.003.

(167) Doyon, Y.; Selleck, W.; Lane, W. S.; Tan, S.; Côté, J. Structural and Functional Conservation of the NuA4 Histone Acetyltransferase Complex from Yeast to Humans. *Mol Cell Biol* **2004**, *24* (5), 1884–1896. https://doi.org/10.1128/MCB.24.5.1884-1896.2004.

(168) Urban, I.; Kerimoglu, C.; Sakib, M. S.; Wang, H.; Benito, E.; Thaller, C.; Zhou, X.; Yan, J.; Fischer, A.; Eichele, G. TIP60/KAT5 Is Required for Neuronal Viability in Hippocampal CA1. *Scientific Reports* **2019**, *9* (1), 16173. https://doi.org/10.1038/s41598-019-50927-1.

(169) Beaver, M.; Bhatnagar, A.; Panikker, P.; Zhang, H.; Snook, R.; Parmar, V.; Vijayakumar, G.; Betini, N.; Akhter, S.; Elefant, F. Disruption of Tip60 HAT Mediated Neural Histone Acetylation Homeostasis Is an Early Common Event in Neurodegenerative Diseases. *Sci Rep* **2020**, *10* (1), 18265. https://doi.org/10.1038/s41598-020-75035-3.

(170) Li, Z.; Rasmussen, L. J. TIP60 in Aging and Neurodegeneration. *Ageing Research Reviews* **2020**, *64*, 101195. https://doi.org/10.1016/j.arr.2020.101195.

(171) Hall, H.; Cooper, B. R.; Qi, G.; Wijeratne, A. B.; Mosley, A. L.; Weake, V. M. Quantitative Proteomic and Metabolomic Profiling Reveals Altered Mitochondrial Metabolism and Folate Biosynthesis Pathways in the Aging Drosophila Eye. *Mol Cell Proteomics* **2021**, *20*, 100127. https://doi.org/10.1016/j.mcpro.2021.100127.

(172) Kounakis, K.; Tavernarakis, N. The Cytoskeleton as a Modulator of Aging and Neurodegeneration. *Adv Exp Med Biol* **2019**, *1178*, 227–245. https://doi.org/10.1007/978-3-030-25650-0_12.

(173) McMurray, C. T. Neurodegeneration: Diseases of the Cytoskeleton? *Cell Death Differ* **2000**, *7* (10), 861–865. https://doi.org/10.1038/sj.cdd.4400764.

(174) Cairns, N. J.; Lee, V. M.-Y.; Trojanowski, J. Q. The Cytoskeleton in Neurodegenerative Diseases. *J Pathol* **2004**, *204* (4), 438–449. https://doi.org/10.1002/path.1650.

(175) Muñoz-Lasso, D. C.; Romá-Mateo, C.; Pallardó, F. V.; Gonzalez-Cabo, P. Much More Than a Scaffold: Cytoskeletal Proteins in Neurological Disorders. *Cells* **2020**, *9* (2), 358. https://doi.org/10.3390/cells9020358.

(176) Liu, Z.; Tabuloc, C. A.; Xue, Y.; Cai, Y.; Mcintire, P.; Niu, Y.; Lam, V. H.; Chiu, J. C.; Zhang, Y. Splice Variants of DOMINO Control Drosophila Circadian Behavior and Pacemaker Neuron Maintenance. *PLOS Genetics* **2019**, *15* (10), e1008474. https://doi.org/10.1371/journal.pgen.1008474.

VITA

Education

Graduate Research Assistant, Biochemistry Department

Fall 2016 – current

Purdue University, West Lafayette, IN

Principal Investigator: Dr. Vikki M. Weake

Bachelor of Science in Biochemistry and Molecular biology

2012-2016,

University of Arizona, Department of Chemistry and Biochemistry, Tucson, AZ

Research

PhD Thesis Research

March 2017 – current

Purdue University, Department of Biochemistry

Thesis Advisor Dr. Vikki Weake

Age-associated changes in photoreceptor neurons.

Professional Development

Oral and Poster *Presentations*

Graduate Student Rotation Talks, (Purdue University, 2016-2017)

Chromatin Group Meeting, (Purdue University, Spring 2018, 2019, 2020, Fall 2021)

Poster Presentation, (ASBMB Annual Conference, San Diego CA, April 2018)

Poster Presentation, (Annual Biochemistry Retreat, Purdue University, August 2018)

Poster Presentation, (Midwest Chromatin Meeting, Purdue University, June 2018)

Mentored Undergraduates

Phyllicia Hemphill (NSF REU Summer Program), May 2017-July 2017

Claire Stamper (Biochemistry undergraduate), August 2017-May 2019

Mikaela Hand (Biochemistry undergraduate), January 2018-May 2018

Aashka Shah (Biochemistry undergraduate), January 2018-May 2020

Nicholas Nelson (NSF REU Summer Program), May 2018-July 2018

Taylor Murray (Biochemistry undergraduate), January 2020-Present

Ryan DeBernardis (Biochemistry undergraduate), January 2020-Present

Brianna Kennedy (Biochemistry undergraduate), August 2021-Present

Mentored Graduate Student Rotation Projects

Stephanie Diaz, Summer 2019

Sarah Stanhope, Fall 2020

Ziyu Dong, Fall 2020

Kratika Singhal, Fall 2021

Anik Paul, Fall 2021

Leadership Experience and Training

Biochemistry Graduate Student Organization -Social Chair (November 2017- August 2018)

NSF REU Summer Research -Mentor (Purdue University, Summer 2017, 2018)

Biochemistry Invited Seminar Committee -Member (Purdue University, Fall 2018)

Biochemistry Graduate Student Recruitment -Host (Purdue University, 2017, 2018, 2019, 2020)

Biochemistry Graduate Student Organization- President (August 2018-July 2019)

Biochemistry Retreat Committee -Member (August 2018, August 2019)

Applied Management Principles, Purdue Krannert School of Management (May 2021)

Awards, Memberships

Rotation Bird Stair Award -Recipient (August 2016-March 2017)

Bird Stair Research Fellowship -Recipient (Spring 2018)

Genetics Society of America -Member (Fall 2019-Present)

Teaching Experience

Biochemistry 309 Lab -Teaching Assistant (Fall 2017)

Biochemistry 100 -Teaching Assistant (Fall 2017)

Biochemistry 101 Lab -Teaching Assistant (Spring 2020)

Publications

Hall,H., Medina, P., Cooper, D. A., **Escobedo, S. E.**, Rounds, J., Brennan, K., Vincent, C., Miura, P., Doerge, R., Weake, V. M. Transcriptome profiling of aging Drosophila photoreceptors reveals gene expression trends that correlate with visual senescence. *BMC Genomics* 2017

Stegeman, R., Hall, H., **Escobedo, S. E**., Chang, H. C., Weake, V. M. Proper splicing contributes to visual function in the aging Drosophila eye, *Aging Cell* 2018

Escobedo, S. E., Zirin, J., Weake, V. M. TRiP stocks contain a previously uncharacterized loss-of-function sevenless allele. *micropublication Biology* 2019

Escobedo, S.E., Shah, A., Easton, A., Hall, H., Weake, V. M. Characterizing a gene expression toolkit for eye- and photoreceptor-specific expression in Drosophila, *Fly* 2021

Jauregui-Lozano, **Escobedo S.E.,** J.,Easton, A., Lanman, N.A., Weake, V.M., Hall, H. *Proper control of R-loop homeostasis is required for maintenance of gene expression and neuronal function during aging, (Revised manuscript submitted for review)*

Escobedo S.E.*, Dong, Z., Stanhope, S.C., Weake V.W. Aging and light stress result in overlapping and unique gene expression changes in photoreceptors (UNDER REVIEW at MDPI GENES)*